

TESIS DOCTORAL

REDUCCIÓN FOTOELECTROQUÍMICA DE CO₂ UTILIZANDO
UN REACTOR DE MEMBRANA EN MODO CONTINUO

PhD THESIS

PHOTOELECTROCHEMICAL REDUCTION OF CO₂ USING A
CONTINUOUS MEMBRANE REACTOR

AUTOR

SERGIO CASTRO GONZÁLEZ

DIRECTORES

DR. JONATHAN ALBO SÁNCHEZ

DR. GUILLERMO DÍAZ SAINZ

UNIVERSIDAD DE CANTABRIA

Escuela de Doctorado de la Universidad de Cantabria

Santander 2023

UNIVERSIDAD DE CANTABRIA



ESCUELA DE DOCTORADO DE LA UNIVERSIDAD DE CANTABRIA

PROGRAMA DE DOCTORADO EN INGENIERÍA QUÍMICA,
DE LA ENERGÍA Y DE PROCESOS

**Photoelectrochemical reduction of CO₂ using a
continuous membrane reactor**

*Reducción fotoelectroquímica de CO₂ utilizando un reactor de
membrana en modo continuo*

Tesis Doctoral presentada para optar al título de Doctor por la
Universidad de Cantabria

Realizada por:

Sergio Castro González

Dirigida por:

Dr. Jonathan Albo Sánchez

Dr. Guillermo Díaz Sainz

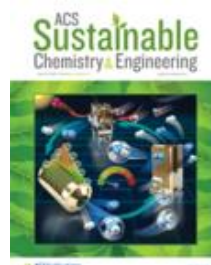
Santander, 2023

La Tesis Doctoral se presenta como un resumen de trabajos previamente publicados en revistas científicas internacionales incluidas en el *Journal of Citation Reports-Science Edition* (JCR), siguiendo la normativa del Programa de Doctorado en Ingeniería Química, de la Energía y de Procesos de la Universidad de Cantabria para la elaboración de Tesis Doctorales a través de un compendio de artículos previamente publicados. El trabajo se ha desarrollado en el grupo de investigación de Desarrollo de Procesos Químicos y Control de Contaminantes (DePRO) del Departamento de Ingenierías Química y Biomolecular de la Universidad de Cantabria, liderado por el Prof. Ángel Irabien Gulías, bajo la supervisión del Dr. Jonathan Albo Sánchez y el Dr. Guillermo Díaz Sainz. A continuación se enumeran las contribuciones científicas publicadas, así como las contribuciones a congresos publicados en libros con ISBN:

a) Artículos en revistas científicas, indicando la lista de autores por orden de firma, año de publicación, título del artículo, título de la revista, número de revista, números de la primera y última página, índice de impacto de la revista, cuartil en el área temática, denominación del área temática de la revista, y posición relativa en el área temática.

1. Sergio Castro, Jonathan Albo, Ángel Irabien, **2018.**

Photoelectrochemical reactors for CO₂ utilization. ACS Sustainable Chemistry & Engineering, 6, 15877-15894. Índice de impacto: 6,970. Q1 y D1; Chemical Engineering 9/138.



2. Sergio Castro, Jonathan Albo, Ángel Irabien, **2020.**

Continuous conversion of CO₂ to alcohols in a TiO₂ photoanode-driven photoelectrochemical system. Journal of Chemical Technology & Biotechnology, 95, 1876-1882. Índice de impacto: 3,174. Q2; Chemical Engineering 63/143.



3. Iván Merino-García¹, Sergio Castro¹, Ángel Irabien, Ignacio

Hernández, Verónica Rodríguez, Rafael Camarillo, Jesusa Rincón, Jonathan Albo, **2022.** Efficient photoelectrochemical conversion of CO₂ to ethylene and methanol using a Cu cathode and TiO₂ nanoparticles synthesized in supercritical medium as photoanode. Journal of Environmental Chemical Engineering, 10, 107441. Índice de impacto: 7,7. Q1; Chemical Engineering 16/140. ¹Iván Merino-García y Sergio Castro han contribuido igualmente a este trabajo como primeros autores.



b) Comunicaciones presentadas en congresos y publicadas en libros con ISBN, detallando la lista de autores por orden de firma, título de la comunicación, congreso, fecha de celebración, lugar de celebración, ISBN y tipo de comunicación.

1. Sergio Castro, Jonathan Albo, Angel Irabien, Continuous photo-electrochemical reduction of CO₂ in a TiO₂ photoanode-driven system, 3rd ANQUE-ICCE International Congress of Chemical Engineering. 19 - 21 junio **2019**, Santander (España). ISBN: 978-84-09-12430-5. Comunicación oral.



2. Sergio Castro, Jonathan Albo, Verónica Rodriguez, Rafael Camarillo, Jesusa Rincón, Angel Irabien, Reducción en continuo de CO₂ utilizando nanopartículas de TiO₂ en una celda fotoelectroquímica, V Workshop de la Red E3TECH / I Workshop Iberoamericano a Distancia E3TECH "Aplicaciones Medioambientales y Energéticas de la Tecnología Electroquímica". 28 – 31 octubre **2020**, Online. ISBN: 978-84-09-24561-1. Comunicación póster.



Esta Tesis Doctoral ha sido desarrollada en el grupo de investigación “Desarrollo de Procesos Químicos y Control de Contaminantes” (DePRO) del Departamento de Ingenierías Química y Biomolecular de la Universidad de Cantabria. Este trabajo ha sido financiado por el Ministerio de Economía y Competitividad a través del proyecto CTQ2013-48280-C3-1-R *“Desarrollo e integración de procesos con membranas para la captura y valorización de dióxido de carbono”*, el Ministerio de Economía, Industria y Competitividad a través del proyecto CTQ2016-76231-C2-1-R *“Diseño multiescala de procesos de captura y utilización de dióxido de carbono”*, y el Ministerio de Ciencia e Innovación a través del proyecto PID2019-104050RA-I00 *“Conversión impulsada por la luz de CO₂ en combustibles utilizando reactores microfluídicos”*.

Durante la ejecución del presente trabajo, su autor, Sergio Castro, ha sido beneficiario de un contrato de investigación en primer lugar, gracias al proyecto CTQ2013-48280-C3-1-R *“Desarrollo e integración de procesos con membranas para la captura y valorización de dióxido de carbono”*, y en segundo lugar, a través del proyecto CTQ2016-76231-C2-1-R *“Diseño multiescala de procesos de captura y utilización de dióxido de carbono”*.

Por todo lo mencionado anteriormente, se expresa el más sincero agradecimiento hacia dichas instituciones y entidades.

AGRADECIMIENTOS

En este momento, a las puertas de la defensa de esta tesis doctoral, toca agradecer a quienes de una forma u otra han seguido de cerca este trabajo y me han brindado su apoyo para conseguirlo.

Toca agradecer de una forma especial a mis directores de tesis: al Dr. Jonathan Albo Sánchez por su colaboración en el día a día y por transmitirme sus conocimientos; al Dr. Guillermo Díaz Sainz por sus consejos y su empuje para culminar este trabajo y, finalmente, pero no menos importante, quiero expresar mi más sincero agradecimiento al que ha sido mi director en los comienzos y gran parte del desarrollo de esta tesis: Prof. Dr. Ángel Irabien. Gracias por saber guiarme y confiar en mí.

Tampoco puedo dejar de agradecer la ayuda y el trato recibido por parte de profesores, técnicos y personal administrativo del Departamento de Ingenierías Química y Biomolecular de la Universidad de Cantabria, así como del grupo de investigación de Desarrollo de Procesos Químicos y Control de Contaminantes (DePRO) del que he formado parte.

Y, por último, una dedicatoria especial para mis padres, mi hermano, familia, amigos y compañeros de despacho y doctorado, por compartir conmigo las alegrías y tristezas de esta etapa.

Muchas gracias a todas aquellas personas que durante estos años estuvieron a mi lado ayudándome a lograr que esto sea posible.

Índice

ÍNDICE

AGRADECIMIENTOS	v
ÍNDICE	vii
RESUMEN	xi
CAPÍTULO 1. PLANTEAMIENTO.....	1
1.1 Marco de la Tesis Doctoral.....	3
1.2 Objetivos y estructura	9
1.3 Referencias del capítulo 1.....	11
CAPÍTULO 2. METODOLOGÍA	19
2.1 Síntesis y caracterización de nanopartículas de TiO ₂	21
2.2 Fabricación de los fotoánodos	22
2.3 Caracterización photoelectroquímica y fisicoquímica de los fotoánodos.....	22
2.4 Sistema experimental para la photoelectroreducción de CO ₂	22
2.5 Figuras de mérito.....	24
2.6 Referencias del capítulo 2.....	26
CAPÍTULO 3. ARTÍCULOS CIENTÍFICOS	27
3.1. Sergio Castro, Jonathan Albo, Angel Irabien. 2018. Photoelectrochemical reactors for CO ₂ utilization. ACS Sustainable Chemistry & Engineering, 6, 12, 15877-15894.	29
3.2. Sergio Castro, Jonathan Albo, Angel Irabien. 2018. Continuous conversion of CO ₂ to alcohols in a TiO ₂ photoanode-driven photoelectrochemical system. Journal of Chemical Technology and Biotechnology, 95, 7, 1876-1882.	49
3.3. Iván Merino García, Sergio Castro, Angel Irabien, Ignacio Hernández, Verónica Rodríguez, Rafael Camarillo, Jesusa Rincón, Jonathan Albo. 2022. Efficient photoelectrochemical conversion of CO ₂ to ethylene and methanol using a Cu cathode and TiO ₂ nanoparticles synthesized in supercritical medium as photoanode. Journal of Environmental Chemical Engineering, 10, 3, 107441.....	59
CAPÍTULO 4. RESUMEN DE RESULTADOS Y CONCLUSIONES.....	71
4.1 Resumen de los principales resultados	73
4.2 Conclusiones	75
4.3 Trabajo futuro	77
ANEXO	79
DIFUSIÓN DE RESULTADOS EN CONGRESOS NACIONALES E INTERNACIONALES	81

Resumen

Este es un resumen de la sección Resumen.

RESUMEN

La reducción de las emisiones de dióxido de carbono (CO_2) en la atmósfera es una prioridad en la agenda política mundial, con el objetivo de lograr una producción de energía en un ciclo neutro en carbono. En este contexto, las tecnologías de Captura, Almacenamiento y Utilización de Carbono (CAUC) han sido objeto de investigación durante las últimas décadas. En particular, la conversión del CO_2 en productos útiles se presenta como una solución para abordar de manera conjunta los desafíos del calentamiento global y la escasez de energía.

Entre las diversas aproximaciones disponibles para activar y convertir el CO_2 en productos útiles (como la conversión química, termoquímica, hidrotérmica, bioquímica, electroquímica o fotoquímica, entre otros), destaca la vía electrocatalítica por su capacidad para almacenar energía renovable intermitente en forma de enlaces químicos. Es decir, la electroreducción no solo proporciona una forma viable de reutilizar el CO_2 , sino también un método para la producción de químicos con valor añadido. Además, la aplicación de luz directa sobre los electrodos durante la electroreducción, la conversión photoelectrocatalítica de CO_2 , ofrece la ventaja de reducir el voltaje externo necesario y, por ende, el consumo de energía requerido para llevar a cabo la reacción. Este voltaje de polarización externo aplicado en el proceso, junto al empleo de celdas divididas, impulsa la separación efectiva de los pares electrón-hueco generados por la luz en el electrodo, superando una de las principales limitaciones de la reducción photocatalítica de CO_2 . Así la photoelectrocatalisis destaca como una alternativa prometedora que combina las ventajas de la electrocatalisis y la fotocatalisis, reduciendo el voltaje necesario requerido en la conversión electroquímica de CO_2 en productos químicos útiles mediante el uso de la luz.

La presente Tesis Doctoral se enmarca en los proyectos de investigación CTQ2013-48280-C3-1-R, CTQ2016-76231- C2-1-R, y PID2019-104050RA-I00, los cuales se centran en el desarrollo de procesos eficientes para la valorización de CO_2 . Bajo la dirección del Prof. Ángel Irabien, el grupo de investigación de Desarrollo de Procesos Químicos y Control de Contaminantes (DePRO) perteneciente al Departamento de Ingenierías Química y Biomolecular de la Universidad de Cantabria, ha logrado avances significativos en la transformación electroquímica de CO_2 en productos de alto valor, como ácido fórmico, alcoholes e hidrocarburos. En esta Tesis Doctoral, se busca desarrollar un proceso continuo de conversión de CO_2 por vía photoelectroquímica, con el fin de reducir los sobrepotenciales necesarios para la conversión de CO_2 mediante el uso directo de la luz, lo cual representa una línea de investigación nueva en el grupo.

Para alcanzar este ambicioso objetivo se llevó a cabo, en primer lugar, una exhaustiva revisión del estado del arte. De esta revisión, se destaca que la configuración más empleada es la de fotoánodo-cátodo a oscuras, aprovechando los beneficios de utilizar semiconductores tipo

n, más abundantes, económicos y estables para la oxidación de H₂O, en lugar de semiconductores tipo *p*.

Posteriormente, se diseña y construye un sistema experimental para llevar a cabo la fotoelectroreducción de CO₂ a metanol y etanol en continuo. Se emplea una celda fotoelectroquímica (PEC) compuesta inicialmente por un fotoánodo basado en TiO₂-P25 en configuración MEA, que se ilumina con luz LED UV (100 mW·cm⁻²), junto con una placa de Cu a oscuras. Con esta configuración, se logra un incremento de hasta 4,3 mA·cm⁻² (2 V vs. Ag/AgCl) al iluminar la superficie del fotoánodo. El funcionamiento del sistema se ve favorecido al aplicar -1,8 V vs. Ag/AgCl con una carga catalítica de TiO₂-P25 de 3 mg·cm⁻², lo que permite alcanzar una velocidad de producción de 9,5 µmol·m⁻²·s⁻¹, una eficiencia Faradaica del 16,2% y una eficiencia energética del 5,2% para metanol, y una velocidad de producción de 6,8 µmol·m⁻²·s⁻¹, eficiencia Faradaica del 23,2% y eficiencia energética del 6,8% para etanol. La producción de metanol se ve favorecida con el incremento de voltaje, mientras que la producción de etanol se ve afectada negativamente. Se puede concluir que es posible mejorar la producción de alcoholes a partir de CO₂ con luz UV, reduciendo la energía requerida en un sistema electroquímico a oscuras.

Tras estos desarrollos, se investiga el empleo de nanopartículas sintetizadas en medio supercrítico (TiO₂-SC) para la preparación de fotoánodos, con el objetivo de mejorar la eficiencia del proceso. La caracterización fotoelectroquímica de los fotoánodos revela que la densidad de corriente alcanzada es significativamente más elevada (12,31 mA·cm⁻²) que la obtenida en el sistema en ausencia de luz (7,18 mA·cm⁻²). Esta corriente también supera la obtenida anteriormente con los fotoánodos fabricados con nanopartículas comerciales de TiO₂-P25 (5,9 mA·cm⁻²) en las mismas condiciones. Esto se atribuye a las propiedades mejoradas del TiO₂-SC, como su morfología, su cristalinidad y área superficial, que influyen en la absorción de luz y la banda prohibida (*o bandgap*, en inglés), permitiendo un mejor acceso de reactivos a los sitios fotoactivos y una mejor separación de cargas. Como resultado, la producción de etileno, un producto de gran interés comercial, se incrementa hasta seis veces (147,4 µmol·m⁻²·s⁻¹) cuando se utilizan superficies de TiO₂-SC como fotoánodos, en comparación con el rendimiento del proceso a oscuras. La formación de metanol también se favorece bajo la luz (4,72 µmol·m⁻²·s⁻¹). Además, las eficiencias Faradaicas tanto para el etileno como para el metanol (46,6% y 15,3%, respectivamente), aumentan con la irradiación de luz, superando los resultados reportados en la literatura para sistemas fotoelectroquímicos en configuración fotoánodo-cátodo. En consecuencia, la eficiencia en la conversión de energía solar en productos mejora en el sistema basado en TiO₂-SC iluminado (5,4% para etileno y 1,9% para metanol), en comparación con el comportamiento de los fotoánodos de TiO₂-P25 (3,7% para etileno y 1% de metanol).

Planteamiento

CAPÍTULO 1. PLANTEAMIENTO

1.1 Marco de la Tesis Doctoral

El uso de combustibles fósiles para generar energía eléctrica y su aplicación en sectores como la agricultura, la industria y el transporte ha ocasionado un constante incremento de las emisiones de dióxido de carbono (CO_2) a la atmósfera desde la Revolución Industrial (Mustafa et al., 2020). Los últimos datos de la Administración Nacional Oceánica y Atmosférica (NOAA, por sus siglas en inglés) muestran que la concentración de CO_2 ha superado las 421 ppm (ESRL Global Monitoring Laboratory, 2023). Estas emisiones son responsables del efecto invernadero, reconocido internacionalmente como la principal causa del cambio climático por el Panel Intergubernamental del Cambio Climático (IPCC, por sus siglas en inglés) (The Intergovernmental Panel on Climate Change, 2023) y la Organización de las Naciones Unidas (ONU) (Naciones Unidas, 2023). El IPCC recomienda limitar el calentamiento global a un aumento de 1,5 °C y, en todo caso, a 2,0 °C, tomando como referencia la época preindustrial, para el año 2100, con el fin de evitar un cambio climático irreversible, tal como se estableció en la Conferencia de las Partes (COP) de París en 2015. En consonancia, la ONU ha definido 17 Objetivos de Desarrollo Sostenible (ODS) (Objetivos de Desarrollo Sostenible, 2023), con diferentes metas en cada uno de ellos, a alcanzar para el año 2030. Entre los ODS se encuentran los números 7 y 13, que se centran en obtener energía asequible y no contaminante, y en la acción por el clima, respectivamente. Estos objetivos abordan distintos aspectos como la implementación de fuentes de energía renovable y la reducción de las emisiones de gases de efecto invernadero. En la misma línea, es importante mencionar el Pacto Verde Europeo, aprobado en 2020 por la Comisión Europea. Este pacto incluye, entre otras cosas, un conjunto de iniciativas políticas con el objetivo de lograr la neutralidad climática de la Unión Europea para el año 2050 (Comisión Europea, 2023).

Para alcanzar estos objetivos, es necesario reemplazar las fuentes de energía con alto contenido de carbono por fuentes renovables, como la energía eólica o solar y, al mismo tiempo, mejorar la eficiencia de los procesos industriales. Sin embargo, la transición hacia la descarbonización avanza lentamente y se prevé una fuerte dependencia de los combustibles fósiles en las próximas décadas (International Energy Agency, 2023). Por lo tanto, se están realizando esfuerzos significativos para promover la tecnologías de CAUC (Irabien et al., 2018), especialmente en aquellos sectores de difícil descarbonización como la producción de acero, cemento, el sector de la aviación o la producción de sustancias químicas básicas, entre otros (Marco Estratégico de Energía y Clima, 2023).

Los procesos tradicionales de captura de CO_2 , como la absorción con aminas, presentan limitaciones debido a los altos costes asociados con la captura, separación y purificación del CO_2 (Vadillo et al., 2022a; Vadillo et al., 2022b). Además, el almacenamiento de CO_2 conlleva un consumo energético significativo, principalmente por el transporte requerido a explotaciones de gas y petróleo o a acuíferos salinos (Aminu et al., 2017). En general, la sociedad tiene una

percepción negativa de estos procesos (Isa et al., 2019). Por lo tanto, existe un creciente interés en la conversión del CO₂ capturado en productos químicos de valor añadido mediante el uso de fuentes de energía renovable. Esto no solo tiene beneficios medioambientales, sino también económicos y sociales (Zhang et al., 2020a, 2020b).

En la actualidad, existen diversas tecnologías para activar y convertir el CO₂ en productos útiles, como es la conversión química, termoquímica, hidrotérmica, bioquímica, electroquímica o fotoquímica, entre otras (Fernández-Caso et al., 2023; Han et al., 2023; Okoye-Chine et al., 2022; Ampelli et al., 2023). Entre ellas, la vía electrocatalítica es especialmente interesante, ya que permite almacenar energías renovables e intermitentes en forma de enlaces químicos (Lin et al., 2023). En otras palabras, la electroreducción no solo es una ruta técnicamente viable para reutilizar el CO₂, sino también una forma de generar productos químicos de valor añadido (Kumar et al., 2023). El CO₂ puede ser reducido a una gran variedad de productos finales, como monóxido de carbono (CO) (Jouny et al., 2019), ácido fórmico (HCOOH) (Fernández-Caso et al., 2023), metanol (CH₃OH) (Duan et al., 2023), metano (CH₄) (Zheng et al., 2022) o etileno (C₂H₄) (Ai et al., 2022), entre otros. En la Tabla 1.1 se presentan los potenciales termodinámicos para la reducción del CO₂ a pH= 7 en disolución acuosa, con un electrodo estándar de hidrógeno (SHE, por sus siglas en inglés) como referencia a 25 °C y presión atmosférica. El avance de la reacción depende en gran medida del catalizador, el electrolito y el potencial del cátodo. Normalmente, se requieren múltiples etapas de transferencia de electrones acoplados a protones, lo que implica importantes barreras cinéticas para la reacción directa (Kumar et al., 2016; Liu et al., 2021; Nandal & Jain, 2022; Verma & Yadav, 2023; Wang et al., 2019).

Tabla 1.1. Reacción de evolución de hidrógeno y de reducción del CO₂ a productos con sus correspondientes potenciales estándar de reducción a pH=7 (Irabien et al., 2018).

Reacción de evolución de hidrógeno	Potencial estándar de reducción vs. SHE (V)
H ₂ O + 2e ⁻ → H ₂ + 2OH ⁻	-0,31
CO ₂ + H ₂ O + 2e ⁻ → CO + 2OH ⁻	-0,52
CO ₂ + 5H ₂ O + 6e ⁻ → CH ₃ OH + 6OH ⁻	-0,39
CO ₂ + 9H ₂ O + 12e ⁻ → C ₂ H ₅ OH + 12OH ⁻	-0,33
CO ₂ + 6H ₂ O + 8e ⁻ → CH ₄ + 8OH ⁻	-0,25
CO ₂ + 8H ₂ O + 12e ⁻ → C ₂ H ₄ + 12OH ⁻	-0,34
CO ₂ + H ₂ O + 2e ⁻ → HCOO ⁻ + OH ⁻	-0,43

Sin embargo, la electroreducción tiene una elevada demanda energética para romper los enlaces de la molécula de CO₂. Este alto sobrepotencial puede comprometer su efectividad como medida de mitigación del cambio climático (Creissen et al., 2022). Por lo tanto, es necesario realizar esfuerzos para reducir el sobrepotencial de reacción tanto en el cátodo como en el ánodo con el fin de mejorar la eficiencia energética del proceso (Kibria et al., 2019). Si bien es posible

combinar cualquier fuente de electricidad renovable con dispositivos electroquímicos, la integración directa de la luz solar ofrece una ventaja adicional, ya que la luz promueve la generación de electrones, reduciendo la necesidad de energía externa para la conversión de CO₂. Esta estrategia integrada reduce las pérdidas de energía e, idealmente, elimina la necesidad de conexión a la red en áreas periféricas, permitiendo el uso directo local (Montoya et al., 2016; Seitz et al., 2016).

En este sentido, los sistemas basados en reactores fotoelectroquímicos (PEC, por sus siglas en inglés) integran la generación de energía asistida por luz y la reducción de CO₂ dentro del mismo dispositivo, maximizando la eficiencia energética al reducir el aporte energético externo necesario debido a la iluminación del fotoelectrodo (Brito et al., 2022; Han et al., 2023). El objetivo es utilizar los electrones generados con la incidencia de fotones sobre un material semiconductor, tal como ocurre en las reacciones de reducción photocatalítica, y utilizarlos en la reducción electroquímica de un par redox seleccionado (Tang & Xiao, 2022; Yaashikaa et al., 2019). Por lo tanto, la fotoelectroreducción de CO₂ se encuentra a medio camino entre la conversión electroquímica y la photocatalítica, aprovechando las oportunidades de ambas. En general, los reactores PEC están compuestos por los propios fotoelectrodos, electrolitos, un circuito externo, y la alimentación de los reactivos (Pitchaimuthu et al., 2022; Zhou et al., 2016). Los electrodos deben estar preferentemente separados mediante una membrana de intercambio iónico para prevenir el transporte de los productos hacia el electrodo opuesto, evitando su reoxidación y facilitando la transferencia de carga entre los compartimentos catódicos y anódicos. Así, la configuración de los fotoelectrodos y reactores desempeñan un papel crucial en la generación de las cargas, su separación, y la inyección extra de electrones para el proceso de reducción de CO₂ (Ochedi et al., 2021).

En cuanto a los materiales, se deben cumplir varios requisitos simultáneamente para lograr el éxito de la fotoelectroreducción (Zhang & Wang, 2023). En primer lugar, y tomando como ejemplo el desarrollo de fotoánodos, el *bandgap* del fotoelectrodo debe ser lo suficientemente bajo como para capturar eficientemente los fotones del espectro solar (<2,2 eV) y debe ser lo suficientemente alto como para proporcionar los electrones excitados para llevar a cabo la reacción de evolución de oxígeno, que es la reacción más común, en el compartimento anódico (>1,23 eV) (Graves et al., 2011). De manera general, los electrodos basados en materiales semiconductores absorben la luz para generar electrones a un nivel de energía más alto que, junto con los huecos generados, son capaces de llevar a cabo las reacciones redox en una interfaz semiconductor/líquido (Zhang& Wang, 2023). Los huecos generados en el fotoánodo, que suele ser un semiconductor de tipo *n*, pueden oxidar el H₂O a O₂, mientras que los electrones generados en el fotocátodo, generalmente un semiconductor de tipo *p*, pueden reducir el CO₂ a CO, HCOOH, CH₃OH o hidrocarburos en presencia o ausencia de un cocatalizador (Xie et al., 2015). Además, el fotoelectrodo debe ser estable y resistente a la corrosión en el electrolito. Por

Lo tanto, la fotoelectroquímica es un campo interdisciplinario que incluye disciplinas como la electroquímica, la física, la óptica y la ciencia de superficies (Jiang et al., 2010).

El TiO₂ ha sido el fotocatalizador más investigado hasta la fecha (Liu et al., 2022; Cortes et al., 2020; Cheng et al., 2019; Cheng et al., 2020; Kobayashi et al., 2020). Esto se debe a que el TiO₂ es un semiconductor de tipo *n* con un amplio *bandgap* de 3,0 eV (Styring et al., 2014) y ha sido considerado como un material económico y respetuoso con el medio ambiente desde que se utilizó por primera vez con este propósito en 1979 (Inoue et al., 1979). Además del TiO₂, existen otros semiconductores que pueden utilizarse como fotoánodos, como por ejemplo el BiVO₄, WO₃ (Li et al., 2019; Wang et al., 2020); Kang et al., 2021) o mezclas entre ambos (Lu et al., 2020), así como el TiO₂ dopado con distintos materiales como CuO (De Brito et al., 2019), ZrO₂ (De Brito et al., 2019), o Si (Liu et al., 2022), entre otros. Entre los fotocátodos más comunes, destacan los materiales basados en Cu₂O (Minggu et al., 2020), CuO (Wang et al., 2022), CuFe₂O₄ (Tarek et al., 2019), Fe₂O₃ (Bharath et al., 2021), o Si (Hu et al., 2023), entre otros. Sin embargo, el desarrollo de fotocátodos eficientes se encuentra menos avanzado que el desarrollo de fotoánodos, ya que requiere combinar la compleja reducción de CO₂ con las propiedades ópticas y semiconductoras del material.

En cuanto a la configuración del reactor PEC, existen cuatro configuraciones mayoritarias (Creissen et al., 2022; Ding et al., 2020): (Figura 1.1): basada en el empleo de fotoánodo - cátodo a oscuras (Cheng et al., 2014, 2015) (Figura 1.1a), fotocátodo – ánodo a oscuras (Bharath et al., 2021a; Liu et al., 2023; Otgonbayar et al., 2023) (Figura 1.1b), fotoánodo – fotocátodo (Kistler et al., 2021) (Figura 1.1c), o los reactores tandem que incorporan elemento fotovoltaicos (Zhang, et al., 2020a) (Figura 1.1d).

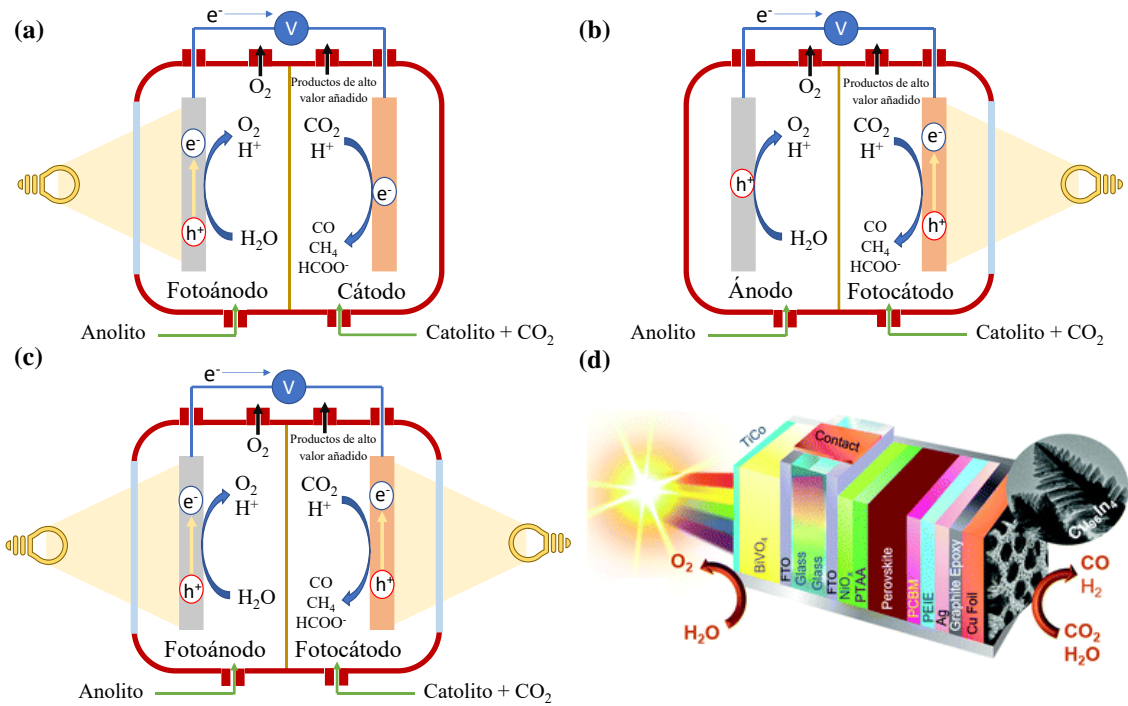


Figura 1.1. Configuración de reactor PEC empleando una configuración: (a) fotoánodo-cátodo a oscuras; (b) photocátodo-ánodo a oscuras, (c) photocátodo y fotoánodo, y (d) sistema tándem (Rahaman et al., 2020.)

Por otro lado, los reactores PEC pueden operar en modo continuo o discontinuo. La operación en modo continuo ha ganado atención en los últimos años debido a su mayor eficiencia y capacidad para tratar volúmenes más grandes de CO_2 , lo que la hace más adecuada para aplicaciones prácticas (Bi et al., 2022; Lu et al., 2020). A su vez, los reactores PEC con operación en continuo pueden contener el catalizador suspendido en una solución electrolítica (lecho fluidizado) o adherido a una superficie (lecho fijo) (Ola & Maroto-Valer, 2015). Los reactores de lecho fluidizado mejoran la transferencia de materia y calor debido al movimiento de las partículas sólidas, pero separar el catalizador del medio de reacción puede dificultar la eficiencia energética y la formación de productos. En comparación, los reactores de lecho fijo tienen áreas de superficie, tasas de conversión y tiempos de reacción más altos que los reactores de lecho fluidizado. Sin embargo, los gradientes de temperatura entre el flujo de gas y el catalizador pueden reducir la eficiencia de conversión. Así, la integración de (foto)electrodos en reactores de lecho fijo puede realizarse en celdas sin dividir (Figura 1.2a), donde en un compartimento único ocurren tanto las reacciones de reducción y oxidación, con un solo electrolito que actúa como catolito y anolito al mismo tiempo.

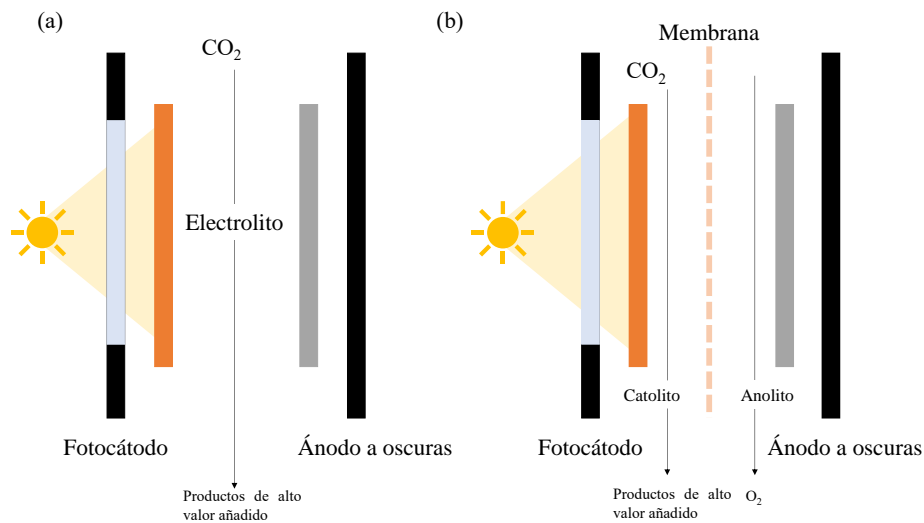


Figura 1.2. (a) Configuración de reactor fotoelectroquímico sin dividir y (b) Configuración de reactor fotoelectroquímico separado por una membrana de intercambio iónico. Adaptada de la referencia Merino-Garcia et al., 2016.

Por otra parte, las celdas divididas por una membrana (Figura 1.2b) impiden la transferencia de productos de reacción de un compartimento a otro, permitiendo el flujo de especies cargadas según su naturaleza (Endrődi et al., 2017). Así, las membranas de intercambio catiónico (CEM) permiten el transporte de protones desde el ánodo hasta el cátodo (Genovese et al., 2013), las membranas de intercambio aniónico (AEM) permiten el transporte selectivo de especies de carga negativa como el OH^- (Kutz et al., 2017), y las membranas bipolares (BPM) hechas de AEM y CEM pueden transportar protones al cátodo y OH^- al ánodo simultáneamente (Gurudayal et al., 2017; Zhou et al., 2016).

Además, se emplean comúnmente estructuras de electrodos de difusión de gas (GDE), tanto para el cátodo como para el ánodo, considerando que ciertos reactivos y productos se encuentran en fase gaseosa. Esta arquitectura de reactor permite superar las limitaciones asociadas con otras configuraciones: i) limitaciones de corriente debido a la baja concentración de CO_2 en la superficie del electrodo, ii) migración de H^+ y acidificación del catolito, o iii) difusión y reoxidación de productos líquidos en el ánodo (Endrődi et al., 2017). En este sentido, es fundamental resaltar también la configuración de ensamblaje membrana-electrodo (MEA), que se compone de una estructura tipo sándwich que consta de tres capas. En primer lugar, se encuentra una membrana de intercambio iónico, comúnmente una membrana de intercambio catiónico, cuya función principal es facilitar la transferencia de protones generados en el ánodo hacia el cátodo. Seguidamente, se sitúa el cátodo, donde se lleva a cabo la reducción del CO_2 . Por último, se encuentra el ánodo, compuesto por materiales activos que generan electrones y, en general, promueven la reacción de evolución de oxígeno (OER). Un aspecto relevante de esta configuración radica en la disminución de las limitaciones de transferencia de materia entre compartimentos a medida que se reduce la distancia entre los electrodos (Ampelli et al., 2012).

En este contexto, el grupo de investigación Desarrollo de Procesos Químicos y Control de Contaminantes (DePRO), liderado por el Prof. Ángel Irabien Gulías, del Departamento de Ingenierías Química y Biomolecular de la Universidad de Cantabria, cuenta con una amplia experiencia y trayectoria en el desarrollo de procesos de utilización de CO₂ mediante la vía electroquímica para la obtención de productos de alto valor añadido en modo continuo en celdas de flujo. Entre los principales antecedentes de este grupo destacan la Tesis Doctoral "*Electrorreducción de dióxido de carbono en fase gas para la producción de hidrocarburos*", realizada por el Dr. Iván Merino García y dirigida por el Prof. Ángel Irabien Gulías y el Dr. Jonathan Albo Sánchez, la Tesis Doctoral "*Valorización electroquímica de CO₂ para la producción de formiato en continuo usando electrodos de difusión de gas (GDEs)*", realizada por el Dr. Andrés del Castillo Martín y dirigida por el Prof. Ángel Irabien Gulías y el Dr. Manuel Álvarez Guerra, y, por último, la Tesis Doctoral "*Utilización de CO₂ por vía electroquímica: desarrollo de un proceso en continuo para la obtención de formiato con alta eficiencia*", realizada por el Dr. Guillermo Díaz Sainz y dirigida por el Prof. Ángel Irabien Gulías y el Dr. Manuel Alvarez Guerra. La presente Tesis Doctoral marca el comienzo de una nueva línea de investigación en el grupo, orientada a la fotoelectrorreducción de CO₂ en continuo mediante el uso de reactores de membrana.

1.2 Objetivos y estructura

La presente Tesis Doctoral se ha llevado a cabo en el marco de tres proyectos de investigación. Por un lado, el proyecto CTQ2013-48280-C3-1-R (MINECO/FEDER,UE) titulado "*Desarrollo e integración de procesos con membranas para la captura y valorización de dióxido de carbono*", subvencionado por el Ministerio de Economía y Competitividad, por otro lado, el proyecto CTQ2016-76231-C2-1-R (AEI/FEDER, UE) titulado "*Diseño multiescala de procesos de captura y utilización de dióxido de carbono*", subvencionado por el Ministerio de Ciencia, Innovación y Universidades, y por último, el proyecto PID2019-104050RA-I00 (AEI /10.13039/501100011033) titulado "*Conversión impulsada por la luz de CO₂ en combustibles utilizando reactores microfluídicos*", subvencionado por el Ministerio de Ciencia e Innovación. Estos proyectos cuentan con el liderazgo y la participación de los investigadores Dr. Jonathan Albo Sánchez y Dr. Guillermo Díaz Sainz, directores de la presente Tesis Doctoral y pertenecientes al grupo de investigación DePRO de la Universidad de Cantabria. Basado en el marco descrito, el objetivo general de la Tesis Doctoral es el análisis, diseño y optimización de un reactor fotoelectroquímico de membrana para la conversión en continuo de CO₂. Con el fin de alcanzar este objetivo principal, se plantean los siguientes objetivos específicos, los cuales son desarrollados en las publicaciones que conforman la Tesis Doctoral:

- Realizar una exhaustiva revisión bibliográfica sobre la valorización fotoelectroquímica de CO₂, prestando especial atención a las diferentes configuraciones de los reactores y

electrodos, los diferentes materiales fotoactivos empleados, así como los productos de reducción obtenidos.

- Diseñar la configuración y operación de un fotoelectroreactor de membrana y su funcionamiento en modo continuo. Para ello, se debe llevar a cabo el diseño y la puesta a punto de un sistema experimental versátil que permita operar con diferentes configuraciones de reactor y electrodos para la conversión de CO₂, tanto en fase líquida como en fase gas.
- Realizar experimentos cinéticos para analizar la influencia de variables clave en el proceso, como la intensidad de la luz suministrada, el voltaje externo aplicado, los caudales de electrolito y CO₂ utilizados, entre otros. Para ello, se ha utilizado TiO₂ como material fotoactivo en el ánodo (TiO₂-P25) y Cu en el cátodo a oscuras.
- Ampliar el estudio de empleo de materiales más allá de aquellos basados en TiO₂ comercial, explorando el funcionamiento de otros materiales semiconductores basados en TiO₂ con propiedades mejoradas, como son las nanopartículas de TiO₂ sintetizadas en medio supercrítico (TiO₂-SC).

De acuerdo con los objetivos específicos, y considerando la normativa vigente en la Universidad de Cantabria y en el Programa de Doctorado de la Ingeniería Química, de la Energía y de los Procesos para la elaboración de Tesis Doctorales por compendio de artículos previamente publicados, el presente trabajo se desarrolla en cuatro capítulos distribuidos de la siguiente forma:

- El **Capítulo 1**: que consiste en el planteamiento de la presente Tesis Doctoral, conteniendo el marco y los objetivos.
- El **Capítulo 2**: que describe la metodología experimental aplicada a lo largo de las diferentes partes que componen la Tesis Doctoral.
- El **Capítulo 3**: que supone el núcleo central de la Tesis Doctoral, incluyendo una copia de los artículos que la sustentan. Estos artículos se integran en el ya mencionado objetivo general de la Tesis Doctoral, incluyendo una revisión bibliográfica sobre la valorización fotoelectroquímica de CO₂ en la publicación "*Photoelectrochemical reactors for CO₂ utilization*", el diseño de la configuración del fotoelectroreactor de membrana y el funcionamiento en modo continuo con materiales basados en TiO₂, así como el estudio de la influencia de variables clave en el proceso con el trabajo "*Continuous conversion of CO₂ to alcohols in a TiO₂ photoanode-driven photoelectrochemical system*", y explorar el empleo de materiales basados en TiO₂ con propiedades mejoradas a través de la publicación "*Efficient photoelectrochemical conversion of CO₂ to ethylene and methanol using a Cu cathode and TiO₂ nanoparticles synthesized in supercritical medium as photoanode*".
- El **Capítulo 4**: que comprende un resumen global de los principales resultados junto con las conclusiones a las que se ha llegado a través de la elaboración de esta Tesis Doctoral.

1.3 Referencias del capítulo 1

- Ai, L., Ng, S. F., & Ong, W. J. (2022). Carbon dioxide electroreduction into formic acid and ethylene: a review. *Environmental Chemistry Letters*, 20, 3555–3612.
- Aminu, M. D., Nabavi, S. A., Rochelle, C. A., & Manovic, V. (2017). A review of developments in carbon dioxide storage. *Applied Energy*, 208, 1389–1419. <https://doi.org/10.1016/j.apenergy.2017.09.015>
- Ampelli, C., Genovese, C., Passalacqua, R., Perathoner, S., & Centi, G., (2012). The use of a solar photoelectrochemical reactor for sustainable production of energy. *Theoretical Foundations of Chemical Engineering*, 46, 651-657. <https://doi.org/10.1134/S0040579512060012>
- Ampelli, C., Tavella, F., Giusi, D., Ronsisvalle, A. M., Perathoner, S., & Centi, G. (2023). Electrode and cell design for CO₂ reduction: A viewpoint. *Catalysis Today*, 421, 114217. <https://doi.org/10.1016/J.CATTOD.2023.114217>
- Bharath, G., Rambabu, K., Hai, A., Ponpandian, N., Schmidt, J. E., Dionysiou, D. D., Abu Hajja, M., & Banat, F. (2021). Dual-functional paired photoelectrocatalytic system for the photocathodic reduction of CO₂ to fuels and the anodic oxidation of furfural to value-added chemicals. *Applied Catalysis B: Environmental*, 298, 120520. <https://doi.org/10.1016/J.APCATB.2021.120520>
- Bi, X., Wang, H., Yang, Z., Zhao, Y., Ma, Z., Liu, T., & Wu, M. (2022). Localized Surface Plasmon Resonance Enhanced Continuous Flow Photoelectrocatalytic CO₂ Conversion to CO. *Energy and Fuels*, 36, 7206–7212. <https://doi.org/10.1021/ACS.ENERGYFUELS.2C01520>
- Cheng, J., Zhang, M., Wu, G., Wang, X., Zhou, J., & Cen, K. (2014). Photoelectrocatalytic reduction of CO₂ into chemicals using Pt-modified reduced graphene oxide combined with Pt-modified TiO₂ nanotubes. *Environmental Science and Technology*, 48, 7076–7084. https://doi.org/10.1021/ES500364G/ASSET/IMAGES/ES-2014-00364G_M005.GIF
- Cheng, J., Zhang, M., Liu, J., Zhou, J., & Cen, K. (2015). A Cu foam cathode used as a Pt–RGO catalyst matrix to improve CO₂ reduction in a photoelectrocatalytic cell with a TiO₂ photoanode. *Journal of Materials Chemistry A*, 3, 12947–12957. <https://doi.org/10.1039/C5TA03026A>
- Cheng, J., Xuan, X., Yang, X., Zhou, J., & Cen, K. (2019). Selective reduction of CO₂ to alcohol products on octahedral catalyst of carbonized Cu(BTC) doped with Pd nanoparticles in a photoelectrochemical cell. *Chemical Engineering Journal*, 358, 860–868. <https://doi.org/10.1016/J.CEJ.2018.10.091>
- Cheng, J., Yang, X., Xuan, X. X., & Zhou, J. (2020). Efficient hybrid solar-to-alcohol system via synergistic catalysis between well-defined Cu–N₄ sites and its sulfide (CuS). *Chemical Engineering Journal*, 392, 123799. <https://doi.org/10.1016/J.CEJ.2019.123799>
- Comisión Europea (2023). Página web del Pacto Verde Europeo. [Consulta 10 de julio de 2023]. Disponible en: https://commission.europa.eu/strategy-and-policy/priorities-2019-2024/european-green-deal_es
- Cortes, M. A. L. R. M., McMichael, S., Hamilton, J. W. J., Sharma, P. K., Brown, A., & Byrne, J. A. (2020). Photoelectrochemical reduction of CO₂ with TiNT. *Materials Science in Semiconductor Processing*, 108, 104900. <https://doi.org/10.1016/j.mssp.2019.104900>

Creissen, C. E., Rivera de la Cruz, J. G., Karapinar, D., Taverna, D., Schreiber, M. W., & Fontecave, M. (2022). Molecular Inhibition for Selective CO₂ Conversion. *Angewandte Chemie International Edition*, 61, e202206279. <https://doi.org/10.1002/ANIE.202206279>

De Brito, J. F., Genovese, C., Tavella, F., Ampelli, C., Boldrin Zanoni, M. V., Centi, G., & Perathoner, S. (2019). CO₂ Reduction of Hybrid Cu₂O-Cu/Gas Diffusion Layer Electrodes and their Integration in a Cu-based Photoelectrocatalytic Cell. *ChemSusChem*, 12, 4274–4284. <https://doi.org/10.1002/CSSC.201901352>

De Brito, J. F. de, Bessegato, G. G., Perini, J. A. L., Torquato, L. D. de M., & Zanoni, M. V. B. (2022). Advances in photoelectroreduction of CO₂ to hydrocarbons fuels: Contributions of functional materials. *Journal of CO₂ Utilization*, 55, 101810. <https://doi.org/10.1016/J.JCOU.2021.101810>

Ding, P., Jiang, T., Han, N., & Li, Y. (2020). Photocathode engineering for efficient photoelectrochemical CO₂ reduction. *Materials Today Nano*, 10, 100077. <https://doi.org/10.1016/J.MTNANO.2020.100077>

Duan, Y. X., Cui, R. C., & Jiang, Q. (2023). Recent progress on the electroreduction of carbon dioxide to C1 liquid products. *Current Opinion in Electrochemistry*, 38, 101219. <https://doi.org/10.1016/J.COELC.2023.101219>

Endrődi, B., Bencsik, G., Darvas, F., Jones, R., Rajeshwar, K., & Janáky, C. (2017). Continuous-flow electroreduction of carbon dioxide. *Progress in Energy and Combustion Science*, 62, 133–154. <https://doi.org/10.1016/J.PECS.2017.05.005>

ESRL Global Monitoring Laboratory (2023). Página web de la oficina Nacional de Administración Oceánica y Atmosférica (NOAA, por sus siglas en inglés). [Consulta 10 de julio de 2023]. Disponible en: <https://www.esrl.noaa.gov/gmd/ccgg/trends/monthly.html>

Fernández-Caso, K., Díaz-Sainz, G., Alvarez-Guerra, M., & Irabien, A. (2023). Electroreduction of CO₂: Advances in the Continuous Production of Formic Acid and Formate. *ACS Energy Letters*, 8, 1992–2024. <https://doi.org/10.1021/acsenergylett.3c00489>

Genovese, C., Ampelli, C., Perathoner, S., & Centi, G. (2013). Electrocatalytic conversion of CO₂ to liquid fuels using nanocarbon-based electrodes. *Journal of Energy Chemistry*, 22, 202–213. [https://doi.org/10.1016/S2095-4956\(13\)60026-1](https://doi.org/10.1016/S2095-4956(13)60026-1)

Graves, C., Ebbesen, S. D., Mogensen, M., & Lackner, K. S. (2011). Sustainable hydrocarbon fuels by recycling CO₂ and H₂O with renewable or nuclear energy. *Renewable and Sustainable Energy Reviews*, 15, 1–23. <https://doi.org/10.1016/j.rser.2010.07.014>

Gurudayal, Bullock, J., Srankó, D. F., Towle, C. M., Lum, Y., Hettick, M., Scott, M. C., Javey, A., & Ager, J. (2017). Efficient solar-driven electrochemical CO₂ reduction to hydrocarbons and oxygenates. *Energy and Environmental Science*, 10, 2222–2230. <https://doi.org/10.1039/C7EE01764B>

Han, G. H., Bang, J., Park, G., Choe, S., Jang, Y. J., Jang, H. W., Kim, S. Y., & Ahn, S. H. (2023). Recent Advances in Electrochemical, Photochemical, and Photoelectrochemical Reduction of CO₂ to C₂⁺ Products. *Small*, 19, 2205765. <https://doi.org/10.1002/smll.202205765>

Hu, J., Fan, N., Chen, C., Wu, Y., Wei, Z., Xu, B., Peng, Y., Shen, M., & Fan, R. (2023). Facet engineering in Au nanoparticles buried in *p*-Si photocathodes for enhanced photoelectrochemical

CO₂ reduction. *Applied Catalysis B: Environmental*, 327, 122438. <https://doi.org/10.1016/J.APCATB.2023.122438>

Inoue, T., Fujishima, A., Konishi, S., & Honda, K. (1979). Photoelectrocatalytic reduction of carbon dioxide in aqueous suspensions of semiconductor powders. *Nature*, 277:5698, 277, 637–638. <https://doi.org/10.1038/277637a0>

International Energy Agency (2023)- World Energy Outlook, 2023. [Consulta 10 de julio de 2023). Disponible en: <https://www.iea.org/>

Irabien, A., Alvarez-Guerra, M., Albo, J., & Domínguez-Ramos, A. (2018). Electrochemical conversion of CO₂ to value-added products, in: Martínez-Huitle, C.A., Rodrigo, M.A., Scialdone, O., (Ed.), *Electrochemical Water and Wastewater Treatment*. Elsevier, pp. 29-59. <https://doi.org/10.1016/C2016-0-04297-3>

Isa, F., Rozali, N. E. M., Suleman, H., Maulud, A., & Shariff, A. M. (2019). Chemical Engineering Research and Design An overview on control strategies for CO₂ capture using absorption / stripping system. *Chemical Engineering Research and Design*, 147, 319–337. <https://doi.org/10.1016/j.cherd.2019.04.034>

Jiang, Z., Xiao, T., Kuznetsov, V. L., & Edwards, P. P. (2010). Turning carbon dioxide into fuel. *Philosophical Transactions of the Royal Society A: Mathematical, Physical and Engineering Sciences*, 368, 3343–3364. <https://doi.org/10.1098/rsta.2010.0119>

Jouny, M., Hutchings, G. S., & Jiao, F. (2019). Carbon monoxide electroreduction as an emerging platform for carbon utilization. *Nature Catalysis*, 2, 1062–1070. <https://doi.org/10.1038/s41929-019-0388-2>

Kang, M. J., Kim, C. W., Cha, H. G., Pawar, A. U., & Kang, Y. S. (2021). Selective liquid chemicals on CO₂ reduction by energy level tuned rGO/TiO₂ dark cathode with BiVO₄ photoanode. *Applied Catalysis B: Environmental*, 295, 120267. <https://doi.org/10.1016/J.APCATB.2021.120267>

Kibria, M. G., Edwards, J. P., Gabardo, C. M., Dinh, C. T., Seifitokaldani, A., Sinton, D., & Sargent, E. H. (2019). Electrochemical CO₂ Reduction into Chemical Feedstocks: From Mechanistic Electrocatalysis Models to System Design. *Advanced Materials*, 31, 1807166. <https://doi.org/10.1002/adma.201807166>

Kistler, T. A., Um, M. Y., Cooper, J. K., Sharp, I. D., & Agbo, P. (2021). Monolithic Photoelectrochemical CO₂ Reduction Producing Syngas at 10% Efficiency. *Advanced Energy Materials*, 11, 2100070. <https://doi.org/10.1002/AENM.202100070>

Kobayashi, K., Lou, S. N., Takatsuji, Y., Haruyama, T., Shimizu, Y., & Ohno, T. (2020). Photoelectrochemical reduction of CO₂ using a TiO₂ photoanode and a gas diffusion electrode modified with a metal phthalocyanine catalyst. *Electrochimica Acta*, 338, 135805. <https://doi.org/10.1016/J.ELECTACTA.2020.135805>

Kumar, B., Brian, J. P., Atla, V., Kumari, S., Bertram, K. A., White, R. T., & Spurgeon, J. M. (2016). New trends in the development of heterogeneous catalysts for electrochemical CO₂ reduction. *Catalysis Today*, 270, 19–30. <https://doi.org/10.1016/j.cattod.2016.02.006>

Kumar, A., Aeshala, L. M., & Palai, T. (2023). Electrochemical reduction of CO₂ to useful fuel: recent advances and prospects. *Journal of Applied Electrochemistry*, 53, 1295-1319. <https://doi.org/10.1007/s10800-023-01850-x>

Kutz, R. B., Chen, Q., Yang, H., Sajjad, S. D., Liu, Z., & Masel, I. R. (2017). Sustainion Imidazolium-Functionalized Polymers for Carbon Dioxide Electrolysis. *Energy Technology*, 5, 929–936. <https://doi.org/10.1002/ENTE.201600636>

Li, K., Han, J., Yang, Y., Wang, T., Feng, Y., Ajmal, S., Liu, Y., Deng, Y., Tahir, M. A., & Zhang, L. (2019). Simultaneous SO₂ removal and CO₂ reduction in a nano-BiVO₄|Cu-In nanoalloy photoelectrochemical cell. *Chemical Engineering Journal*, 355, 11–21. <https://doi.org/10.1016/J.CEJ.2018.08.093>

Lin, J., Zhang, Y., Xu, P., & Chen, L. (2023). CO₂ electrolysis: Advances and challenges in electrocatalyst engineering and reactor design. *Materials Reports: Energy*, 3, 100194. <https://doi.org/10.1016/j.matre.2023.100194>

Liu, L., Zhang, Y., & Huang, H. (2021). Junction Engineering for Photocatalytic and Photoelectrocatalytic CO₂ Reduction. *Solar RRL*, 5, 2000430. <https://doi.org/10.1002/SOLR.202000430>

Liu, B., Wang, T., Wang, S., Zhang, G., Zhong, D., Yuan, T., Dong, H., Wu, B., & Gong, J. (2022). Back-illuminated photoelectrochemical flow cell for efficient CO₂ reduction. *Nature Communications*, 13, 7111. <https://doi.org/10.1038/s41467-022-34926-x>

Liu, Y., Xia, M., Ren, D., Nussbaum, S., Yum, J. H., Grätzel, M., Guijarro, N., & Sivula, K. (2023). Photoelectrochemical CO₂ Reduction at a Direct CuInGaS₂/Electrolyte Junction. *ACS Energy Letters*, 8, 1645–1651. https://doi.org/10.1021/ACSENERGYLETT.3C00022/ASSET/IMAGES/LARGE/NZ3C00022_0004.JPEG

Lu, W., Zhang, Y., Zhang, J., & Xu, P. (2020). Reduction of Gas CO₂ to CO with High Selectivity by Ag Nanocube-Based Membrane Cathodes in a Photoelectrochemical System. *Industrial and Engineering Chemistry Research*, 59 (13), 5536–5545. <https://doi.org/10.1021/ACS.IECR.9B06052>

Marco Estratégico de Energía y Clima (2023). Estrategia de descarbonización a largo 2050. [Consulta 10 de julio de 2023]. Disponible en: https://ec.europa.eu/clima/sites/lts/lts_es_es.pdf

Merino-Garcia, I., Alvarez-Guerra, E., Albo, J., & Irabien, A. (2016). Electrochemical membrane reactors for the utilisation of carbon dioxide. *Chemical Engineering Journal*, 305, 104–120. <https://doi.org/10.1016/J.CEJ.2016.05.032>

Minggu, L. J., Salehmin, M. N. I., Mohamed, M. A., Arifin, K., Yunus, R. M., & Kassim, M. B. (2020). A low overpotential photoelectrochemical reduction of carbon dioxide to methanol with highly photoactive hierarchical structured cuprous oxide. *Ceramics International*, 46, 26004–26016. <https://doi.org/10.1016/J.CERAMINT.2020.07.091>

Montoya, J. H., Seitz, L. C., Chakthranont, P., Vojvodic, A., Jaramillo, T. F., & Nørskov, J. K. (2016). Materials for solar fuels and chemicals. *Nature Materials*, 16, 70–81. <https://doi.org/10.1038/NMAT4778>

Mustafa, A., Lougou, B. G., Shuai, Y., Wang, Z., & Tan, H. (2020). Current technology development for CO₂ utilization into solar fuels and chemicals: A review. *Journal of Energy Chemistry*, 49, 96–123. <https://doi.org/10.1016/j.jechem.2020.01.023>

Naciones Unidas (2023). Página web de la Organización de las Naciones Unidas (UN, por sus siglas en inglés). [Consulta 10 de julio de 2023]. Disponible en: <https://www.un.org/es/>

Nandal, N., & Jain, S. L. (2022). A review on progress and perspective of molecular catalysis in photoelectrochemical reduction of CO₂. *Coordination Chemistry Reviews*, 451, 214271. <https://doi.org/10.1016/J.CCR.2021.214271>

Objetivos y metas de desarrollo sostenible (2023). Página web de los objetivos del Desarrollo Sostenible (ODS, por sus siglas en inglés). [Consulta 10 de julio de 2023]. Disponible en: <https://www.un.org/sustainabledevelopment/es/objetivos-de-desarrollo-sostenible/>

Ochedi, F. O., Liu, D., Yu, J., Hussain, A., & Liu, Y. (2021). Photocatalytic, electrocatalytic and photoelectrocatalytic conversion of carbon dioxide: a review. *Environmental Chemistry Letters*, 19, 941–967. <https://doi.org/10.1007/S10311-020-01131-5>

Okoye-Chine, C. G., Otun, K., Shiba, N., Rashama, C., Ugwu, S. N., Onyeaka, H., & Okeke, C. T. (2022). Conversion of carbon dioxide into fuels - A review. *Journal of CO₂ Utilization*, 62, 102099. <https://doi.org/10.1016/j.jcou.2022.102099>

Ola, O., & Maroto-Valer, M. M. (2015). Review of material design and reactor engineering on TiO₂ photocatalysis for CO₂ reduction. *Journal of Photochemistry and Photobiology C: Photochemistry Reviews*, 24, 16–42. <https://doi.org/10.1016/J.JPHOTOCHEMREV.2015.06.001>

Otgongbayar, Z., Yoon, C. M., & Oh, W. C. (2023). Photoelectrocatalytic CO₂ reduction with ternary nanocomposite of MXene (Ti₃C₂)-Cu₂O-Fe₃O₄: Comprehensive utilization of electrolyte and light-wavelength. *Chemical Engineering Journal*, 464, 142716. <https://doi.org/10.1016/J.CEJ.2023.142716>

Pitchaimuthu, S., Sridharan, K., Nagarajan, S., Ananthraj, S., Robertson, P., Kuehnel, M. F., Irabien, Á., & Maroto-Valer, M. (2022). Solar Hydrogen Fuel Generation from Wastewater—Beyond Photoelectrochemical Water Splitting: A Perspective. *Energies*, 15, 7399. <https://doi.org/10.3390/EN15197399>

Rahaman, M., Andrei, V., Pornrungroj, C., Wright, D., Baumberg, J. J., & Reisner, E. (2020). Selective CO production from aqueous CO₂ using a Cu₉₆In₄ catalyst and its integration into a bias-free solar perovskite–BiVO₄ tandem device. *Energy & Environmental Science*, 13, 3536–3543. <https://doi.org/10.1039/D0EE01279C>

Seitz, L. C., Dickens, C. F., Nishio, K., Hikita, Y., Montoya, J., Doyle, A., Kirk, C., Vojvodic, A., Hwang, H. Y., Norskov, J. K., & Jaramillo, T. F. (2016). A highly active and stable IrO_x/SrIrO₃ catalyst for the Oxygen evolution reaction. *Science*, 353, 1011–1014. <https://doi.org/10.1126/science.aaf5050>

Styring, P., Quadrelli, E.A., & Armstrong, K. (2014). Carbon Dioxide Utilisation: Closing the Carbon Cycle. ISBN 9780444627469.

Tang, B., & Xiao, F. X. (2022). An Overview of Solar-Driven Photoelectrochemical CO₂ Conversion to Chemical Fuels. *ACS Catalysis*, 12, 9023–9057. <https://doi.org/10.1021/ACSCATAL.2C01667>

Tarek, M., Rezaul Karim, K. M., Sarkar, S. M., Deb, A., Ong, H. R., Abdullah, H., Cheng, C. K., & Rahman Khan, M. M. (2019). Hetero-structure CdS–CuFe₂O₄ as an efficient visible light active photocatalyst for photoelectrochemical reduction of CO₂ to methanol. *International Journal of Hydrogen Energy*, 44, 26271–26284. <https://doi.org/10.1016/J.IJHYDENE.2019.08.074>

The Intergovernmental Panel on Climate Change (**2023**). Página web del Panel Intergubernamental del Cambio Climático (IPPC, por sus siglas en inglés). [Consulta el 10 de julio de 2023]. Disponible en: <https://www.ipcc.ch/>

Vadillo, J. M., Díaz-Sainz, G., Gómez-Coma, L., Garea, A., & Irabien, A. (**2022a**). Chemical and Physical Ionic Liquids in CO₂ Capture System Using Membrane Vacuum Regeneration. *Membranes*, *12*, 785. <https://doi.org/10.3390/membranes12080785>

Vadillo, J.M., Gomez-Coma, L., Garea, A., & Irabien, A. (**2022b**). Non-dispersive CO₂ separation process using vacuum desorption and ionic liquids as carbon capture and utilization innovative technology. *Separation and Purification Technology*, *301*, 121923. <https://doi.org/10.1016/j.seppur.2022.121923>

Verma, S., & Yadav, A. (**2023**). Emerging Single-Atom Catalysts and Nanomaterials for Photoelectrochemical Reduction of Carbon Dioxide to Value-Added Products: A Review of the Current State-of-the-Art and Future Perspectives. *Energy and Fuels*, *37*, 5712-5742 [https://doi.org/10.1021/ACS.ENERGYFUELS.3C00311/ASSET/IMAGES/LARGE/EF3C00311_0024.JPG](https://doi.org/10.1021/ACS.ENERGYFUELS.3C00311/ASSET/IMAGES/LARGE/EF3C00311_0024.JPEG)

Wang, Y., He, D., Chen, H., & Wang, D. (**2019**). Catalysts in electro-, photo- and photoelectrocatalytic CO₂ reduction reactions. *Journal of Photochemistry and Photobiology C: Photochemistry Reviews*, *40*, 117–149. <https://doi.org/10.1016/J.JPHOTOCHEMREV.2019.02.002>

Wang, Y., Zhu, Y., Sun, L., & Li, F. (**2020**). Selective CO Production by Photoelectrochemical CO₂ Reduction in an Aqueous Solution with Cobalt-Based Molecular Redox Catalysts. *ACS Applied Materials and Interfaces*, *12*(37), 41644–41648. <https://doi.org/10.1021/ACSMI.0C14533>

Wang, K., Liu, Y., Wang, Q., Zhang, Y., Yang, X., Chen, L., Liu, M., Qiu, X., Li, J., & Li, W. (**2022**). Asymmetric Cu-N sites on copper oxide photocathode for photoelectrochemical CO₂ reduction towards C₂ products. *Applied Catalysis B: Environmental*, *316*, 121616 <https://doi.org/10.1016/J.APCATB.2022.121616>

Xie, S., Zhang, Q., Liu, G., & Wang, Y. (**2015**). Photocatalytic and photoelectrocatalytic reduction of CO₂ using heterogeneous catalysts with controlled nanostructures. *Chemical Communications*, *52*(1), 35–59. <https://doi.org/10.1039/C5CC07613G>

Yaashikaa, P. R., Senthil Kumar, P., Varjani, S. J., & Saravanan, A. (**2019**). A review on photochemical, biochemical and electrochemical transformation of CO₂ into value-added products. *Journal of CO₂ Utilization*, *33*, 131–147. <https://doi.org/10.1016/j.jcou.2019.05.017>

Zhang, H., Chen, Y., Wang, H., Wang, H., Ma, W., Zong, X., & Li, C. (**2020a**). Carbon Encapsulation of Organic–Inorganic Hybrid Perovskite toward Efficient and Stable Photo-Electrochemical Carbon Dioxide Reduction. *Advanced Energy Materials*, *10*, 2002105. <https://doi.org/10.1002/AENM.202002105>

Zhang, M., Xuan, X., Wang, W., Ma, C., Lin, Z., Zhang, M., Wang, W., Ma, C., Lin, Z., & Xuan, X. (**2020b**). Anode Photovoltage Compensation-Enabled Synergistic CO₂ Photoelectrocatalytic Reduction on a Flower-Like Graphene-Decorated Cu Foam Cathode. *Advanced Functional Materials*, *30*, 2005983. <https://doi.org/10.1002/ADFM.202005983>

Zhang, L., & Wang, Y. (**2023**). Decoupled Artificial Photosynthesis. *Angewandte Chemie International Edition*, *62*, e202219076. <https://doi.org/10.1002/ANIE.202219076>

Zheng, H., Yang, Z., Kong, X., Geng, Z., & Zeng, J. (2022). Progresses on carbon dioxide electroreduction into methane. *Chinese Journal of Catalysis*, 43, 1634–1641. [https://doi.org/10.1016/S1872-2067\(21\)63967-0](https://doi.org/10.1016/S1872-2067(21)63967-0)

Zhou, X., Liu, R., Sun, K., Chen, Y., Verlage, E., Francis, S. A., Lewis, N. S., & Xiang, C. (2016). Solar-Driven Reduction of 1 atm of CO₂ to Formate at 10% Energy-Conversion Efficiency by Use of a TiO₂-Protected III-V Tandem Photoanode in Conjunction with a Bipolar Membrane and a Pd/C Cathode. *ACS Energy Letters*, 1, 764–770. <https://doi.org/10.1021/acsenergylett.6b00317>

Metodología

CAPÍTULO 2. METODOLOGÍA

Este capítulo proporciona una descripción detallada de los materiales empleados, del sistema experimental, y los procedimientos utilizados a lo largo de la Tesis Doctoral.

2.1 Síntesis y caracterización de nanopartículas de TiO₂

La síntesis de nanopartículas de TiO₂ en CO₂ supercrítico (TiO₂-SC) se ha llevado a cabo utilizando un sistema experimental diseñado específicamente en el Departamento de Ingeniería Química de la Universidad de Castilla-La Mancha (Camarillo et al., 2017), con el que el grupo DePRO de la Universidad de Cantabria ha establecido una colaboración a lo largo de los últimos años. El sistema experimental consta de un baño termostático, una bomba de alta presión y un reactor de síntesis de alta presión como componentes principales. Las nanopartículas de TiO₂ se obtienen mediante la hidrólisis térmica del isopropóxido de titanio (TTIP), como precursor, utilizando etanol como disolvente y CO₂ supercrítico como medio de reacción. Las condiciones de síntesis fueron una presión de 20 MPa, una temperatura de 300 °C, una relación molar de 28 mmol de precursor por mmol de alcohol y un tiempo de reacción de 2 horas. Una vez finalizado el procedimiento de síntesis, los sólidos obtenidos se extrajeron del reactor y se secaron a 105 °C durante 12 horas para asegurar la total eliminación de agua. Posteriormente, el material se somete a una calcinación a 400 °C durante 6 horas para eliminar impurezas de carbono y aumentar la cristalinidad del TiO₂. Se utiliza, además, como material comercial de referencia, TiO₂-P25 (Sigma, Aldrich, P25), con un tamaño de partícula promedio de 21 nm.

Los materiales fotoactivos se caracterizan mediante diversas técnicas. Estas técnicas incluyen microscopía electrónica de barrido (SEM) para analizar la morfología y la composición atómica, difracción de rayos X (XRD) para identificar las caras expuestas y la composición de los diferentes elementos presentes, y al mismo tiempo, comprobar la eficiencia en el proceso de síntesis, análisis BET para determinar la superficie del catalizador y espectroscopia infrarroja transformada de Fourier (FTIR) para analizar la composición de los materiales. Para medir las propiedades ópticas, se utiliza un espectrómetro Cary 6000i con una esfera integradora para mediciones de espectroscopia de reflectancia difusa (DRS) en el rango UV-Vis-NIR, y un fluorómetro de doble rejilla FLSP 920 de Edinburgh Instruments equipado con una lámpara de xenón y un tubo fotomultiplicador Hamamatsu R928. Estos instrumentos permiten realizar el análisis de fotoluminiscencia (PL) tanto de emisión como de excitación, lo que permite estudiar las propiedades ópticas tanto de TiO₂-SC como de TiO₂-P25.

2.2 Fabricación de los fotoánodos

Para el desarrollo de los fotoánodos, se emplea la técnica de aerografía manual con una tinta compuesta por una mezcla del catalizador de TiO_2 , Nafion (Alfa Aesar, 5% en peso) como aglutinante e isopropanol (99,5%, Sigma Aldrich) como disolvente. La relación mísica entre el TiO_2 y el Nafion es de 70:30, con un porcentaje en peso de sólidos (TiO_2 y Nafion) del 3% (97% en peso de isopropanol). La tinta se introduce en un baño de ultrasonidos durante 30 minutos antes de ser depositada sobre el papel de carbono Toray (TGP-H60).

El proceso se lleva a cabo sobre una placa calefactora a 100 °C, para favorecer la evaporación del isopropanol. Posteriormente, el fotoánodo de TiO_2 (carga catalítica entre 1 y 3 $\text{mg}\cdot\text{cm}^{-2}$) se acopla mediante prensado en caliente con una membrana de intercambio catiónica de Nafion (Nafion 117). Esta membrane se activa en HCl durante 30 minutos y, posteriormente, se enjuaga con agua desionizada antes de su uso, formando un ensamblaje membrana-electrodo (MEA) capaz de mejorar el transporte de cargas y reducir las limitaciones a la transferencia de materia (Albo et al., 2017; Merino-Garcia et al., 2017).

2.3 Caracterización fotoelectroquímica y fisicoquímica de los fotoánodos

Las propiedades PEC de los fotoánodos se determinan, en primer lugar, mediante voltamperometría de barrido lineal (LSV), tanto con iluminación de luz LED como sin ella, mientras se alimenta continuamente CO_2 al reactor en un rango de potenciales de entre -1,2 y -2 V (vs. Ag/AgCl). Además, se investiga el comportamiento de los fotoánodos de TiO_2 mediante ensayos de cronoamperometría a una velocidad de escaneo de $50 \text{ mV}\cdot\text{s}^{-1}$ después de 20 ciclos, con y sin iluminación.

Adicionalmente, las superficies se caracterizan mediante difracción de rayos X (XRD) utilizando un difractómetro de polvo (Phillips X'Pert MDP). Esta caracterización se lleva a cabo antes y después de 150 minutos de operación continua bajo radiación, con el objetivo de determinar la composición y cristalinidad de los materiales, así como su estabilidad.

2.4 Sistema experimental para la fotoelectroreducción de CO_2

La fotoelectroreducción de CO_2 en continuo se lleva a cabo en un reactor electroquímico de tipo filtro prensa comercial (Electrocell A/S, Dinamarca) que se adapta con tapas transparentes para poder ser iluminado en ambos compartimentos. La Figura 2.1 muestra una vista detallada de la configuración de la celda, mientras que la Figura 2.2. muestra un esquema del sistema experimental. Este sistema incluye cuatro tanques, para las disoluciones electrolíticas de entrada y salida, dos bombas peristálticas para circular el líquido a un caudal de $10 \text{ mL}\cdot\text{min}^{-1}$, dos

indicadores de presión y controladores de caudal másico para fijar el caudal de entrada de CO₂ en 180 mL·min⁻¹. Además, se utiliza un potenciómetro (AutoLabPGSTAT 302N) para controlar el potencial aplicado y medir la densidad de corriente generada.

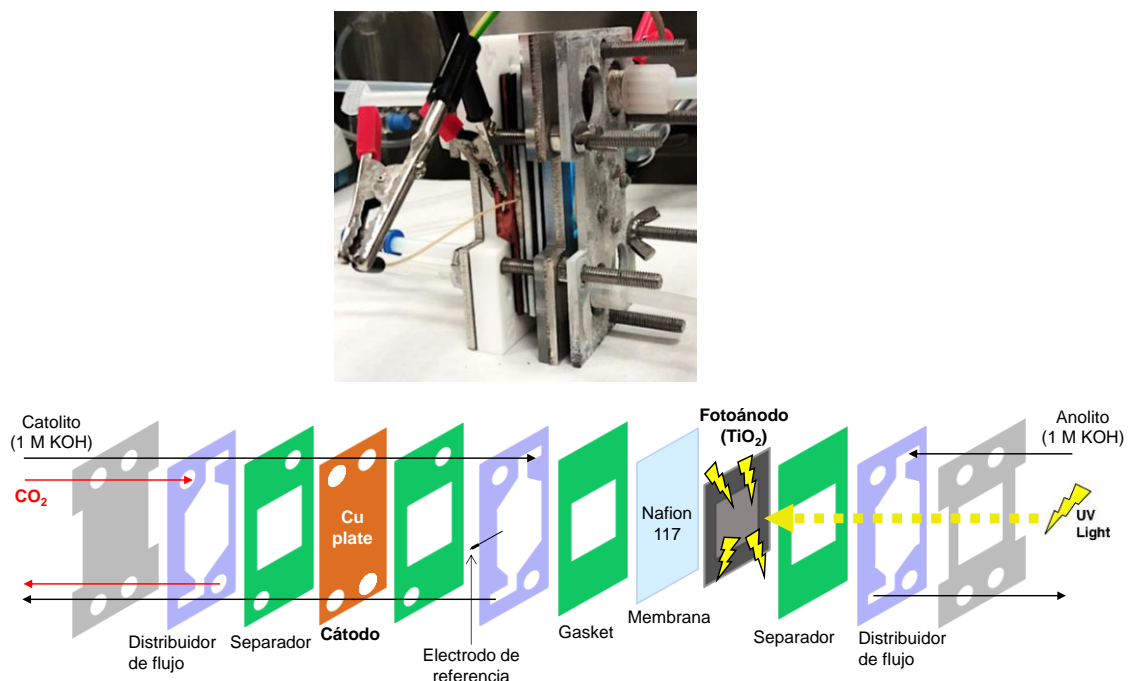


Figura 2.1. Reactor PEC de tipo filtro prensa iluminado (arriba) y esquema gráfico de los componentes internos de la celda (abajo).

Se emplea una placa de Cu como cátodo y los diferentes MEAs preparados como fotoánodos, que actúan como separador de los compartimentos de la celda PEC. Como catolito y anolito, se utiliza una disolución acuosa de 1 mol·L⁻¹ de KOH, y una fuente de luz LED UV fría (365 nm) para iluminar el área fotoactiva (10 cm²) del fotoánodo. La intensidad de la luz se mide con un radiómetro (Fotorradiómetro Delta OMH) y se controla ajustando la intensidad del LED y la distancia entre el microreactor y el LED.

En el lado del cátodo, hay dos entradas: el catolito y la alimentación gaseosa de CO₂; y una salida: el catolito con los productos de reacción (líquidos y gaseosos). La placa de Cu actúa como electrodo de trabajo, el fotoelectrodo de TiO₂ como contraelectrodo y Ag/AgCl (1 mm) como electrodo de referencia. La placa de Cu se limpia antes de cada experimento con una solución de HCl (37%) para garantizar que Cu(0) sea la especie mayoritaria (Kim et al., 1988). La reducción de CO₂ se realiza en condiciones ambientales.

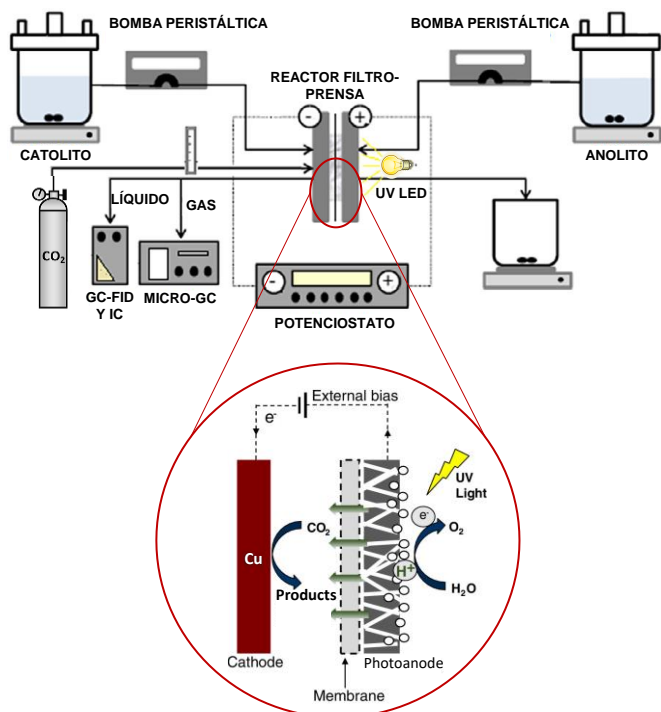


Figura 2.2. Sistema experimental para la conversión PEC de CO_2 en continuo que incluye una representación esquemática de la configuración fotoánodo (MEA)/cátodo a oscuras.

Los ensayos fotoelectroquímicos de reducción de CO_2 se llevan a cabo al menos por duplicado en modo continuo durante 50 minutos, cuando se alcanza un rendimiento pseudoestable. Las muestras de gas y líquido se toman a la salida del reactor (compartimento catódico) cada 10 minutos para calcular la concentración del producto a la salida. Se utiliza un cromatógrafo de gases (GCMSQP2010 Ultra, Shimadzu) equipado con un detector de ionización de llama (GC-FID) para medir la formación de productos líquidos, como alcoholes. La producción de formiato en fase líquida también se analiza mediante cromatografía iónica (IC, Dionex ICS 1100). Además, se miden muestras gaseosas utilizando un microcromatógrafo de gases instalado en línea (3000 Micro GC, Inficon). Se descartan los resultados de concentración dos veces por debajo o por encima del valor promedio para, posteriormente, calcular las principales figuras de méritos.

2.5 Figuras de mérito

El funcionamiento del proceso se evalúa teniendo en cuenta las siguientes figuras de mérito: (i) velocidad de formación de productos, (ii) eficiencia Faradaica (EF), (iii) eficiencia energética (EE) y (iv) eficiencia de conversión de energía solar en productos (STF, *Solar-to-fuel*, en inglés).

En primer lugar, la velocidad de formación de productos se define como los moles de producto obtenidos por unidad de tiempo y unidad de área geométrica de electrodo, como se muestra en la ecuación 2.1:

$$\text{Velocidad de producción } (\mu\text{mol} \cdot \text{m}^{-2} \cdot \text{s}^{-1}) = \frac{n}{A \cdot t} \quad (\text{Ecuación 2.1})$$

Donde n es el número de moles de producto generado (μmol producto), A es el área geométrica de electrodo (m^2) y t es el tiempo total del experimento (s).

Por otro lado, la EF expresa el porcentaje de la energía total suministrada que se ha utilizado para obtener el producto deseado. Se puede calcular utilizando la ecuación 2.2:

$$EF (\%) = \frac{z \cdot n \cdot F}{Q \cdot t} \cdot 100 \quad (\text{Ecuación 2.2})$$

Donde z es la relación entre el número de electrones intercambiados en el proceso de reducción de CO_2 y el número de moles de producto generado ($\text{mol electrones} \cdot \text{mol producto}^{-1}$), n es el número de moles de producto generado (mol producto), F es la constante de Faraday ($96.485 \text{ C} \cdot \text{mol electrones}^{-1}$), Q es la carga total aplicada en el sistema (A) y t es el tiempo total del experimento (s).

La EE se define como el porcentaje de la energía total utilizada para la formación de un determinado producto, de acuerdo a la ecuación 2.3:

$$EE (\%) = \frac{E_t}{E} \cdot EF \quad (\text{Ecuación 2.3})$$

Donde E es el potencial externo aplicado (V), E_t representa el voltaje teórico necesario para la formación de cada producto y EF es la eficiencia Faradaica. Los potenciales teóricos para el etileno y el metanol (V vs. Ag/AgCl a pH 7) son $-0,539 \text{ V}$ y $-0,589 \text{ V}$, respectivamente (Irabien et al., 2018).

Por último, STF representa la eficiencia del proceso para la generación de productos utilizando la luz de acuerdo a la Ecuación 2.4:

$$STF (\%) = \frac{P_{f,o} + P_{e,o}}{P_S + P_{e,i}} = \frac{I_{op} \cdot E_{f,o} \cdot EF}{P_S + P_{e,i}} \quad (\text{Ecuación 2.4})$$

Donde $P_{f,o}$ es la potencia de salida contenida en el combustible químico (W), $P_{e,o}$ es la potencia de salida en forma de electricidad (W), P_S es la potencia de entrada por radiación solar y $P_{e,i}$ es la entrada externa de potencia eléctrica (W). Además, I_{op} es la corriente operativa (A), $E_{f,o}$ es la diferencia de potencial (V) entre las dos semirreacciones (es decir, el producto de reducción de CO_2 y el O_2 de la oxidación del agua) y EF es la eficiencia Faradaica.

2.6 Referencias del capítulo 2

Albo, J., Vallejo, D., Beobide, G., Castillo, O., Castaño, P., & Irabien, A. (2017). Copper-Based Metal–Organic Porous Materials for CO₂ Electrocatalytic Reduction to Alcohols. *ChemSusChem*, 10, 1100–1109. <https://doi.org/10.1002/cssc.201600693>

Camarillo, R., Tostón, S., Martínez, F., Jiménez, C., & Rincón, J. (2017). Preparation of TiO₂-based catalysts with supercritical fluid technology: characterization and photocatalytic activity in CO₂ reduction. *Journal of Chemical Technology & Biotechnology*, 92, 1710–1720. <https://doi.org/10.1002/JCTB.5169>

Irabien, A., Alvarez-Guerra, M., Albo, J., & Domínguez-Ramos, A. (2018). Electrochemical conversion of CO₂ to value-added products, in: Martínez-Huitle, C.A., Rodrigo, M.A., Scialdone, O., (Ed.), *Electrochemical Water and Wastewater Treatment*. Elsevier, pp. 29-59. <https://doi.org/10.1016/C2016-0-04297-3>

Kim, J. J., Summers, D. P., & Frese, K. W. (1988). Reduction of CO₂ and CO to methane on Cu foil electrodes. *Journal of Electroanalytical Chemistry and Interfacial Electrochemistry*, 245, 223–244. [https://doi.org/10.1016/0022-0728\(88\)80071-8](https://doi.org/10.1016/0022-0728(88)80071-8)

Merino-Garcia, I., Albo, J., & Irabien, A. (2017). Productivity and Selectivity of Gas-Phase CO₂ Electroreduction to Methane at Copper Nanoparticle-Based Electrodes. *Energy Technology*, 5, 922–928. <https://doi.org/10.1002/ente.201600616>

Artículos científicos

CAPÍTULO 3. ARTÍCULOS CIENTÍFICOS

A continuación, se presentan los artículos científicos publicados que forman parte de la Tesis Doctoral, junto con sus correspondientes resúmenes en español.

3.1. Sergio Castro, Jonathan Albo, Ángel Irabien. 2018. Photoelectrochemical reactors for CO₂ utilization. ACS Sustainable Chemistry & Engineering, 6, 12, 15877-15894.

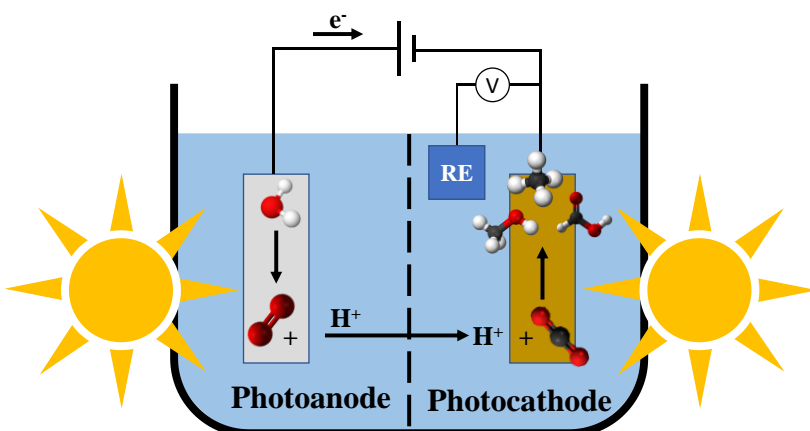


Figura 3.1. Resumen gráfico del artículo: "Photoelectrochemical reactors for CO₂ utilization".

Este artículo de revisión se centra en la reducción fotoelectroquímica de CO₂ utilizando energía solar para la producción sostenible de combustibles y productos químicos de alto valor añadido. Esta línea de investigación ha despertado un gran interés recientemente entre la comunidad científica, debido a su potencial para contribuir a resolver los problemas asociados al calentamiento global. Los esfuerzos de investigación realizados hasta la fecha se han centrado en el desarrollo de materiales activos, prestando una menor atención a la influencia de la configuración del reactor y electrodos en el rendimiento del proceso. Por lo tanto, el objetivo de esta revisión es proporcionar un análisis exhaustivo de la fotoelectroreducción de CO₂, centrándose en las celdas fotoelectroquímicas y fotoelectrodos empleados, así como en los materiales fotoactivos utilizados y los productos obtenidos para cada configuración, considerando las variables clave en el proceso. Así, la revisión se estructura de la siguiente manera: (i) configuraciones de reactores fotoelectroquímicos, (ii) materiales empleados para los fotoelectrodos, (iii) principales productos de reducción, y (iv) conclusiones y desafíos futuros. El objetivo final es recopilar toda la información disponible hasta la fecha y avanzar hacia la aplicación práctica de la fotoelectrocatalisis para la conversión de CO₂.

El diseño de un reactor fotoelectroquímico debe basarse en una cuidadosa evaluación de diversos factores, como es la fuente de luz, la configuración geométrica, el material de construcción, el intercambio de calor, las características de mezcla y las características de flujo,

entre otros. Dos de los parámetros clave del proceso son las fases involucradas y el modo de operación (discontinuo, semidiscontinuo y continuo). El ánodo y el cátodo deben estar, preferiblemente, en forma de películas delgadas separadas por una membrana conductora de protones y depositadas sobre sustratos porosos. Esto permite un transporte y separación eficiente de electrones. Para una fotoconversión de CO₂ eficiente, se necesita también de la reacción de evolución del oxígeno en el lado del ánodo, así como una apropiada difusión de CO₂ en el lado del cátodo.

En los últimos años se está empleando mayoritariamente la configuración fotoánodo con un cátodo a oscuras debido a los beneficios de utilizar semiconductores de tipo *n*, que son más abundantes, económicos y estables para la oxidación de H₂O, en lugar de semiconductores tipo *p*. Otra opción de creciente interés es la aplicación de un sistema compuesto de un fotocátodo y un ánodo en ausencia de luz. El fotocátodo está compuesto por un semiconductor de tipo *p* debido a su alta energía de banda de conducción adecuada para la reducción de CO₂, pero su eficiencia es limitada. Finalmente, el empleo de un material semiconductor tipo *p* para la reducción de CO₂ en el fotocátodo con un fotoánodo basado en un semiconductor tipo *n* para la oxidación de H₂O, donde idealmente puede no ser necesario la aplicación de energía externa, salvo la luz.

En resumen, la reducción photoelectrocatalítica del CO₂ es una solución tecnológica prometedora que combina las ventajas de la electrocatálisis y la fotocatálisis, reduciendo el voltaje necesario en electrocatálisis para convertir el CO₂ en productos útiles. Sin duda, aún existen grandes retos por resolver antes de que estos procesos tengan aplicación práctica real, pero esta tecnología presenta un gran potencial para alcanzar una mayor eficiencia en la reducción de CO₂ mediante el empleo de energía solar.

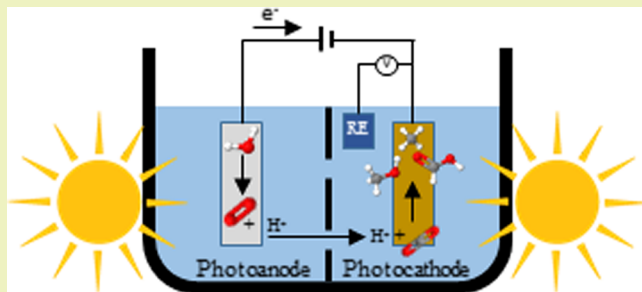
Photoelectrochemical Reactors for CO₂ Utilization

Sergio Castro,*^{ID} Jonathan Albo,^{ID} and Angel Irabien

Department of Chemical & Biomolecular Engineering, University of Cantabria, Avda. Los Castros s/n, 39005 Santander, Spain

ABSTRACT: The photoelectrochemical reduction of CO₂ to renewable fuels and valuable chemicals using solar energy is a research topic that has attracted great attention recently due to its potential to provide value-added products under the Sun, solving the issues related to global warming at the same time. This review covers the main research efforts made on the photoelectrochemical reduction of CO₂. Particularly, the study focuses in the configuration of the applied reactor, which is a topic scarcely explored in the literature. This includes the main materials used as photoelectrodes and their configuration in the photoelectrochemical reactor, which are discussed for technical uses. The review provides an overview of the state-of-the-art processes and aims to help in the development of enhanced photoelectroreactors for an efficient CO₂ utilization.

KEYWORDS: Photoelectrocatalysis, CO₂ reduction, Reactor configurations, Photoelectrodes, Climate change



INTRODUCTION

The reduction of fossil fuels and the growing emission of carbon dioxide (CO₂) have accelerated research activities to produce fuels and chemicals from wasted CO₂ as a carbon source. CO₂ can be considered an unlimited, renewable, and valuable carbon source instead of a greenhouse gas emission. However, due to the chemical properties of CO₂, its transformation requires a high level of energy since the bond dissociation energy of C=O is ~750 kJ·mol⁻¹, higher than other chemical bonds such as C—H (~430 kJ·mol⁻¹) and C—C (~336 kJ·mol⁻¹).¹ Nowadays, there are several technologies able to chemically reduce CO₂ to value-added products, among them, thermochemical processes (i.e., hydrogenation, reforming), mineralization, electrochemical reduction, and photo/photoelectrochemical reduction.² Compared to thermochemical processes, mineralization processes present limitations that should be solved through further technological developments due to the low carbonation rates, high cost, and energy penalties. It is also possible to dissociate CO₂ and H₂O by thermolysis at extremely high temperatures. Electrochemical processes, however, permit dissociation to H₂O or CO₂ at ambient conditions using electricity and have attracted worldwide interest due to their potential environmental and economic benefits.³ This technology not only offers a viable route to reuse CO₂ but also an excellent alternative to store intermittent energy from renewable sources in the form of chemical bonds.^{4,5} When electrochemical reduction integrates a light source, a photoelectrochemical device is obtained, which has attracted intense progress in recent years.^{6,7} In principle, such integration reduces the system capital cost and enables higher efficiency by reducing losses in transporting electricity to the electrolysis cell, eliminating current collectors and interconnections between devices. The operation of a photoelectrochemical (PEC) cell is inspired by natural

photosynthesis in which carbohydrates are formed from CO₂. The goal is to use excited electrons that are generated when the semiconductor absorbs light to effect electrochemistry on a redox couple strategically chosen to produce the desired chemicals.⁸

The concept of a photoelectrochemical cell is comparable to a conventional electrochemical cell, except that energy necessary to cause redox reactions is partially provided by the light. This concept is represented in Figure 1. A

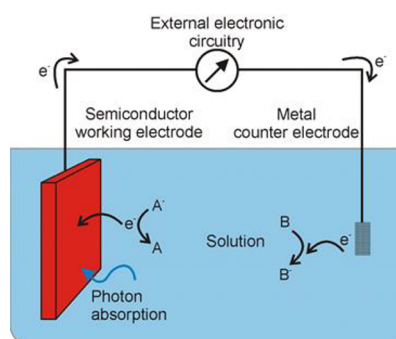


Figure 1. Photoelectrochemical setup.⁹

semiconductor material absorbs the light at the working electrode, exciting electrons to a higher energy level that, together with the corresponding holes generated, are able of carrying out reduction and oxidation reactions at a semiconductor/liquid interface. In practice, several characteristics of the photoelectrodes must be satisfied simultaneously; the

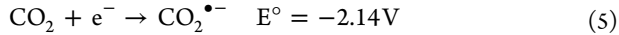
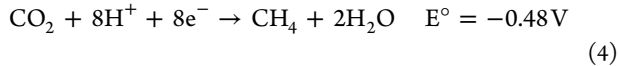
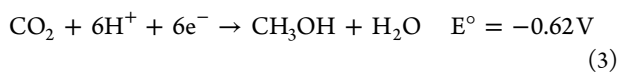
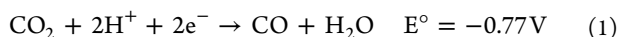
Received: July 30, 2018

Revised: October 11, 2018

Published: October 19, 2018

electronic band gap of the photoelectrode must be low enough for efficient photon collecting from the solar spectrum (<2.2 eV) and high enough such that the excited electrons have enough energy to split water (>1.23 eV or typically at least 1.6–1.7 eV for sufficient rates), the band edges must cover the water electrolysis redox potentials, and the photoelectrode must be stable and resistant to corrosion in the aqueous electrolyte.¹⁰ The photoelectrochemistry is therefore a thrilling and interdisciplinary research field that includes electrochemistry, surface science, solid-state physics, and optics.¹¹

CO_2 can be converted to a wide range of products such as CO , H_2 , HCOOH , CH_3OH , CH_4 , etc.¹² Equations 1–5 shows the thermodynamic potentials for CO_2 reduction products at neutral pH in aqueous solution versus a saturated calomel electrode (SCE) and 25°C and atmospheric pressure¹³



The extent to which the reaction progresses depends mainly on the catalytic systems, as well as the reaction media and potential applied.¹² Typically, multiple proton coupled electron transfer steps must be orchestrated, presenting kinetic barriers to the forward reaction.¹³ Also, part of the energy supplied to the system may be consumed by the competitive reaction for H_2 production from water electrolysis in the Hydrogen Evolution Reaction (HER). The state-of-the-art process for the production of value-added products from CO_2 using solar energy is still far from practical consideration, but knowledge has been accumulated through the years.¹⁴ Since the first report in 1978 on CO_2 photoelectrochemical reduction by Halman,¹⁵ many review articles have been written about different aspects of this photoelectrochemical technology, as shown in Table 1. In 2014, Ibrahim et al.⁹ collected the available knowledge about photoelectrochemical reactions to produce biofuel from biomass. In 2015, Sudha et al.¹⁶ review the recent developments in the synthesis and application of composite photocatalysts derived from TiO_2 , CdS , WO_3 , SnS , and ZnO . Moreover, Nikokavoura et al.¹⁷ presented alternative photocatalysts to TiO_2 for the photoelectroreduction of CO_2 . Inorganic and carbon-based semiconductors, mixed-metal oxides, salt composites, and other groups of photocatalysts were examined in this review. Moreover, a simplified energetic and economic feasibility assessment for a solar refinery (including photoelectrochemical means) for the production of methanol was developed by Herron et al.,^{18,19} concluding that at least a 15% solar-to-fuel efficiency is required in order to compete with industrial methanol production. Also, one of the most important factors affecting the CO_2 reduction performance is the configuration of the photoreactor. A complete discussion on photoreactor analysis and design was carried out by Yue in 1985.²⁰ In this paper, the author presented an overview of the important engineering problems in the modeling and design of photoreactors. More recently, Cassano et al.²¹ in 2005 described the most important technical tools that are needed

Table 1. List of Review Articles on CO_2 Photoelectrochemical Reduction

Author (year)	Publication title	ref
A. J. Bard (1979)	Photoelectrochemistry and heterogeneous photocatalysis at semiconductors	22
D. A. Tryk (2000)	Recent topics in photoelectrochemistry: Achievements and future prospects	23
B. Kumar (2012)	Photochemical and photoelectrochemical reduction of CO_2	13
A. Harriman (2013)	Prospects for conversion of solar energy into chemical fuels: The concept of a solar fuels industry	7
S. N. Habisreutinger (2013)	Photocatalytic reduction of CO_2 on TiO_2 and other semiconductors	24
N. Ibrahim (2014)	Biofuel from biomass via photoelectrochemical reactions: An overview	9
J. Zhao (2014)	Hybrid catalysts for photoelectrochemical reduction of carbon dioxide: A prospective review on semiconductor/metal complex cocatalyst systems	25
J. Highfield (2015)	Advances and recent trends in heterogeneous photo-(electro)-catalysis for solar fuels and chemicals	26
Y. Yan (2015)	Photoelectrocatalytic reduction of carbon dioxide	8
C. Ampelli (2015)	Electrolyte-less design of PEC cells for solar fuels: Prospects and open issues in the development of cells and related catalytic electrodes	27
D. Sudha (2015)	Review on the photocatalytic activity of various composite catalysts	16
S. Xie (2016)	Photocatalytic and photoelectrocatalytic reduction of CO_2 using heterogeneous catalysts with controlled nanostructures	28
A. Nikokavoura (2017)	Alternative photocatalysts to TiO_2 for the photocatalytic reduction of CO_2	17
L. Y. Ozer (2017)	Inorganic semiconductors-graphene composites in photo(electro)catalysis: Synthetic strategies, interaction mechanisms and applications	29
P. Wang (2018)	Recent progress on photo-electrocatalytic reduction of carbon dioxide	30

to design photoreactors using computer simulation of a rigorous mathematical description of the reactor performance, both in the laboratory and on a commercial scale.

In any case, it seems that the effect of reactor configuration in the CO_2 photoreduction performance has not been discussed in the literature as much as the development of active materials. To fill this gap, the aim of the present review is to provide a deeper analysis on the photoelectroreduction of CO_2 in terms of photoelectrochemical cell and photoelectrodes configuration, together with a discussion on photoactive materials applied and obtained products for each configuration as key variables in process performance. The discussion is structured as follows: (i) photoelectrochemical reactor configurations, (ii) photoelectrode materials, (iii) main reduction products and finally, (iv) conclusions and future challenges. This compilation aims to be a step further toward real application of photoelectroreactors for CO_2 conversion.

■ SUMMARY OF STUDIES

PEC Reactor Configuration. The reactor can be considered the heart of a photoelectrochemical system. In a PEC reactor, the illumination of the photoactive surface becomes crucial, together with other common variables in reactors such as mass transfer, mixing, or reaction kinetics.³¹ The design should be made based on a careful evaluation of different factors influencing reaction performance:^{20,21} (i) light source and geometrical configuration, (ii) construction material, (iii) heat exchange, (iv) mixing and flow characteristics, and (v) phases involved and mode of operation.³² These are discussed as follows:

Reactor design	Advantages	Disadvantages
Fluidized and slurry reactor (multiphase)	Temperature gradients inside the beds can be reduced through vigorous movements caused by the solid passing through the fluids. Heat and mass transfer increase due to agitated movement of solid particles. High catalyst loading.	Filters (liquid phase) and scrubbers (gas) are needed. Flooding tends to reduce the effectiveness of the catalyst. Difficulty of separating the catalyst from the reaction mixture. Low light utilization efficiency due to absorption and scattering of the light by the reaction medium. Restricted processing capacities due to limitations in mass transfer.
Fixed bed reactor	High surface area. Fast reaction time. The conversion rate per unit mass of the catalyst is high due to the flow regime close to plug flow. Low operating cost due to a reduced pressure drop.	Temperature gradient between gas and solid surface.
Monolith reactor	High surface to volume ratio and low pressure drop with high flow rate. Configuration can be easily modified.	Low light efficiency due to opacity of channels of the monolith.
Optical fiber reactor	High surface area and light utilization efficiency. Efficient processing capacities of the catalyst.	Maximum use of the reactor volume is not achieved. Heat buildup of fibers can lead to rapid catalyst deactivation.

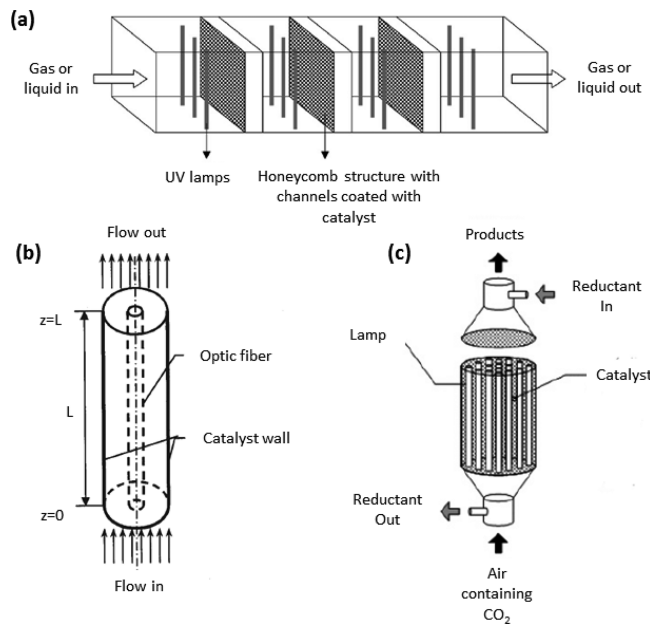


Figure 2. (a) Monolith photoreactor.⁵⁰ (b) Optical fiber photoreactor.⁵¹ (c) Fixed bed photoreactor.⁴⁵

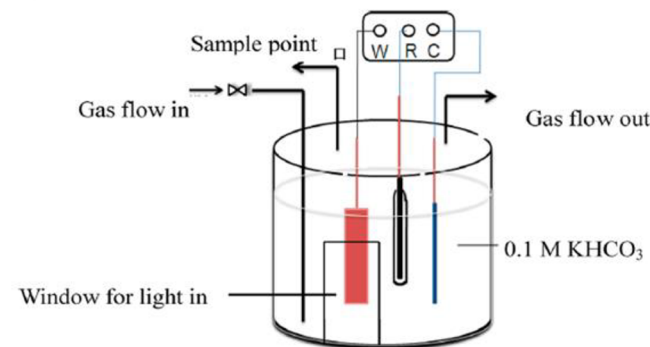


Figure 3. Single compartment cell (W = working electrode, R = reference electrode, and C = counter electrode).⁵⁹

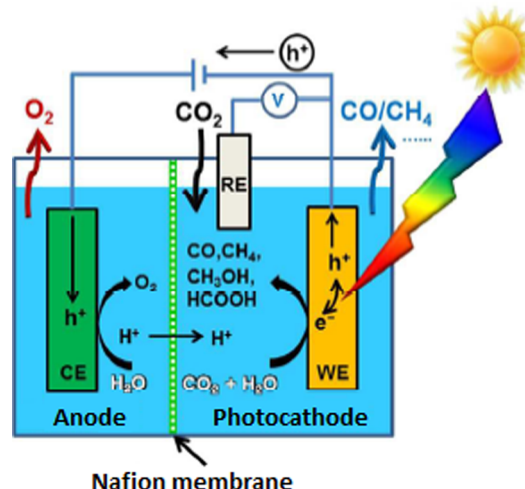


Figure 4. Dual compartment cell.⁶⁴

(i) For optimum results, light needs to be distributed homogeneously through the entire photoactive surface.³³ The

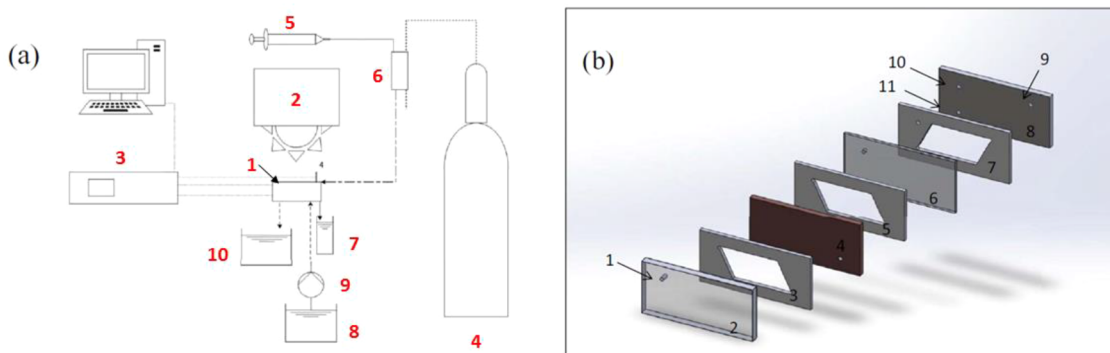


Figure 5. (a) Schematic diagram of the CFPR setup: (1) CFPR, (2) solar simulator, (3) electrochemical workstation, (4) CO₂ tank, (5) syringe pump, (6) fresh catholyte from a gas mixing chamber, (7) catholyte collector, (8) fresh anolyte, (9) pump, and (10) anolyte collector. The electrical connections to the electrodes are marked as WE, CE, and RE for the cathode, anode, and reference electrode, respectively. (b) Schematic diagram of the CFPR itself consisting of (1) catholyte inlet and location of the reference electrode, (2) optical window (transparent slab), (3) microchannel arrays slab on top of the cathode, (4) cathode, (5) microchannel arrays underneath the cathode, (6) ion exchange membrane, (7) microchannel arrays on top of the anode, (8) anode, (9) outlet of anolyte, (10) outlet of catholyte, and (11) inlet of anolyte.⁷³

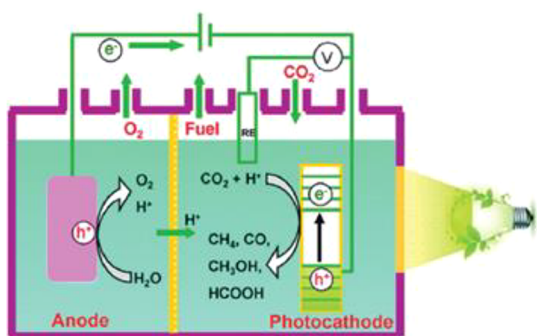


Figure 6. Semiconductor as photocathode.²⁸

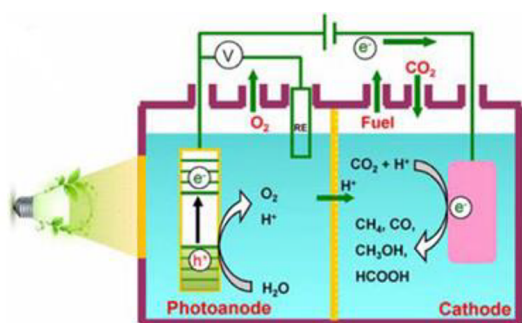


Figure 7. Semiconductor as photoanode.²⁸

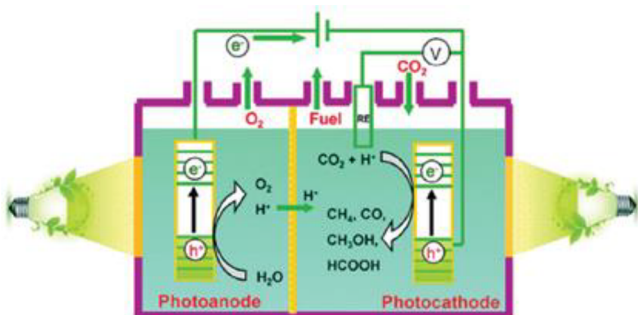


Figure 8. Semiconductors as both photocathode and photoanode.²⁸

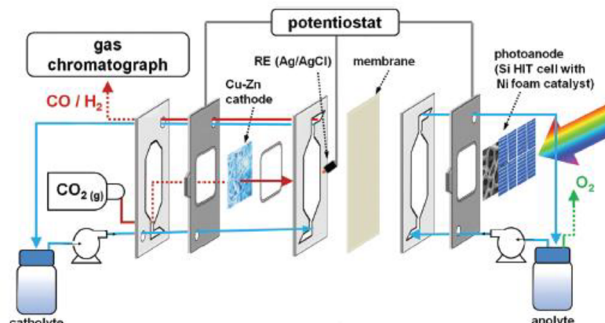


Figure 9. Filter-press reactor including a Cu–Zn cathode and a Si/Ni foam photoanode.⁴²

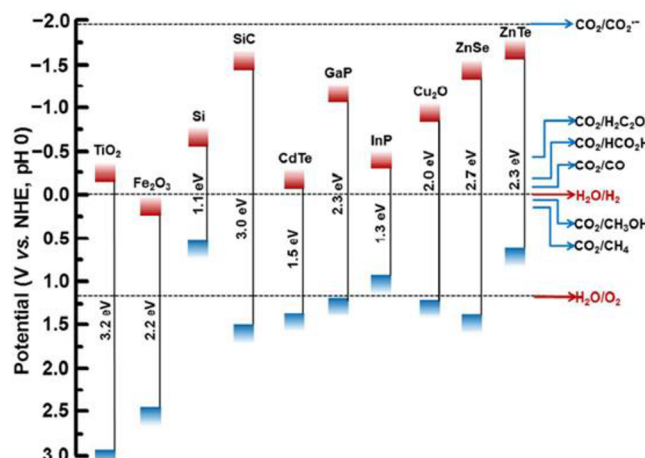


Figure 10. Conduction band (in red) and valence band (in blue) positions of some semiconductors and the redox potentials (vs NHE) for CO₂ reduction and water splitting at pH 0.⁶⁴

choice of the most suitable light source can be made by evaluating the reaction energy requirements with respect to the lamp specifications. The well-known xenon arc lamp seems to be the most employed lamp in the literature. This lamp produces a bright white light that closely mimics natural sunlight when electricity passes through the ionized Xe gas at high pressure.^{34,35} If solar energy is being considered, it should be noticed that sunlight mainly consists of three different

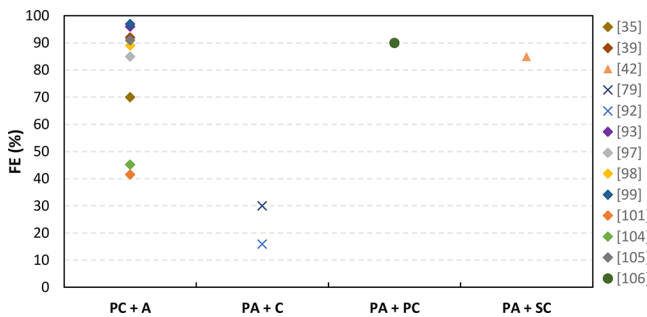


Figure 11. FEs for CO at different electrode configurations in PEC cells.

wavelengths: ultraviolet ($\lambda < 400$ nm), visible ($\lambda = 400\text{--}800$ nm), and infrared ($\lambda > 800$ nm), accounting for 4%, 53%, and 43% of the total solar energy, respectively.³⁶ Moreover, it is recommended to give a certain pattern of irradiation by mounting the light source inside a glass sheath or some suitable optical assembly as Ampelli et al.³⁷ evaluated where the Xe-arc lamp of 300 W was protected by a housing and a set of lenses were employed. Regarding geometrical configuration, it is necessary to determine the optical path of the light inside the reactor in a way to obtain the maximum benefit from the irradiation pattern and a good absorption of light photons. For photoreactors, other aspects such as the spatial relation between reactor and light source and geometry are crucial. In all cases, the irradiation takes place normal to the reactor surface.

(ii) In photoreactors, the requirements of light transmission influenced in the construction material election. The choice is usually limited to different types of glass being the Pyrex glass the most used in the bibliography for its adequate light transmission and cost,^{38–40} although quartz glass is more expensive, but generally gives the best performance in terms of light transmission. At short wavelengths ($\lambda < 300$ nm), quartz seems to be the only appropriate material. In some cases, the glass has been substituted by the plastic Plexiglas, except the reactor window, which is continuously being made of glass to allow UV light transmittance. For instance, Cheng et al.⁴¹ reduced CO₂ using a PEC Plexiglas reactor with a quartz window achieving a light intensity at the anode surface of 10 mW·cm⁻² with a 300 W Xe-arc lamp. Another important factor is the thickness of the reactor wall, which decreases the light transmission and limited the size of the reactor and the

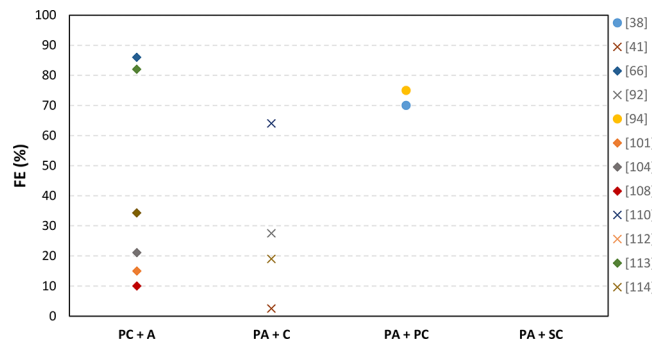


Figure 13. FEs for HCOOH at different electrode configurations in PEC cells.

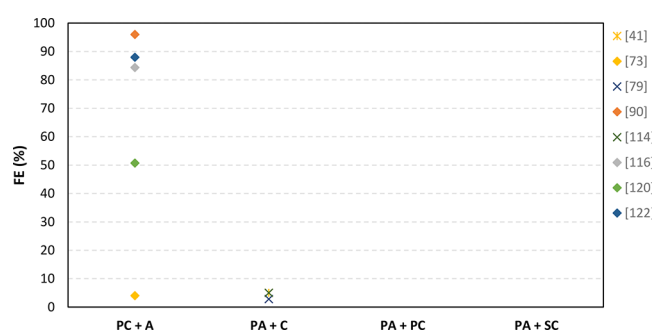


Figure 14. FEs for CH₃OH at different electrode configurations in PEC cells.

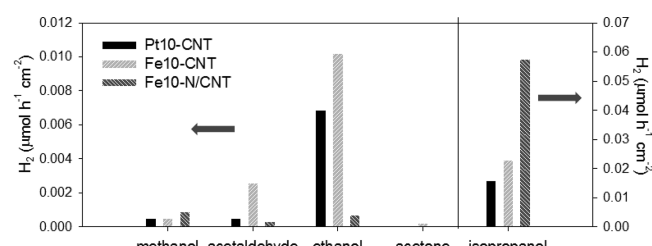


Figure 15. Electroreduction of CO₂ in the gas phase over Nafion 117/Pt or Fe(10%)/CNT 20% carbon GDEs.¹²⁴

operating temperature and pressure. Others authors^{42,43} use a different design to illuminate the photocatalyst surface, avoiding the problems of construction materials and light transmission by combining the PEC cell with a solar panel

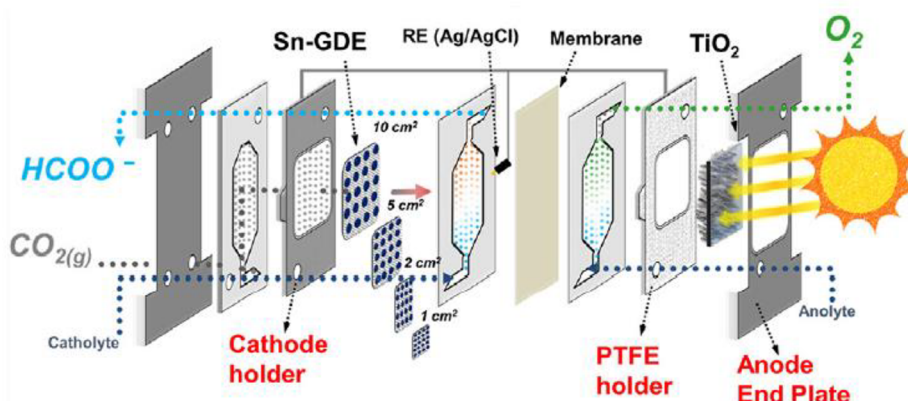


Figure 12. Photoelectrochemical flow cell scheme using a TiO₂ photoanode.¹¹⁰

Table 3. Experimental Conditions and Main Products in Photocathode–Dark Anode Configuration

Photocathode	Anode	Light source/Intensity	Electrode potential (V vs SCE)	Product	FE/Productivity	ref
p-GaP	Carbon rod	Hg lamp ($\lambda = 365$ nm)	-1 V	CH_2O ; HCOOH ; CH_3OH	—	15
p-GaAs	Pt	150W Tungsten lamp ($\lambda > 380$ nm)	-1.2 V	CO	47%	97
p-GaP	Pt	150W Tungsten lamp ($\lambda > 380$ nm)	-1 V	CO	85%	97
p-InP	Pt	500 W Xe lamp ($\lambda > 370$ nm)	-1.1 V	CO	89%	98
p-GaAs	Pt	500 W Xe lamp ($\lambda > 370$ nm)	-1.6 V	CO	74%	98
p-Si	Pt	500 W Xe lamp ($\lambda > 370$ nm)	-1.8 V	CO	75%	98
p-InP/deposited-metal [Pb, Ag, Au, Pd, Cu and Ni]	Pt	5000 W Xe lamp ($\lambda > 300$ nm)	-2.5 V	CO; HCOOH	—	77
p-GaAs	Pt	5000 W Xe lamp ($\lambda > 300$ nm)	-2.4 V	CO; HCOO^-	CO: 24.9%; HCOO^- : 14%	101
p-InP	Pt	5000 W Xe lamp ($\lambda > 300$ nm)	-2.5 V	CO; HCOO^-	CO: 41.5%; HCOO^- : 15%	101
p-GaP	Carbon rod	200 W Hg–Xe-arc light ($\lambda > 365$ nm)	-0.4 V	CH_3OH	88%–100%	90
p-InP	Pt	5000 W Xe lamp ($\lambda > 300$ nm)	-2.4 V to -2.8 V	CO; HCOOH	CO at -2.7 V: 45.2%; HCOOH at -2.6 V: 21.1%	104
p-Si	Pt	150 quartz halogen lamp ($\lambda < 1000$ nm)	-0.6 V	CO	97%	99
p-InP-Zn	[Ru(L-L) (CO) ₂] _n	Xe light (400 nm < $\lambda < 800$ nm)	-0.6 V	HCOO^-	34.3%	112
$\text{Cu}_2\text{ZnSnS}_4$ (CZTS)	[RuCE + RuCA	(400 nm < $\lambda < 800$ nm)	-0.4 V	HCOO^-	82%	113
meso-tetraphenylporphyrin FeIII chloride at p-type Si	$\text{CF}_3\text{CH}_2\text{OH}$	Halogen fiber optic lamp ($\lambda_{\max} = 650$ nm)	-1.1 V	CO	92%	39
Mg-doped CuFeO_2	Pt	75 W Xe (350 nm < $\lambda > 1350$ nm)	-0.9 V	HCOO^-	10%	108
Cu/Cu ₂ O	Pt	125 W Hg lamp	0.2 V	CH_3OH	—	115
Cu/Cu ₂ O	Pt	LED light (435 nm < $\lambda > 450$ nm)	-2.0 V	CH_4 ; C_2H_4	C_2H_4 : 32.69%	59
Wedge N-doped CuO	Pt	Xe lamp ($\lambda \geq 420$ nm)	-1.2 V	CH_3OH	84.4%	116
Ordered mesoporous TiO ₂	Pt	300 W Xe-arc lamp	-0.4 V	CH_4 ; CO	—	88
p-type CuO/Cu ₂ O	Stainless steel	(AM 1.5) Solar simulator (Newport Model 91160)	-0.3 V	$\text{C}_2\text{H}_5\text{OH}$; $\text{C}_3\text{H}_8\text{O}$; CH_3OH	$\text{C}_2\text{H}_5\text{OH}$: 52%; $\text{C}_3\text{H}_8\text{O}$: 40%; CH_3OH : 4%	59
Cu/Cu ₂ O	Pt	125 W Hg lamp	0.20 V	CH_3OH ; $\text{C}_2\text{H}_5\text{OH}$; CH_2O ; $\text{C}_2\text{H}_4\text{O}$; CH_3COCH_3	—	117
Cu–Co ₃ O ₄ NTs	Pt	300 W Xe lamp	-0.9 V	HCOO^-	—	109
$\text{Cu}_2\text{O}-\text{TiO}_{2-x}$	—	150 W Xe lamp (AM 1.5)	-0.07 V to -0.77 V	CH_3OH ; HCOOH	—	34
NiO	Pt	LED with an output of 1000 lm	-0.4 V	H_2	—	75
Ru(bpy) ₂ dppz-Co ₃ O ₄ /CA 1T@2H-MoS ₂	graphite plate	Xe lamp ($\lambda > 420$ nm)	-0.84 V	HCOO^-	86%	66
	Pt	Visible-light illumination (400 nm < $\lambda > 800$ nm)	-0.6 V	—	—	126
Au ₃ Cu NP/Si NW	—	—	-0.8 V	CO	—	127
Si with RA-treated Au thin film mesh	—	100 mW cm ⁻²	-0.73 V	CO	91%	105
Cu ₂ O/graphene/TNA	Pt	300 W Xe-arc lamp ($\lambda > 400$ nm)	-0.8 V vs SCE	CH_3OH	45 $\mu\text{mol cm}^{-2} \text{ h}^{-1}$	40
Ti/ZnO–Fe ₂ O ₃	Pt	300 W Xe lamp (400 nm < $\lambda < 800$ nm)	-0.5 V	CH_3OH ; HCOOH ; CH_2O	CH_3OH : 0.773 mmol/cm ²	74
Cu-ZnO/GaN/n ⁺ -p Si	—	300 W Xe lamp	-0.6 V	CO	70%	35
Cu ₂ O	Pt	LS 150 with AM1.5 G filter	-0.3 V	CH_3OH	23.6%	120
Cu ₂ O/TiO ₂ – Cu ⁺	Pt	LS 150 with AM1.5 G filter	-0.3 V	CH_3OH	50.7%	120
CdSeTe NPs/TiO ₂ NTs	Pt	500W Xe lamp ($\lambda \geq 420$ nm)	-1.2 V	CH_3OH	88%	122
CdSeTe NSs/TiO ₂	Pt	500W Xe lamp ($\lambda \geq 420$ nm)	-1.2 V	CH_3OH	25%	122
SnO ₂ NRs/Fe ₂ O ₃ NTs	Pt	Xenon lamp ($\lambda \geq 420$ nm)	-1.1 V	CH_3OH	87.04%	121
Cu ₂ O	Graphite sheet	100 mW cm ⁻²	-0.6 V	$\text{C}_2\text{H}_5\text{OH}$	0.071 mmol·cm ⁻² ·h ⁻¹	125

Table 3. continued

Photocathode	Anode	Light source/Intensity	Electrode potential (V vs SCE)	Product	FE/Productivity	ref
0D/2D CND/pCN	Pt	300 W Xe-arc lamp ($\lambda > 400$ nm)	-0.5 V	CH ₄ CO	CH ₄ : 2.9 $\mu\text{mol}\cdot\text{g}_{\text{catalyst}}^{-1}\cdot\text{h}^{-1}$ CO: 5.8 $\mu\text{mol}\cdot\text{g}_{\text{catalyst}}^{-1}\cdot\text{h}^{-1}$	44
Si/Au	Graphite rod	100 mW cm ⁻²	0 V	CO	96%	93

(PEC-photosolar cell tandem). Thus, the photomaterial is directly illuminated, the light is not disturbed by aqueous media, and H₂O could be oxidized in the photoanode without applying external bias.

(iii) Heat exchange should be particularly considered, especially in gas–solid systems. Suitable devices must be designed to remove the heat generated by the lamp because of the glass low thermal conductivity.³² For example, Ong et al.⁴⁴ positioned a water jacket between the PEC cell systems and the Xe-arc lamp to lessen the effects of heat on the Na₂SO₄ electrolyte solution during irradiation.

(iv) Mixing and flows depend on the phases involved in the process and are also important factors to take into account. It is recommended to mix. In the case of heterogeneous photo-reactions, contact between reactants, photons, and catalysts should be promoted with, for example, agitation of the reacting mixture using a stirrer.³²

(v) Photoreactors applied for CO₂ photoconversion can be classified according to the phases involved (i.e., gas–solid, liquid–solid, gas–liquid–solid, etc.) and the mode of operation (i.e., batch, semibatch, or continuous). Moreover, the materials can be generally in suspended (fluidized bed) or immobilized forms (fixed bed) in reactors. The main pros and cons of different current photoreactor systems for CO₂ transformation are summarized in Table 2.³³ Figure 2 shows the schematic configuration of various types of photocatalytic reactors, which may serve as a reference for the design of new photoelectrocatalytic reactors (i.e., light incidence, flows inlet/outlet, photoactive surface configuration, etc.).

The recirculation of unconverted CO₂ also must be taken into account when designing an effective photoelectroreactor since the separation of the products from CO₂ could account for 6%–17% of the total energy required in the process.⁵³ Moreover, undivided photoelectrochemical reactors (Figure 3), in which plate-type electrodes are separated by a liquid phase that acts as both anolyte and catholyte, have been commonly used. In these type of cells, the process costs increase due to the extra separation step required for the product recuperation.⁵⁴ For a practical use of PEC cells, the separation in two distinct compartments where CO₂ reduction and water oxidation take place is more appealing than the single compartment process, since one can deal with one reaction at a time. As a result, the efficiency of the redox reactions increase, as so the charge and products separation.^{37,55,56} The election between single and dual compartment cell does not follow a determinant rule and depends on the case, although dual compartment cells are usually preferred.^{37,38,40}

Also, in order to allow an efficient collection/transport of electrons over the entire film as well as the diffusion of protons through the membrane (Figure 4), both anode and cathode should be in the form of a thin film separated by a proton-conducting membrane (Nafion or other materials)^{37,57} and fixed onto a porous conductive substrate in the PEC cell. For CO₂ photoreduction, an efficient evolution of oxygen on the

anode side is also needed, together with an efficient evolution of CO₂ and diffusion of reaction products on the cathode side. Moreover, the use of gas diffusion electrodes (GDEs) and gas phase operation on the cathode compartment is preferable, in order to avoid the limitations of CO₂ solubility in water.^{37,58}

The mass transport in the electrode is a limiting factor as better catalyst are progressively becoming available. For this, several elements have been considered: high pressure operation, the use of GDEs, and no aqueous electrolytes.⁶⁰ GDEs usually consists of a carbon fiber substrate (CFS), a microporous layer (MPL), typically is composed of carbon powder and polytetrafluoroethylene (PTFE), and a catalyst layer (CL). Del Castillo et al.⁶¹ compared a Sn-GDE with a Sn plate electrode and obtained higher rates for the Sn-GDE than for Sn plate electrode, demonstrating the exceptional performance of GDEs for CO₂ reduction.^{60,62} Gas phase CO₂ transformation by using GDEs can be also applied to enhance CO₂ transfer, allowing the operation at higher current densities in the cell as demonstrated by Merino-Garcia et al.,⁶³ in a dual compartment cell for methane and ethylene production by using a Cu-based membrane electrode assembly (MEA).

Moreover, the type of ion transport membrane applied is key in the CO₂ photoelectrochemical reduction performance, where proton exchange membranes (PEMs) are preferred due to their favored protons transport from the anode to the cathode than the anion exchange membranes (AEMs), with anions transported from the cathode to the anode compartment, but of course, it may depend on the reaction conditions and cell configuration.⁵⁴ The expected reactions in a PEM-based reactors are as follows:

Cathode:

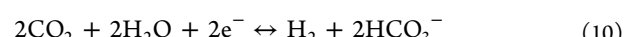
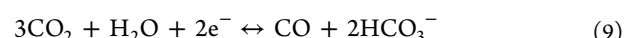


Anode:

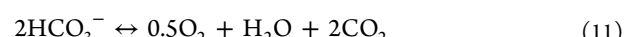


While the expected reactions in a AEM are as follows:⁵⁵

Cathode:



Anode:



There are many examples on the use of PEMs in photoelectroreduction,^{5,65,66} while AEMs are not usually employed, although some examples are reported in electrochemical devices where current densities as high as 130 mA·cm⁻² can be achieved.⁶⁷ This is the case for the new anion-conductive polystyrene methyl methylimidazolium chloride (trade named Sustainion) AEM membrane developed by

Table 4. Experimental Conditions and Main Products in Photoanode–Dark Cathode Configuration

Cathode	Photoanode	Light source/Intensity	Electrode potential (V vs SCE)	Product	FE/Productivity	ref
Pt	<i>n</i> -TiO ₂	500 W Xe lamp	-2 V	CH ₃ OH	100%	14
	Pt-TNT	300 W Xe-arc lamp	-2 V	C ₂ H ₅ OH; CH ₃ COOH; CH ₃ OH; HCOOH	CH ₃ OH: 5%; HCOOH: 2.5%; CH ₃ COOH: 20%; C ₂ H ₅ OH: 45%	41
Cu	WO ₃	500 W Hg lamp (λ > 420 nm)	-1.39 V	CO; CH ₄ ; C ₂ H ₄	CO: 0.6%; CH ₄ : 67%; C ₂ H ₄ : 2.7%	92
Sn/SnO _x	WO ₃	500 W Hg lamp (λ > 420 nm)	-1.34 V	CO; HCOOH	CO: 15.9%; HCOOH: 27.5%	92
Pt-RGO/Cu	TiO ₂ nanotube	300 W Xe-arc lamp (320 nm < λ > 410 nm)	-2 V	HCOOH; CH ₃ COOH; C ₂ H ₅ COOH; CH ₃ OH; C ₂ H ₅ OH	—	78
Pt-RGO	Pt-TNT	300 W Xe-arc lamp (320 nm < λ > 410 nm)	-2 V	C ₂ H ₅ OH; CH ₃ COOH; CH ₃ OH; HCOOH; CO	C ₂ H ₅ OH: 1350 nmol·cm ⁻² ·h ⁻¹ ; CH ₃ COOH: 1150 nmol·cm ⁻² ·h ⁻¹ ; CH ₃ OH: 875 nmol·cm ⁻² ·h ⁻¹ ; HCOOH: 820 nmol·cm ⁻² ·h ⁻¹	128
Pt	Cu-RGO-TiO ₂ /ITO	150 W Xe-arc lamp	-0.61 V	HCOOH; CH ₃ OH	CH ₃ OH: 255 mmol·cm ⁻² ·h ⁻¹ ; HCOOH: 189.06 mmol·cm ⁻² ·h ⁻¹	129
Pt-RGO	Pt (5%)-TNT	300 W Xe-arc lamp (320 nm < λ > 410 nm)	-2 V	HCOOH; CH ₃ OH; CH ₃ COOH; C ₂ H ₅ OH	HCOOH: 80 nmol·cm ⁻² ·h ⁻¹ ; CH ₃ OH: 75 nmol·cm ⁻² ·h ⁻¹ ; CH3COOH: 250 nmol·cm ⁻² ·h ⁻¹ ; C ₂ H ₅ OH: 280 nmol·cm ⁻² ·h ⁻¹	65
Cu ₂ O	TiO ₂	100 mW·cm ⁻² AM 1.5G	-1.49 V	CH ₄ ; CO; CH ₃ OH	CH ₄ : 54.63%; CO: 30.03%; CH ₃ OH: 2.79%	79
Pt	b-Si/TiO ₂ /Co(OH) ₂	150 W Xe lamp light	1.04 V	—	—	91
Pt/GA/CF	TiO ₂	300 W Xe-arc lamp (320 nm < λ > 410 nm)	-2 V	HCOOH; C ₃ COOH; C ₂ H ₅ COOH; CH ₃ OH;	HCOOH: 19%; CH ₃ COOH: 24%; C ₂ H ₅ COOH: 23%; CH ₃ OH: 5%; C ₂ H ₅ OH: 29%	114
Sn-GDE	TiO ₂	300 W Xe lamp	-1.12 V	HCOO ⁻	40%–65%	1110
Cu	TiO ₂ NWs	250 W lamp (λ < 400 nm)	0 V	CH ₄	2596 μL·g _{catalyst} ⁻¹ ·h ⁻¹	123
Pd/C	GaAs/InGaP/TiO ₂ /Ni	100 mW·cm ⁻² AM 1.5G	0 V	HCOO ⁻	94%	69

Table 5. Experimental Conditions and Main Products in Photocathode–Photoanode Configuration

Photocathode	Photoanode	Light source/Intensity	Electrode Potential (V vs SCE)	Product	FE/Productivity	ref
InP/[MCE]s	TiO ₂ /Pt	1 sun (AM 1.5)	0 V	HCOO ⁻	70%	38
<i>p</i> -type Si nanowire	<i>n</i> -type TiO ₂ nanotube	Photocathode: 150W Xe lamp (AM 1.5); Photoanode: 25W Hg arc lamp	-1.5 V	CO; CH ₄ ; C ₄ H ₈ ; C ₂ H ₄ ; C ₃ H ₈ ; C ₄ H ₁₀	CO: 824 nmol/cm ² ·h; CH ₄ : 121.5 nmol/cm ² ·h; C ₂ H ₄ : 80 nmol/cm ² ·h	80
InP/Ru complex	TiO ₂	1 sun, air mass 1.5	0 V	HCOO ⁻	75%	94
Si NWs@ CoP/CN	TiO ₂ NWs@ CoP/CN	—	-0.81 V	CO; CH ₄	CO: 90%	106
NiO-RuRe	CoO _x /TaON	300 W Xe lamp ($\lambda > 460$ nm)	-0.3 V	CO	—	95

Table 6. Experimental Conditions and Main Products in PEC–Solar Cell Tandem Configuration

Photo/cathode	Photo/anode	Light source/Intensity	Electrode Potential (V vs SCE)	Product	FE/Productivity	ref
ZnTe based	Co-Ci	100 mW cm ⁻²	0 V	CO	—	130
GaN	Pt	300 W xenon lamp	—	CH ₄	19%	131
Cu _x O	WO ₃	200 W xenon lamp (AM 1.5)	0 V	CO; HCOO ⁻	—	132
Cu-Zn	Si/Ni	150 W xenon lamp (AM 1.5)	0 V	CO	85%	42

Masel and co-workers, which exceeded standards for product selectivity and current density with commercially available AEM.⁶⁷

Moreover, bipolar membranes (BPM), made of an anion and cation exchange membranes, have recently gained interest for CO₂ transformation due to their ability to separate anode and cathode compartments and the high sensitivity on pH required to facilitate different electrolyte conditions for the anode and for the cathode by the selective transport of OH⁻ to the anode and H⁺ to the cathode.^{68,69} Maintaining the pH constant, BPMs allow the use of new Earth-abundant metal anodes that are stable in basic conditions and highly active acid-stable cathodes for CO₂ reduction, which cannot be realized by using PEMs and AEMs.⁶² Recently, Zhou et al.⁶⁹ reported a FE > 94% to HCOOH (8.5 mA·cm⁻²) using a GaAs/InGaP/TiO₂/Ni photoanode and a Pd/C nanoparticle-coated Ti mesh cathode, employing as electrolytes 1.0 M KOH (pH 13.7) and 2.8 M KHCO₃ (pH 8.0) separated by a BPM that facilitated the separation of redox reactions to achieve higher efficiencies and produce lower total overpotentials in comparison to a single compartment cell.

In addition, the formation of liquid products from CO₂ reduction has mostly focused on batch PEC reactors.^{3,4,70,71} Only a few researchers deal with the concept of continuous flow photoelectrochemical reactors,⁷² required in the production at industrial scale, minimizing capital costs and maximizing product consistency as demonstrated in case of electrochemical systems for CO₂ continuous reduction. To this end, a continuous flow PEC reactor (CFPR) was developed in 2015 by Homayoni et al.⁷³ to produce alcohols from CO₂ employing a CuO/Cu₂O photocathode (Figure 5). The results show long-chain alcohol products up to C₂–C₃ (ethanol and isopropanol) with a production rate of 0.22 mL·m⁻²·h⁻¹, that was approximately 6 times higher than in a batch design.

Furthermore, there are different electrode configurations for the PEC systems on dependence on which electrode (i.e., anode, cathode, or both) acts as photoelectrode,⁶⁵ as described in the following subsections.

Photocathode–Dark Anode. Most of the studies employed a photocathode made of a *p*-type semiconductor, with a high

conduction band energy suitable for CO₂ reduction, and an anode made of metal (Figure 6).^{74,75} The first study was reported by Halmann in 1978, where a *p*-GaP semiconductor was used as photocathode, carbon rod as counter electrode, and a buffered aqueous solution as electrolyte.¹⁵ A 6 mA·cm⁻² current was detected when *p*-GaP was illuminated with an Hg lamp, and a voltage bias of -1 V vs SCE was applied. HCOOH, HCHO, and CH₃OH were formed. More recently, this type of configuration was implemented by Qin et al.⁷⁶ using TiO₂ as photocathode and an electrode of Pt as anode to obtain HCOOH, HCHO, and CH₃OH as main products.

Unfortunately, the valence band in *p*-type semiconductors does not cover H₂O oxidation, and a bias potential is required. Also, these materials are usually expensive, toxic, and unstable and two-electron compounds, such as CO and HCOOH, are obtained as it was demonstrated by Kaneko et al.⁷⁷ when a metal-doped (Pb, Ag, Au, Pd, Cu, and Ni) *p*-InP photocathode and a Pt foil as counter electrode was applied at -2.5 V vs SCE potential. Overall, the efficiency of *p*-type semiconductor-based systems is low, and the improvement required in photocathode efficiency remains a challenge.

Photoanode–Dark Cathode. The use of a *n*-type semiconductor (e.g., TiO₂, ZnO, BiVO₄, or WO₃), which are Earth-abundant, cheap, and stable as a photoanodes for H₂O oxidation, and a metallic electrocatalyst active for CO₂ reduction as the cathode to assemble a photoanode–dark cathode PEC reactor is also an attractive option (Figure 7).^{41,78} CO₂ reduction in a photoanode–dark cathode PEC depends on two components: cathode catalysts and photoanode activity. This cell could improve CO₂ reduction values obtained in electrocatalytic systems and reduce energy input over the photoanode catalyst, requiring a lower external bias for an effective CO₂ reduction than the photocathode–dark anode configuration.^{28,65} In this configuration, the photoanode plays a dual role during CO₂ reduction. On the one hand, the voltage generated by the light in the anode supplies an extra negative potential to the cathode for CO₂ reduction, and on the other hand, protons and electrons for CO₂ reduction in the cathode were provided by the oxidation of water in the anode.⁶⁵ Chang and co-workers⁷⁹ used TiO₂ as a model photoanode and Cu₂O as a dark cathode to devise a stable

system for photoconversion with a FE of 87.4% and a selectivity of 92.6% for carbonaceous products from CO₂. For instance, a Pt-modified reduced graphene oxide (Pt-RGO) cathode and a Pt-modified TiO₂ nanotubes (Pt-TNT) photoanode converted CO₂ into HCOOH, CH₃OH, CH₃COOH, and C₂H₅OH under UV-vis irradiation, applying a potential of 2 V.⁴¹ In further investigations, the cathode was substituted by Pt-RGO/Cu foam⁷⁸ and Pt-RGO/Ni foam⁶⁵ to improve products selectivity.

Photocathode–Photoanode. Another option for the photoelectrodes in an assembly of PECs is the combination of a photocathode made of a *p*-type semiconductor for CO₂ reduction with a photoanode made of a *n*-type semiconductor for H₂O oxidation (Figure 8). This configuration, in contrast to the other two, allows realizing the transformation of CO₂ with H₂O without external electrical energy. In this case, the conduction band edge of the photoanode for H₂O oxidation must be more negative than the valence band edge of the photocathode for CO₂ reduction to guarantee the electron transfer from photoanode to photocathode through the external wire.²⁸ Sato et al.³⁸ employed this PEC configuration to produce HCOOH in a two-compartment Pyrex cell separated by a PEM using InP/[MCE]s and TiO₂/Pt as photocathode and photoanode, respectively. By applying a light source, the two-compartment PEC cell could be run without external applied electrical energy. Not all the photocathode and a photoanode PEC cell configurations reported in the literature are able to reduce CO₂ without an external potential. Some need extra electrical energy to overcome parasitic losses and reaction overpotentials, such as a *p*-type Si nanowire/*n*-type TiO₂ nanotube where traces of C₃–C₄ hydrocarbons, CH₄, and C₂H₄ were formed under band gap illumination and at 1.5 V vs Ag/AgCl.⁸⁰

PEC–Solar Cell Tandem. Traditionally, PEC cells and PV electrolyzers are considered as different approaches, although some authors as Jacobsson et al.⁸¹ suggest that in many cases both approaches have certain similarities and should be considered under the acronym photo-driven catalytic (PDC) devices. To be clear, a distinction should be made between the solar panel coupled in the photoanode⁴² (PEC–solar cell tandem, Figure 9), and the photovoltaic panels used as electric source to the PEC cell (PV electrolyzers), which is the same as electroreduction using renewable energy.^{43,82,83} In order to value the potential importance that can develop the PEC–solar cell tandem configuration in photoelectroreduction, the authors consider treating this configuration as one more added to the previous.

The main benefit of using a PEC cell (i.e., photocathode–anode, cathode–photoanode, photocathode–photoanode, or PEC–solar cell tandem) rather than PV electrolyzers is the possibility to deal with the generation of electrons required and the oxidation of H₂O (if a photoanode is employed) or adjust the redox potential to the interest product (if a photocathode is used) in the same device.

Figure 9 is an example of a PEC–solar cell tandem. An experimental setup using Si heterojunction solar cells in combination with Ni foam as the photoanode and Zn-coated Cu foam as the cathode was applied, reaching CO FEs up to 85% at 0.12 V vs SCE (0.8 V vs RHE) with a CO current density of 39.4 mA·cm⁻², the highest reported for a Zn catalyst at such low overpotential. This reactor concept enhances the solar CO₂ conversion by the use of the well known and developed Si heterojunction technology, which is nontoxic,

abundant, and cheap, and it is being used in the photovoltaic industry nowadays.⁴²

Photoelectrode Materials. The next section briefly discusses on the main photoactive materials applied in the different PEC configurations for the reduction of CO₂.²⁴ The two basic requirements for photoelectrode materials are optical response, to effectively absorb sunlight, and catalytic activity, required for the CO₂ reduction and H₂O oxidation reactions. In order to satisfy these requirements, the processing of materials with enhanced performance characteristics need to include a high solar energy conversion efficiency, stability in aquatic environments, and low cost.⁹ In addition, the particle size of the photoelectrode material has a considerable effect on CO₂ photoreduction efficiency due to changes in CO₂ adsorption, available active surface area, and transfer pathways for charge carriers to reach its surface. The performance can be normally enhanced at smaller particle sizes, although the smaller the size is, the more the boundary of the particles, which leads also to a lower activity. Furthermore, it has been proved that the best way to improve the activity of photomaterials is controlling the facets of the photocatalysts applied.⁸⁴

Typically, photoelectrocatalysis, in contrast to common electrodes used in electrocatalysis, employs semiconductor electrodes. In addition, graphene-based nanocatalyst and organometallic complexes are commonly applied.² Semiconductor-based electrodes absorb light to generate electron–hole pairs. The holes generated at the photoanode, typically, a *n*-type semiconductor, oxidize H₂O to O₂, while the electrons photogenerated at the cathode, usually a *p*-type semiconductor, reduce the CO₂ to valuable products such as CO, HCOOH, CH₃OH, or hydrocarbons in the presence or absence of a cocatalyst.²⁸ TiO₂, ZnO, CdS, and SiC are the most employed inorganic binary compounds as semiconductor materials.

TiO₂ Photoelectrodes. TiO₂ is the most investigated semiconductor material for photocatalytic processes. It is a *n*-type semiconductor that possesses a wide band gap (3.0 eV)⁸ and has been considered a cheaper and more environmental friendly material since the first report in 1979.⁸⁵ TiO₂ has three kinds of polycrystalline phases, (anatase, brookite, and rutile),⁸⁶ with different symmetries, slip directions, theoretical crystal densities, close stacking planes, and available interstitial positions, altering also the defect distribution and density. As an example, Liu et al.⁸⁷ studied the photocatalytic reduction of CO₂ on three TiO₂ nanocrystal polymorphs pretreated with helium and concluded that for TiO₂ surfaces engineered with defect sites, brookite provided the highest yield for CO and CH₄, followed by anatase and rutile, probably due to a lower formation energy of oxygen vacancies (V_O) on brookite.

The literature shows that TiO₂ has been tested for the photocatalytic reduction of CO₂ under various structures, such as nanosheets, nanocrystals, nanotube arrays, nanorods, carbon-TiO₂ nanocomposites, and mesoporous TiO₂-based materials.⁸⁸ Zhao et al.⁸⁹ reviewed the effects of surface point defects in the production of solar fuels from CO₂ photoreduction in H₂O. In TiO₂, oxygen vacancies, impurities, Ti interstitials, Ti vacancies, and defects at interfaces are examples of point defects. The defective TiO₂ materials show superior performance than pristine TiO₂ for CO₂ photoreduction, probably due to an enhanced dissociative adsorption of CO₂, an improved solar energy absorption due to a change in the electronic band structure, and a reduced charge recombination

due to the presence of charge traps. Unfortunately, TiO_2 mainly absorbs UV radiation,⁹ which is only a small part of solar radiation. Although progresses have been made with TiO_2 , it seems that different materials should be considered in order to enhance the photocatalytic transformation of CO_2 to useful products.

Alternative Photocatalyst to TiO_2 . Apart from TiO_2 , other semiconductor-based photoelectrodes could be used. Figure 10 shows the band gap positions of other semiconductor materials and the standard reduction potentials for CO_2 reduction to different products. However, the photogenerated electrons in the conduction band edge of all the candidate semiconductors do not have enough driving force to carry out the activation of CO_2 to $\text{CO}_2^{\bullet-}$ (−2.14 V vs SCE), which defines the efficiency for CO_2 photoreduction.⁶⁴

Barton et al.⁹⁰ presented a selective and efficient conversion of CO_2 to CH_3OH at a *p*-type semiconductor electrode made of a narrow band single crystal *p*-GaP (111) in a pyridine solution. The current efficiency is 100% at −0.3 V vs SCE. Recently, Yu et al.⁹¹ developed a novel material by depositing a conformal, ultrathin, amorphous TiO_2 film by low-temperature atomic layer deposition on top of black Si. A photocurrent density of $32.3 \text{ mA}\cdot\text{cm}^{-2}$ at an external potential of 0.87 V vs SCE (1.48 V vs RHE) in 1 M NaOH electrolyte could be achieved. ZnO , a *n*-type semiconductor with a wide band gap energy, has been also tested as photocatalytic material due to its photoluminescence properties (including good transparency and high electron mobility) that shows potential for scintillator applications.¹⁶ WO_3 is also suitable and stable enough for sustained reduction of CO_2 . A PEC system using WO_3 as a photoanode and Cu or Sn/SnO_x as a cathode has been shown to achieve reduction of CO_2 at low bias potentials under visible light.⁹² Si is also considered as a promising material due to its Earth abundance, but a cocatalyst is required to enhance its CO_2 reduction. Song and co-workers⁹³ employed a Si photoelectrode with a nanoporous Au film as cocatalyst in a photocathode–dark anode configuration. Applying a light intensity of $100 \text{ mW}\cdot\text{cm}^{-2}$ a 91% FE to CO was achieved.

Doping the photocatalysts surface with a cocatalyst is another used procedure to achieve enhancements on both conversion efficiency and product selectivity.⁸⁴ In many cases, a combination of a photocathode with a cocatalyst able to activate CO_2 molecules is needed since *p*-type semiconductor photocathodes do not act as a true catalyst for the activation of CO_2 molecules but just as light harvesters to generate electrons and holes. For this purpose, metal complexes have attracted much attention, where the interface interaction between the semiconductor and the complex plays a decisive factor in the electron transfer and thus the CO_2 photoreduction efficiency.^{25,28} Besides, Huang et al.⁶⁶ employed Co_3O_4 as the light harvester and $\text{Ru}(\text{bpy})_2\text{dppz}$ as an electron transfer mediator and a CO_2 activator to obtain HCOOH as a main product. The results show a 380-fold increase in CO_2 concentration on this hybrid interface than that on $\text{Co}_3\text{O}_4/\text{FTO}$. The CO_2 conversion to HCOO^- occurred at an onset potential of −0.7 V vs SCE (−0.45 V vs NHE) under photoelectrochemical conditions, 160 mV more positive than its thermodynamic redox potential. At −0.85 V vs SCE (−0.60 V vs NHE), the selectivity of the HCOO^- yield reached 99.95%, with a production of $110 \mu\text{mol}\cdot\text{cm}^{-2}\cdot\text{h}^{-1}$ and a FE of 86%. HCOO^- was obtained by Morikawa et al.⁹⁴ conjugating a *p*-InP:Zn photocathode with a Ru complex–polymer electrocatalyst $[\text{Ru}(\text{L-L})(\text{CO})_2]_n$, for CO_2 transformation with a

TiO_2 photoanode for water oxidation. The conversion efficiency was 0.04%, which is closed to that value obtained in natural photosynthesis. Sahara et al.⁹⁵ reported the first example of a molecular/semiconductor photocatalyst hybrid-constructed PEC to transform CO_2 under visible light in the presence of water, using a Ru(II)–Re(I) photocathode and a CoO_x/TaON photoanode.

Main Reduction Products. The most common products from the photoelectrochemical reduction of CO_2 are summarized hereafter. H_2 is a side reaction in CO_2 electroreduction, and so it is not thoroughly discussed in the section.

Carbon Monoxide. CO_2 reduction to CO can be seen as the simplest route for CO_2 conversion. CO is also an intermediate product for the synthesis of other products, such as CH_3OH and hydrocarbon fuels.⁹⁶ Petit and co-workers⁹⁷ proposed the reduction CO_2 to CO in a photocathode–dark anode configuration using two systems: *p*-GaAs/0.1 M KClO_4 , H_2O , $\text{Ni}(\text{cyclam})^{2+}$, and *p*-GaP/0.1 M NaClO_4 , H_2O , $\text{Ni}(\text{cyclam})^{2+}$, which assist a selective photoreduction at −0.44 V vs SCE (−0.2 V vs SHE) using an anode of Pt, separated from the working-electrode compartment by glass frits. Using a similar photocathode (*p*-GaAs)–dark anode (Pt) cell configuration as Petit and co-workers in a one compartment cell, Hirota et al.⁹⁸ reduced CO_2 to CO photoelectrochemically in $\text{CO}_2 + \text{CH}_3\text{OH}$ at high-pressure conditions (40 atm). *p*-InP and *p*-Si as photoelectrodes were tested at different applied potentials. For $50 \text{ mA}\cdot\text{cm}^{-2}$, *p*-InP required −1.1 V, *p*-GaAs −1.6 V, and *p*-Si −1.8 V, demonstrating that CO_2 can be converted to CO at more positive potentials than for a Cu under similar experimental conditions and without illumination. Moreover, Kumar and co-workers⁹⁹ using a one compartment cell configuration and a *p*-type H-Si photocathode with a $\text{Re}(\text{bipy-Bu}^t)(\text{CO})_3\text{Cl}$ ($\text{bipy-Bu}^t = 4,4'$ -di-*tert*-butyl-2,2'-bipyridine) electrocatalyst achieved a 600 mV lower potential (FE = 97%) than with a Pt electrode. The photocathode + anode electrode configuration is usually employed to produce CO, since two-electron chemical products are commonly found over *p*-type semiconductors. More recently, Sahara et al.⁹⁵ generated CO using a dual photocathode–photoanode cell configuration with an external electrical (0.3 V) and chemical bias (0.10 V) in a hybrid photocathode of NiO-RuRe and a photoanode of CoO_x/TaON . The work can be considered the first example of a molecular–semiconductor hybrid PEC cell using water to reduce CO_2 . Different photoelectrodes, apart from those mentioned above, are also reported with good results such as *p*-type silicon nanowire with nitrogen-doped graphene quantum sheets (N-GQSS),¹⁰⁰ *p*-GaAs and *p*-InP,¹⁰¹ CoSn(OH)_6 ,¹⁰² and NiO-RuRe .¹⁰³ Figure 11 compares the FEs reported in the literature for CO for the different electrode configurations in the PEC: photocathode–dark anode (PC+A), photoanode–dark cathode (PA+C), and photocathode–photoanode (PA+PC). The results seem to show an enhanced reaction performance for a PC+A configuration.

Formic Acid. Particular reference is made in the literature to the formation of HCOOH , this being a product for which there is a growing demand and which is currently made by processes that are neither straightforward nor environmentally friendly.¹² Morikawa and co-workers⁹⁴ successfully achieved the photoreduction of CO_2 to HCOOH without applying any electrical bias, employing a photocathode–photoanode configuration separated by a PEM membrane, using water as a proton source and electron donor by conjugating an InP/Ru

complex for CO₂ reduction with a TiO₂ photocatalyst for water oxidation. HCOOH was generated continuously with a FE of >75%. However, the TiO₂ high band gap critically reduce its excitation wavelength to the UV range. Jiang et al.¹⁰⁷ expanded the TiO₂ optical absorption region from the UV absorption to the visible light region by depositing Fe₂O₃ (Fe₂O₃/TiO₂ NTs) with an onset wavelength of ~600 nm. The maximum selectivity was 99.89% with a rate of HCOOH production of 74896.13 nmol·h⁻¹·cm⁻² under optimal conditions in a photocathode–dark anode dual chamber cell using Pt as counter electrode. Employing a similar photoelectroreactor configuration, Gu and co-workers¹⁰⁸ reduced CO₂ to HCOOH without the need for a cocatalyst at an unparalleled underpotential. However, FE was limited due to the competitive reaction for H₂ formation (HER). In his work, a *p*-type Mg-doped CuFeO₂ electrode was found to reduce CO₂ to HCOOH photoelectrochemically with a maximum conversion efficiency at -0.9 V vs SCE using a LED source (470 nm) in experiments of 8 to 24 h. Shen and co-workers¹⁰⁹ reported in 2015 one of the highest yields to HCOOH. In this work, CO₂ was reduced using a photocathode–dark anode configuration at Cu nanoparticles decorated with Co₃O₄ nanotube arrays achieving a selectivity of nearly 100% employing a single compartment cell. The production of HCOOH was as high as 6.75 mmol·L⁻¹·cm⁻² in 8 h of experimental time. One year later, Huang et al.⁶⁶ improved the yield reported by Shen and co-workers employing also Co₃O₄ as the light harvester and Ru(bpy)₂dppz as the electron transfer mediator and CO₂ activator. The photoelectroreduction of CO₂ to HCOOH has been realized for 8 h with an onset potential as low as -0.69 V vs SCE (-0.45 V vs NHE) and an anode made of graphite. At an applied potential of -0.84 V vs SCE (-0.60 V vs NHE), the selectivity for HCOOH reached 99.95%, with a FE of 86% and a production of 110 μmol·cm⁻²·h⁻¹.

Nowadays, improvements in HCOOH formation continues with new strategies. Irtem and co-workers, continuing with their research line using Sn,^{110,111} proposed two strategies: concentration of solar light on the photoanode and adjustment of cathode area. At a voltage of 1.2 V and with a TiO₂ photoanode and a Sn cathode, FEs of 40%–65% for HCOO⁻ production were obtained, with energy efficiencies as high as 70% using a two-compartment cell (Figure 12). This study demonstrated that a stable photoanode optimized the system efficiency using a GDE as a cathode to enhance mass transfer and provide a wide photovoltage for O₂ evolution reaction (OER). Also, three PEC cell electrode configurations can be found in the literature for HCOOH production, where PC+A seems to be beneficial (Figure 13).

Methanol. CH₃OH as a key commodity has become an important part of our global economy. Several articles deal with CH₃OH production^{115–117} since it may directly replace fossil fuels without modifications of the actual energy distribution infrastructure.^{3,96,118} Moreover, CH₃OH is used in paints, building blocks for plastics, and organic solvents, among others. Ogura and Uchida¹⁴ were one of the first reporting the formation of CH₃OH by photoelectroreduction of CO₂ using a *n*-TiO₂ photoanode and a metal complex-confined Pt cathode separated by a PEM and a 500 W Xe lamp. In their experiments, it was observed that the feasibility for CO₂ reduction in a photocell depended mainly on the anolyte pH. pH higher than 12 led to CH₃OH formation in the cathode, and O₂ evolved at the photoanode. The photo-

reduction of CO₂ only occurred at a pH below 11 when applying external energy.

Yuan et al.¹¹⁹ proposed the photoelectroreduction of CO₂ using a Cu₂O photocathode and a graphite sheet as dark anode, obtaining a concentration and FE for CH₃OH formation of 1.41 mmol and 29.1%, respectively, after 1.5 h of operation at 1.5 V vs SCE in a single compartment cell with an irradiation of 100 mW·cm⁻² emitted from a Xe lamp. The formation rate of CH₃OH was 23.5 μmol·cm⁻²·h⁻¹. A higher rate for CH₃OH (45 μmol·cm⁻²·h⁻¹) was achieved in a light-driven two compartment reactor using Cu₂O/graphene/TiO₂ nanotube array (TNA) heterostructures and Pt as working electrode and counter electrode, respectively by Li et al.⁴⁰ An intensity of 100 mW·cm⁻² was applied by a 300 W Xe-arc lamp with a UV cutoff filter. Similar materials, but with different structure and in a single compartment cell, were employed by Lee and co-workers,¹²⁰ enhancing FE and stability toward CH₃OH production from CO₂ using Cu₂O nanowires photocathodes with a TiO₂–Cu⁺ shell. The FE after 2 h of operation improved from 23.6% for a Cu₂O photocathode to 56.5% for Cu₂O with a TiO₂–Cu⁺ shell mainly due to a lower resistance to charge transfer and an increased CO₂ adsorption. Recently, Yang et al.¹²¹ compared the CH₃OH formation at different catalytic processes (PEC, photocatalysis, electrocatalysis) on a SnO₂ NRs/Fe₂O₃ NTs photocathode and a Pt wire anode employing a single compartment cell. The largest CH₃OH production (2.05 mmol·L⁻¹·cm⁻²), obtained under visible light (1.1 V extra), was far higher than that individually electro- or photocatalytic reduction. As it is, the case for CO and HCOOH, the production of CH₃OH can be enhanced with a PC+A configuration (Figure 14). The extraordinary high FE obtained for CH₃OH formation (>100%) for PA+C system using TiO₂ as photoanode and Pt as cathode¹⁴ has been removed for a clear comparison.

Methane. Kaneko et al.¹⁰⁴ demonstrated that the selectivity for the photoelectrochemical reduction of CO₂ can be tuned by adding metal particles into the catholyte to form CH₄ in a dual compartment cell by adding Cu particles suspended CH₃OH using a *p*-InP and a Pt foil as photocathode and anode, respectively. A maximum FE for CH₄ of 0.56% was achieved at 265 K under a 5000 W Xe lamp. In order to enhance the CH₄ production efficiency, Wang and co-workers⁸⁸ presented the use of ordered mesoporous TiO₂ as photocathode and Pt as anode for CO₂ reduction to CH₄. The ordered mesoporous TiO₂ exhibits a higher and stable production efficiency for CH₄ (0.192 μmol·g_{catalyst}⁻¹·h⁻¹) which is 71 and 53 times higher than that for a commercial TiO₂ (P25) and disordered mesoporous TiO₂, respectively. Employing a photoanode–dark cathode electrode configuration in a dual cell compartment, a FE of 67% for CH₄ at -1.39 V vs SCE (-0.75 V vs RHE) and 71.6% for all carbon-containing products at -1.34 V vs SCE (-0.65 V vs RHE) was achieved by Magesh et al.⁹² using Cu as a cathode electrocatalyst and WO₃ as photoanode under bias potential. Moreover, in a photocathode–dark anode electrode configuration, Ong and co-workers⁴⁴ reached 2.923 μmol·g_{catalyst}⁻¹·h⁻¹ of CH₄ under visible light irradiation employing a carbon nanodot/g-C₃N₄ (CND/pCN) hybrid heterojunction photocatalyst with a mass loadings of 3% of CNDs and a Pt foil as anode. This improved in 3.6 times the CH₄ generated with pCN pure. Thompson et al.¹²³ reported an initial conversion rate of 2596 μL·g_{catalyst}⁻¹·h⁻¹ of CH₄, the highest reported to date, employing Cu as cathode and TiO₂ as photoanode

without using an external wire. Only UV light as an energy source was employed to reduce CO₂. In any case, FEs to CH₄ are rarely reported with values ranging from 54.6% to 67% for a PA+C configuration.^{79,92}

Long-Chain Hydrocarbons. Attending to thermodynamics, CO₂ reduction to long-chain hydrocarbons is more challenging because of the number of electron required.⁴ For instance, CO₂ reduction to CH₃OH requires a 6-electron process, while CO₂ reduction to isopropanol is a 18-electron reduction. These liquid fuels have higher energy densities and are more convenient for transport and storing. Ampelli et al.^{37,124} reduced CO₂ to liquid fuels (mainly CH₃CH(OH)CH₃) employing carbon-nanotube based electrodes, Pt/CNT and Fe/CNT, and nanostructured TiO₂ as photoanodes in a homemade Plexiglas-quartz window PEC reactor, reaching a production of 2.28·10⁻²·μmol·h⁻¹·cm⁻² of CH₃CH(OH)CH₃ for the Fe/CNT cathode. As seen in Figure 15, better results were achieved when instead of Fe-CNT, Fe-nitrogen-doped carbon nanotubes were employed (5.74·10⁻² μmol·h⁻¹·cm⁻²).

Genovese et al.⁵⁷ employed the same material but operated under a gas-phase electrocatalytic cell using electrodes based on metal nanoparticles supported and TiO₂ as photoanode. Long C-chain products (i.e., CH₃CH(OH)CH₃ and C₈–C₉) were obtained from CO₂. Employing also a TiO₂ photoanode and a nanostructured Pt/graphene aerogel deposited onto a Cu foam (Pt/GA/CF), Zhang and co-workers¹¹⁴ revealed that the Pt/GA/CF electrode improved CO₂ reduction significantly and facilitated the conversion of C₁ to high-order products due to enhanced charge transportation. HCOOH, CH₃COOH, C₂H₅COOH, CH₃OH, and C₂H₅OH were the main products detected. Recently, Yuan et al.¹²⁵ showed in his study an outstanding performance for C₂H₅OH production. At a Cu₂O foam cathode, the solar-driven conversion of CO₂ to C₂H₅OH led to a formation rate as high as 71.67 μmol·cm⁻²·h⁻¹ at only 131 mV within 1.5 h. There are a variety of FEs reported for different hydrocarbons, with values ranging from 32.6% to 52% for PC+A configurations^{59,73} and 2.7 to 45% for PA+C configurations.^{41,92,114}

Finally, Tables 3, 4, 5, and 6 summarize the literature on the topic, paying special attention to the reactor/electrode configuration but also including photoelectrocatalytic materials, main products obtained, and process conditions.

CONCLUSIONS AND FUTURE PERSPECTIVES

The photoelectrocatalytic reduction of CO₂ is a promising technological alternative that combines the advantages of electrocatalysis and photocatalysis, reducing the applied voltage needed in CO₂ conversion to useful chemicals. Undoubtedly, many issues remain to be solved before photoelectrocatalytic processes come to reality, although the technology presents potential for an enhanced CO₂ reduction efficiency under the Sun.

The design of a photoelectrochemical reactor should be made based on a careful evaluation of different factors, such as light source, geometrical configuration, construction material, heat exchange, mixing and flow characteristics, etc. Two key parameters in the process are the phases involved and the mode of operation (i.e., batch, semibatch, or continuous). Photocatalysts can be generally tested in either fluidized or fixed bed reactors. Besides, the anode and cathode in the photoelectrochemical device should be preferably in the form of thin films separated by a proton-conducting membrane and deposited over porous substrates, which allows an efficient

collection/transport of electrons as well as the diffusion of protons through the membrane. For CO₂ photoreduction, an efficient evolution of oxygen on the anode side is also needed, as well as an efficient diffusion of CO₂ on the cathode side.

A photocathode–dark anode configuration has been commonly reported for CO₂ reduction. This configuration employs a photocathode made of a *p*-type semiconductor because of their high conduction band energy suitable for CO₂ reduction, but its efficiency is limited. In the last years, the photoanode–dark cathode configuration is being used more frequently due to the benefits of using *n*-type semiconductors instead of *p*-type semiconductors, which are Earth abundant, cheap, and stable for H₂O oxidation. Another option for the arrangement of the photoelectrodes in the photoelectrochemical is the combination of a photocathode made of a *p*-type semiconductor for CO₂ reduction with a photoanode made of a *n*-type semiconductor for H₂O oxidation. This configuration, in contrast to the other two, allows realizing the reduction of CO₂ with H₂O without an external electric bias.

AUTHOR INFORMATION

Corresponding Author

*E-mail: sergio.castro@unican.es.

ORCID

Sergio Castro: 0000-0002-3814-9420

Jonathan Albo: 0000-0001-6781-5704

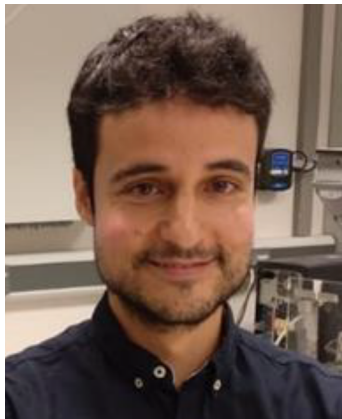
Notes

The authors declare no competing financial interest.

Biographies



Sergio Castro studied Chemical Engineering at University of Cantabria (2015), where he obtained his Master's (2017) in Chemical Engineering. At present, he is a Predoctoral Researcher in the Department of Chemical and Biomolecular Engineering and member of the DePRO research group headed by Prof. Irabien (<http://grupos.unican.es/depro/>) in the same university. The primary focus of his research areas are in the field of the electro- and photoelectrocatalytic conversion of CO₂ into valuable products.



Jonathan Albo obtained his MSc in Chemical Engineering (2010) from the University of Cantabria. In 2012, he completed his PhD in Chemical Engineering at the same University, focused on the development of new membrane-based processes for CO₂ separation. He next held a JSPS postdoctoral fellowship (2013) at Hiroshima University and then joined the University of the Basque Country as a Juan de la Cierva researcher (2014–2016). At present, he is Ramón y Cajal senior researcher at the Chemical and Biomolecular Engineering Department, University of Cantabria. His main research interests are in the field of electro-photoelectro-and-photocatalytic conversion of CO₂ to value-added chemicals.



Angel Irabien is Full Professor of Chemical Engineering in the Department of Chemical and Biomolecular Engineering at the University of Cantabria (Spain) after his PhD thesis, Associated Professor position in the Basque Country University and Academic Visitor stays in the Kings College (U London, UK), Friedrich Alexander Universität (Germany) and Oxford University (UK). His research interest include the development of carbon capture and utilization processes based on electrochemical reactors and renewable energy and the application of Life Cycle Thinking to the Chemical and Process Engineering.

ACKNOWLEDGMENTS

The authors acknowledge the financial support from the Spanish Ministry of Economy and Competitiveness (MINECO) under the project CTQ2016-76231-C2-1-R and Ramón y Cajal programme (RYC-2015-17080).

REFERENCES

- (1) Peng, Y. P.; Yeh, Y. T.; Wang, P. Y.; Huang, C. P. A solar cell driven electrochemical process for the concurrent reduction of carbon dioxide and degradation of azo dye in dilute KHCO₃ electrolyte. *Sep. Purif. Technol.* **2013**, *117*, 3–11.
- (2) Zheng, Y.; Zhang, W.; Li, Y.; Chen, J.; Yu, B.; Wang, J.; Zhang, L.; Zhang, J. Energy related CO₂ conversion and utilization: Advanced materials/ nanomaterials, reaction mechanisms and technologies. *Nano Energy* **2017**, *40*, 512–539.
- (3) Albo, J.; Alvarez-Guerra, M.; Castaño, P.; Irabien, A. Towards the electrochemical conversion of carbon dioxide into methanol. *Green Chem.* **2015**, *17*, 2304–2324.
- (4) Albo, J.; Irabien, A. Cu₂O-loaded gas diffusion electrodes for the continuous electrochemical reduction of CO₂ to methanol. *J. Catal.* **2016**, *343*, 232–239.
- (5) Albo, J.; Beobide, G.; Castaño, P.; Irabien, A. Methanol electrosynthesis from CO₂ at Cu₂O/ZnO prompted by pyridine-based aqueous solutions. *J. CO₂ Util.* **2017**, *18*, 164–172.
- (6) Das, S.; Daud, W. M. A. Photocatalytic CO₂ transformation into fuel: A review on advances in photocatalyst and photoreactor. *Renewable Sustainable Energy Rev.* **2014**, *39*, 765–805.
- (7) Harriman, A. Prospects for conversion of solar energy into chemical fuels: the concept of a solar fuels industry. *Philos. Trans. R. Soc., A* **2013**, *371*, 20110415–20110415.
- (8) Yan, Y.; et al. Photoelectrocatalytic Reduction of Carbon Dioxide. In *Carbon Dioxide Utilisation*; Styring, P., Quadrelli, E. A., Armstrong, K., Eds.; Elsevier B.V., 2015.
- (9) Ibrahim, N.; Kamarudin, S. K.; Minggu, L. J. Biofuel from biomass via photo-electrochemical reactions: An overview. *J. Power Sources* **2014**, *259*, 33–42.
- (10) Graves, C.; Ebbesen, D.; Mogensen, M.; Lackner, S. Sustainable hydrocarbon fuels by recycling CO₂ and H₂O with renewable or nuclear energy. *Renewable Sustainable Energy Rev.* **2011**, *15*, 1–23.
- (11) Jiang, Z.; Xiao, Z.; Kuznetsov, V. L.; Edwards, P. P. Turning carbon dioxide into fuel. *Philos. Trans. R. Soc., A* **2010**, *368*, 3343–3364.
- (12) Chaplin, R. P. S.; Wragg, A. A. Effects of process conditions and electrode material on reaction pathways for carbon dioxide electro-reduction with particular reference to formate formation. *J. Appl. Electrochem.* **2003**, *33*, 1107–1123.
- (13) Kumar, B.; Llorente, M.; Froehlich, J.; Dang, T.; Sathrum, A.; Kubiak, C. P. Photochemical and Photoelectrochemical Reduction of CO₂. *Annu. Rev. Phys. Chem.* **2012**, *63*, 541–69.
- (14) Ogura, K.; Uchida, H. Electrocatalytic reduction of CO₂ to methanol. *J. Electroanal. Chem. Interfacial Electrochem.* **1987**, *220*, 333–337.
- (15) Halmann, M. Photoelectrochemical reduction of aqueous carbon dioxide on *p*-type gallium phosphide in liquid junction solar cells. *Nature* **1978**, *275*, 115–116.
- (16) Sudha, D.; Sivakumar, P. Review on the photocatalytic activity of various composite catalysts. *Chem. Eng. Process.* **2015**, *97*, 112–133.
- (17) Nikokavoura, A.; Trapalis, C. Alternative photocatalysts to TiO₂ for the photocatalytic reduction of CO₂. *Appl. Surf. Sci.* **2017**, *391*, 149–174.
- (18) Herron, J. A.; Kim, J.; Upadhye, A. A.; Huber, G. W.; Maravelias, C. T. A general framework for the assessment of solar fuel technologies. *Energy Environ. Sci.* **2015**, *8*, 126–157.
- (19) Herron, J. A.; Maravelias, C. T. Assessment of solar-to-fuels strategies: photocatalysis and electrocatalytic reduction. *Energy Technol.* **2016**, *4*, 1369–1391.
- (20) Yue, P. L. Introduction to the modelling and design of photoreactors. In *Photoelectrochemistry, Photocatalysis and Photoreactors*; Schiavello, M., Eds.; Springer: Dordrecht, 1985.
- (21) Cassano, A. E.; Alfano, O. M. Design and Analysis of Homogeneous and Heterogeneous Photoreactors. In *Chemical Engineering: Trends and Developments*; Galán, M. A.; Del Valle, E. M., Eds.; John Wiley & Sons, Ltd: Chichester, U.K., 2005.
- (22) Bard, A. J. Photoelectrochemistry and heterogenous photocatalysis at semiconductors. *J. Photochem.* **1979**, *10*, 59–75.
- (23) Tryk, D. A.; Fujishima, A.; Honda, K. Recent topics in photoelectrochemistry: achievements and future prospects. *Electrochim. Acta* **2000**, *45*, 2363–2376.

- (24) Habisreutinger, S. N.; Schmidt-Mende, L.; Stolarczyk, J. K. Photocatalytic Reduction of CO₂ on TiO₂ and Other Semiconductors. *Angew. Chem., Int. Ed.* **2013**, *52*, 7372–7408.
- (25) Zhao, J.; Wang, X.; Xu, Z.; Loo, J. S. C. Hybrid catalysts for photoelectrochemical reduction of carbon dioxide: a prospective review on semiconductor/metal complex co-catalyst systems. *J. Mater. Chem. A* **2014**, *2*, 15228–15233.
- (26) Highfield, J. Advances and Recent Trends in Heterogeneous Photo (Electro)-Catalysis for Solar Fuels and Chemicals. *Molecules* **2015**, *20*, 6739–6793.
- (27) Ampelli, C.; Centi, G.; Passalacqua, R.; Perathoner, S. Electrolyte-less design of PEC cells for solar fuels: prospects and open issues in the development of cells and related catalytic electrodes. *Catal. Today* **2016**, *259*, 246–258.
- (28) Xie, S.; Zhang, Q.; Liu, G.; Wang, Y. Photocatalytic and photoelectrocatalytic reduction of CO₂ using heterogeneous catalysts with controlled nanostructures. *Chem. Commun.* **2016**, *52*, 35–59.
- (29) Ozer, L. Y.; Garlisi, C.; Oladipo, H.; Pagliaro, M.; Sharief, S. A.; Yusuf, A.; Almheiri, S.; Palmisano, G. Inorganic semiconductors-graphene composites in photo(electro)catalysis: Synthetic strategies, interaction mechanisms and applications. *J. Photochem. Photobiol., C* **2017**, *33*, 132–164.
- (30) Wang, P.; Wang, S.; Wang, H.; Wu, Z.; Wang, L. Recent Progress on Photo-Electrocatalytic Reduction of Carbon Dioxide. *Part. Part. Syst. Charact.* **2018**, *35*, 1700371.
- (31) Chen, D.; Sivakumar, M.; Ray, A. K. Heterogeneous Photocatalysis in Environmental Remediation. *Dev. Chem. Eng. Miner. Process.* **2000**, *8*, 505–550.
- (32) Ampelli, C.; Passalacqua, R.; Perathoner, S.; Centi, G. Nano-engineered materials for H₂ production by water photo-electrolysis. *Chem. Eng. Trans.* **2009**, *17*, 1011–1016.
- (33) Ola, O.; Maroto-Valer, M. M. Review of material design and reactor engineering on TiO₂ photocatalysis for CO₂ reduction. *J. Photochem. Photobiol., C* **2015**, *24*, 16–42.
- (34) Szaniawska, E.; Bienkowski, K.; Rutkowska, I. A.; Kulesza, P. J.;olarska, R. Enhanced photoelectrochemical CO₂-reduction system based on mixed Cu₂O- nonstoichiometric TiO₂ photocathode. *Catal. Today* **2018**, *300*, 145–151.
- (35) Chu, S.; Fan, S.; Wang, Y.; Rossouw, D.; Wang, Y.; Botton, G. A.; Mi, Z. Tunable Syngas Production from CO₂ and H₂O in an Aqueous Photoelectrochemical Cell. *Angew. Chem., Int. Ed.* **2016**, *55*, 14262–14266.
- (36) Li, K.; Peng, B.; Peng, T. Recent Advances in Heterogeneous Photocatalytic CO₂ Conversion to Solar Fuels. *ACS Catal.* **2016**, *6*, 7485–7527.
- (37) Ampelli, C.; Centi, G.; Passalacqua, R.; Perathoner, S. Synthesis of solar fuels by a novel photoelectrocatalytic approach. *Energy Environ. Sci.* **2010**, *3*, 292–301.
- (38) Sato, S.; Arai, T.; Morikawa, T.; Uemura, K.; Suzuki, M.; Tanaka, H.; Kajino, T. Selective CO₂ Conversion to Formate Conjugated with H₂O Oxidation Utilizing Semiconductor/Complex Hybrid Photocatalysts. *J. Am. Chem. Soc.* **2011**, *133*, 15240–15243.
- (39) Alenezi, K.; Ibrahim, K.; Li, P.; Pickett, J. Solar Fuels: Photoelectrosynthesis of CO from CO₂ at *p*-Type Si using Fe Porphyrin Electrocatalysts. *Chem. - Eur. J.* **2013**, *19*, 13522–13527.
- (40) Li, F.; Zhang, L.; Tong, J.; Liu, Y.; Xu, S.; Cao, Y.; Cao, S. Photocatalytic CO₂ conversion to methanol by Cu₂O/graphene/TNA heterostructure catalyst in a visible-light-driven dual-chamber reactor. *Nano Energy* **2016**, *27*, 320–329.
- (41) Cheng, J.; Zhang, M.; Wu, G.; Wang, X.; Zhou, J.; Cen, K. Photoelectrocatalytic Reduction of CO₂ into Chemicals Using Pt-Modified Reduced Graphene Oxide Combined with Pt-Modified TiO₂ Nanotubes. *Environ. Sci. Technol.* **2014**, *48*, 7076–7084.
- (42) Urbain, F.; Tang, P.; Carretero, N. M.; Andreu, T.; Gerling, L. G.; Voz, C.; Arbiol, J.; Morante, J. R. A prototype reactor for highly selective solar-driven CO₂ reduction to synthesis gas using nanosized earth-abundant catalysts and silicon photovoltaics. *Energy Environ. Sci.* **2017**, *10*, 2256.
- (43) Schreier, M.; Héroguel, F.; Steier, L.; Ahmad, S.; Luterbacher, J. S.; Mayer, M. T.; Luo, J.; Grätzel, M. Solar conversion of CO₂ to CO using Earth-abundant electrocatalysts prepared by atomic layer modification of CuO. *Nature Energy* **2017**, *2*, 17087.
- (44) Ong, W. J.; Putri, L. K.; Tan, Y. C.; Tan, L. L.; Li, N.; Ng, Y. H.; Wen, X.; Chai, S. P. Unravelling charge carrier dynamics in protonated g-C₃N₄ interfaced with carbon nanodots as co-catalysts toward enhanced photocatalytic CO₂ reduction: A combined experimental and first-principles DFT study. *Nano Res.* **2017**, *10* (5), 1673–1696.
- (45) Usuharatana, P.; McMakin, D.; Veawab, A.; Tontiwachwuthikul, P. Photocatalytic Process for CO₂ Emission Reduction from Industrial Flue Gas Streams. *Ind. Eng. Chem. Res.* **2006**, *45*, 2558–2568.
- (46) Nguyen, T. V.; Wu, J. C. S. Photoreduction of CO₂ in an optical-fiber photoreactor: Effects of metals addition and catalyst carrier. *Appl. Catal., A* **2008**, *335*, 112–120.
- (47) Du, P.; Carneiro, J. T.; Moulijn, J. A.; Mul, G. A novel photocatalytic monolith reactor for multiphase heterogeneous photocatalysis. *Appl. Catal., A* **2008**, *334*, 119–128.
- (48) Perego, C.; Peratello, S. Experimental methods in catalytic kinetics. *Catal. Today* **1999**, *52*, 133–145.
- (49) Mukherjee, P. S.; Ray, A. K. Major Challenges in the Design of a Large-Scale Photocatalytic Reactor for Water Treatment. *Chem. Eng. Technol.* **1999**, *22* (3), 253–260.
- (50) Van Gerven, T.; Mul, G.; Moulijn, J.; Stankiewicz, A. A review of intensification of photocatalytic processes. *Chem. Eng. Process.* **2007**, *46*, 781–789.
- (51) Lin, H.; Valsaraj, K. T. An Optical Fiber Monolith Reactor for Photocatalytic Wastewater Treatment. *AIChE J.* **2006**, *52* (6), 2271–2280.
- (52) Sun, R.; Nakajima, A.; Watanabe, I.; Watanabe, T.; Hashimoto, K. TiO₂-coated optical fiber bundles used as a photocatalytic filter for decomposition of gaseous organic compounds. *J. Photochem. Photobiol., A* **2000**, *136*, 111–116.
- (53) Kondratenko, E. V.; Mul, G.; Baltrusaitis, J.; Larrazábal, G. O.; Pérez-Ramírez, J. Status and perspectives of CO₂ conversion into fuels and chemicals by catalytic, photocatalytic and electrocatalytic processes. *Energy Environ. Sci.* **2013**, *6*, 3112–3135.
- (54) Merino-García, I.; Alvarez-Guerra, E.; Albo, J.; Irabien, A. Electrochemical membrane reactors for the utilization of carbon dioxide. *Chem. Eng. J.* **2016**, *305*, 104–120.
- (55) Delacourt, C.; Ridgway, P. L.; Kerr, J. B.; Newman, J. Design of an electrochemical cell making syngas (CO + H₂) from CO₂ and H₂O reduction at room temperature. *J. Electrochem. Soc.* **2008**, *155*, B42–B49.
- (56) Currao, A. Photoelectrochemical Water Splitting. *Chimia* **2007**, *61*, 815–819.
- (57) Genovese, C.; Ampelli, C.; Perathoner, S.; Centi, G. Electrocatalytic conversion of CO₂ to liquid fuels using nanocarbon-based electrodes. *J. Energy Chem.* **2013**, *22*, 202–213.
- (58) Singh, M. R.; Clark, E. L.; Bell, A. T. Effects of electrolyte, catalyst, and membrane composition and operating conditions on the performance of solar-driven electrochemical reduction of carbon dioxide. *Phys. Chem. Chem. Phys.* **2015**, *17*, 18924–18936.
- (59) Ba, X.; Yan, L.; Huang, S.; Yu, J.; Xia, X.; Yu, Y. New Way for CO₂ Reduction under Visible Light by a Combination of a Cu Electrode and Semiconductor Thin Film: Cu₂O Conduction Type and Morphology Effect. *J. Phys. Chem. C* **2014**, *118*, 24467–24478.
- (60) Kim, B.; Hillman, F.; Ariyoshi, M.; Fujikawa, S.; Kenis, P. J. A. Effects of composition of the micro porous layer and the substrate on performance in the electrochemical reduction of CO₂ to CO. *J. Power Sources* **2016**, *312*, 192–198.
- (61) Del Castillo, A.; Alvarez-Guerra, M.; Irabien, A. Continuous Electroreduction of CO₂ to Formate Using Sn Gas Diffusion Electrodes. *AIChE J.* **2014**, *60*, 3557–3564.
- (62) Salvatore, D. A.; Weekes, D. M.; He, J.; Dettelbach, K. E.; Li, Y. C.; Mallouk, T. E.; Berlinguet, C. P. Electrolysis of Gaseous CO₂ to

- CO in a Flow Cell with a Bipolar Membrane. *ACS Energy Lett.* **2018**, *3*, 149–154.
- (63) Merino-Garcia, I.; Albo, J.; Irabien, A. Tailoring gas-phase CO₂ electroreduction selectivity to hydrocarbons at Cu nanoparticles. *Nanotechnology* **2018**, *29*, 014001.
- (64) Chang, X.; Wang, T.; Gong, J. CO₂ Photo-reduction: Insights into CO₂ Activation and Reaction on Surfaces of Photocatalysts. *Energy Environ. Sci.* **2016**, *9*, 2177–2196.
- (65) Zhang, M.; Cheng, J.; Xuan, X.; Zhou, J.; Cen, K. CO₂ Synergistic Reduction in a Photoanode-Driven Photoelectrochemical Cell with a Pt-Modified TiO₂ Nanotube Photoanode and a Pt Reduced Graphene Oxide Electrocathode. *ACS Sustainable Chem. Eng.* **2016**, *4*, 6344–6354.
- (66) Huang, X.; Shen, Q.; Liu, J.; Yang, N.; Zhao, G. CO₂ adsorption-enhanced semiconductor/metal-complex hybrid photoelectrocatalytic interface for efficient formate production. *Energy Environ. Sci.* **2016**, *9*, 3161–3171.
- (67) Kutz, R. B.; Chen, Q.; Yang, H.; Sajjad, S. D.; Liu, Z.; Masel, I. R. Sustainion Imidazolium-Functionalized Polymers for Carbon Dioxide Electrolysis. *Energy Technol.* **2017**, *5*, 929–936.
- (68) Li, Y. C.; Zhou, D.; Yan, Z.; Gonçalves, R. H.; Salvatore, D. A.; Berlinguet, C. P.; Mallouk, T. E. Electrolysis of CO₂ to Syngas in Bipolar Membrane-Based Electrochemical Cells. *ACS Energy Lett.* **2016**, *1*, 1149–1153.
- (69) Zhou, X.; Liu, R.; Sun, K.; Chen, Y.; Verlage, E.; Francis, S. A.; Lewis, N. S.; Xiang, C. Solar-Driven Reduction of 1 atm of CO₂ to Formate at 10% Energy-Conversion Efficiency by Use of a TiO₂-Protected III–V Tandem Photoanode in Conjunction with a Bipolar Membrane and a Pd/C Cathode. *ACS Energy Lett.* **2016**, *1*, 764–770.
- (70) Albo, J.; Sáez, A.; Solla-Gullón, J.; Montiel, V.; Irabien, A. Production of methanol from CO₂ electroreduction at Cu₂O and Cu₂O/ZnO-based electrodes in aqueous solution. *Appl. Catal., B* **2015**, *176–177*, 709–717.
- (71) Albo, J.; Vallejo, D.; Beobide, G.; Castillo, O.; Castaño, P.; Irabien, A. Copper-Based Metal–Organic Porous Materials for CO₂ Electrocatalytic Reduction to Alcohols. *ChemSusChem* **2017**, *10*, 1100–1109.
- (72) Endrodi, B.; Bencsik, G.; Darvas, F.; Jones, R.; Rajeshwar, K.; Janáky, C. Continuous-flow electroreduction of carbon dioxide. *Prog. Energy Combust. Sci.* **2017**, *62*, 133–154.
- (73) Homayoni, H.; Chanmanee, W.; de Tacconi, R.; Dennis, H.; Rajeshwar, K. Continuous Flow Photoelectrochemical Reactor for Solar Conversion of Carbon Dioxide to Alcohols. *J. Electrochem. Soc.* **2015**, *162* (8), E115–E122.
- (74) Xia, S.; Meng, Y.; Zhou, X.; Xue, J.; Pan, G.; Ni, Z. Ti/ZnO–Fe₂O₃ composite: Synthesis, characterization and applications as a highly efficient photoelectrocatalyst for methanol from CO₂ reduction. *Appl. Catal., B* **2016**, *187*, 122–133.
- (75) Wood, J.; Summers, H.; Clark, A.; Kaeffer, N.; Braeutigam, M.; Carbone, L.; D'Amario, L.; Fan, K.; Farre, Y.; Narbey, S.; Oswald, F.; Stevens, A.; Parmenter, D. J.; Fay, W.; La Torre, A.; et al. A comprehensive comparison of dye-sensitized NiO photocathodes for solar energy conversion. *Phys. Chem. Chem. Phys.* **2016**, *18*, 10727–10738.
- (76) Qin, G.; Zhang, Y.; Ke, X.; Tong, X.; Sun, Z.; Liang, M.; Xue, S. Photocatalytic reduction of carbon dioxide to formic acid, formaldehyde, and methanol using dye-sensitized TiO₂ film. *Appl. Catal., B* **2013**, *129*, 599–605.
- (77) Kaneko, S.; Katsumata, H.; Suzuki, T.; Ohta, K. Photoelectrocatalytic reduction of CO₂ in LiOH/methanol at metal-modified p-InP electrodes. *Appl. Catal., B* **2006**, *64*, 139–145.
- (78) Cheng, J.; Zhang, M.; Liu, J.; Zhou, J.; Cen, K. Cu foam cathode used as Pt-RGO catalyst matrix to improve CO₂ reduction in a photoelectrocatalytic cell with TiO₂ photoanode. *J. Mater. Chem. A* **2015**, *3*, 12947–12957.
- (79) Chang, X.; Wang, T.; Zhang, P.; Wei, Y.; Zhao, J.; Gong, J. Stable Aqueous Photoelectrochemical CO₂ Reduction by a Cu₂O Dark Cathode with Improved Selectivity for Carbonaceous Products. *Angew. Chem., Int. Ed.* **2016**, *55*, 1–6.
- (80) La Tempa, T. J.; Rani, S.; Bao, N.; Grimes, C. A. Generation of fuel from CO₂ saturated liquids using a p-Si nanowire // n-TiO₂ nanotube array photoelectrochemical cell. *Nanoscale* **2012**, *4*, 2245–2250.
- (81) Jacobsson, T. J.; Fjällström, V.; Edoff, M.; Edvinsson, T. Sustainable solar hydrogen production: from photoelectrochemical cells to PV-electrolyzers and back again. *Energy Environ. Sci.* **2014**, *7*, 2056.
- (82) Asadi, M.; Kim, K.; Liu, C.; Addepalli, A. V.; Abbasi, P.; Yasaei, P.; Phillips, P.; Behrangiin, A.; Cerrato, J. M.; Haasch, R.; Zapol, P.; Kumar, B.; Klie, R. F.; Abiade, J.; Curtiss, L. A.; Salehi-Khojin, A. Nanostructured transition metal dichalcogenide electrocatalysts for CO₂ reduction in ionic liquid. *Science* **2016**, *353*, 467–470.
- (83) White, J. L.; Herb, J. T.; Kaczur, J. J.; Majsztrik, P. W.; Bocarsly, A. B. Photons to formate: Efficient electrochemical solar energy conversion via reduction of carbon dioxide. *J. CO₂ Util.* **2014**, *7*, 1–5.
- (84) Li, K.; An, X.; Park, K. H.; Khraisheh, M.; Tang, J. A critical review of CO₂ photoconversion: Catalysts and reactors. *Catal. Today* **2014**, *224*, 3–12.
- (85) Inoue, T.; Fujishima, A.; Konishi, S.; Honda, K. Photoelectrocatalytic reduction of carbon dioxide in aqueous suspensions of semiconductor powders. *Nature* **1979**, *277*, 637–638.
- (86) Sekiya, T.; Ichimura, K.; Igarashi, M.; Kurita, S. Absorption spectra of anatase TiO₂ single crystals heat-treated under oxygen atmosphere. *J. Phys. Chem. Solids* **2000**, *61*, 1237–1242.
- (87) Liu, L.; Zhao, H.; Andino, J. M.; Li, Y. Photocatalytic CO₂ Reduction with H₂O on TiO₂ Nanocrystals: Comparison of Anatase, Rutile, and Brookite Polymorphs and Exploration of Surface Chemistry. *ACS Catal.* **2012**, *2* (8), 1817–1828.
- (88) Wang, T.; Meng, X.; Li, P.; Ouyang, S.; Chang, K.; Liu, G.; Mei, Z.; Ye, J. Photoreduction of CO₂ over the well-crystallized ordered mesoporous TiO₂ with the confined space effect. *Nano Energy* **2014**, *9*, 50–60.
- (89) Zhao, H.; Pan, F.; Li, Y. A review on the effects of TiO₂ surface point defects on CO₂ photoreduction with H₂O. *J. Materomics* **2017**, *3*, 17–32.
- (90) Barton, E.; Rampulla, M.; Bocarsly, B. Selective Solar-Driven Reduction of CO₂ to Methanol Using a Catalyzed p-GaP Based Photoelectrochemical Cell. *J. Am. Chem. Soc.* **2008**, *130*, 6342–6344.
- (91) Yu, Y.; Zhang, Z.; Yin, X.; Kvít, A.; Liao, Q.; Kang, Z.; Yan, X.; Zhang, Y.; Wang, X. Enhanced photoelectrochemical efficiency and stability using a conformal TiO₂ film on a black silicon photoanode. *Nature Energy* **2017**, *2*, 17045.
- (92) Magesh, G.; Kim, E. S.; Kang, H. J.; Banu, M.; Kim, J. Y.; Kim, J. H.; Lee, J. S. A versatile photoanode-driven photoelectrochemical system for conversion of CO₂ to fuels with high faradaic efficiencies at low bias potentials. *J. Mater. Chem. A* **2014**, *2*, 2044–2049.
- (93) Song, J. T.; Ryo, H.; Cho, M.; Kim, J.; Kim, J. G.; Chung, S. Y.; Oh, J. Nanoporous Au Thin Films on Si Photoelectrodes for Selective and Efficient Photoelectrochemical CO₂ Reduction. *Adv. Energy Mater.* **2017**, *7*, 1601103.
- (94) Morikawa, T.; Sato, S.; Arai, T.; Uemura, K.; Yamanaka, K. I.; Suzuki, T. M.; Kajino, T.; Motohiro, T. Selective CO₂ Reduction Conjugated with H₂O Oxidation Utilizing Semiconductor/Metal-Complex Hybrid Photocatalysts. *AIP Conf. Proc.* **2012**, *1568*, 11–15.
- (95) Sahara, G.; Kumagai, H.; Maeda, K.; Kaeffer, N.; Artero, V.; Higashi, M.; Abe, R.; Ishitani, O. Photoelectrochemical Reduction of CO₂ Coupled to Water Oxidation Using a Photocathode With a Ru(II)–Re(I) Complex Photocatalyst and a CoO_x/TaON Photoanode. *J. Am. Chem. Soc.* **2016**, *138*, 14152–14158.
- (96) Hu, B.; Guild, C.; Suib, S. L. Thermal, electrochemical, and photochemical conversion of CO₂ to fuels and value-added products. *J. CO₂ Util.* **2013**, *1*, 18–27.
- (97) Petit, J. P.; Chartier, P.; Beley, M.; Deville, J. P. Molecular catalysts in photoelectrochemical cells Study of an efficient system for the selective photoelectroreduction of CO₂: p-GaI or p-GaAs/Ni(cyclam)²⁺, aqueous medium. *J. Electroanal. Chem. Interfacial Electrochem.* **1989**, *269*, 267–281.

- (98) Hirota, K.; Tryk, A.; Yamamoto, T.; Hashimoto, K.; Okawa, M.; Fujishima, A. Photoelectrochemical reduction of CO₂ in a high-pressure CO₂ + methanol medium at *p*-type semiconductor electrodes. *J. Phys. Chem. B* **1998**, *102*, 9834–9843.
- (99) Kumar, B.; Smieja, J. M.; Kubiak, C. P. Photoreduction of CO₂ on *p*-type Silicon Using Re(bipy-But)(CO)₃Cl: Photovoltages Exceeding 600 mV for the Selective Reduction of CO₂ to CO. *J. Phys. Chem. C* **2010**, *114*, 14220–14223.
- (100) Yang, K. D.; Ha, Y.; Sim, U.; An, J.; Lee, C. W.; Jin, K.; Kim, Y.; Park, J.; Hong, J. S.; Lee, J. H.; Lee, H.-E.; Jeong, H.-Y.; Kim, H.; Nam, K. T. Graphene Quantum Sheet Catalyzed Silicon Photocathode for Selective CO₂ Conversion to CO. *Adv. Funct. Mater.* **2016**, *26*, 233–242.
- (101) Kaneko, S.; Katsumata, H.; Suzuki, T.; Ohta, K. Photoelectrochemical reduction of carbon dioxide at *p*-type gallium arsenide and *p*-type indium phosphide electrodes in methanol. *Chem. Eng. J.* **2006**, *116*, 227–231.
- (102) Lin, X.; Gao, Y.; Jiang, M.; Zhang, Y.; Hou, Y.; Dai, W.; Wang, S.; Ding, Z. Photocatalytic CO₂ reduction promoted by uniform perovskite hydroxide CoSn(OH)₆ nanocubes. *Appl. Catal., B* **2018**, *224*, 1009–1016.
- (103) Sahara, G.; Abe, R.; Higashi, M.; Morikawa, T.; Maeda, K.; Ueda, Y.; Ishitani, O. Photoelectrochemical CO₂ reduction using a Ru(II)-Re(I) multinuclear metal complex on a *p*-type semiconducting NiO electrode. *Chem. Commun.* **2015**, *51*, 10722–10725.
- (104) Kaneko, S.; Ueno, Y.; Katsumata, H.; Suzuki, T.; Ohta, K. Photoelectrochemical reduction of CO₂ at *p*-InP electrode in copper particle-suspended methanol. *Chem. Eng. J.* **2009**, *148*, 57–62.
- (105) Song, J.; Ryoo, H.; Cho, M.; Kim, J.; Kim, J. G.; Chung, S.; Oh, J. Nanoporous Au Thin Films on Si Photoelectrodes for Selective and Efficient Photoelectrochemical CO₂ Reduction. *Adv. Energy Mater.* **2017**, *7*, 1601103.
- (106) Weng, B.; Wei, W.; Yiligungum, Wu, H.; Alenizi, A. M.; Zheng, G. Bifunctional CoP and CoN Porous Nanocatalysts Derived from ZIF-67 In Situ Grown on Nanowire Photoelectrodes for Efficient Photoelectrochemical Water Splitting and CO₂ Reduction. *J. Mater. Chem. A* **2016**, *4*, 15353–1536.
- (107) Jiang, M.; Wu, H.; Li, Z.; Ji, D.; Li, W.; Liu, Y.; Yuan, D.; Wang, B.; Zhang, Z. Highly selective photoelectrochemical conversion of carbon dioxide to formic acid. *ACS Sustainable Chem. Eng.* **2018**, *6* (1), 82–87.
- (108) Gu, J.; Wuttig, A.; Krizan, J. W.; Hu, Y.; Detweiler, Z. M.; Cava, R. J.; Bocarsly, A. B. Mg-Doped CuFeO₂ Photocathodes for Photoelectrochemical Reduction of Carbon Dioxide. *J. Phys. Chem. C* **2013**, *117*, 12415–12422.
- (109) Shen, Q.; Chen, Z.; Huang, X.; Liu, M.; Zhao, G. High-yield and Selective Photoelectrocatalytic Reduction of CO₂ to Formate by Metallic Copper Decorated Co₃O₄ Nanotube Arrays. *Environ. Sci. Technol.* **2015**, *49*, 5828–5835.
- (110) Irtem, E.; Hernández-Alonso, M. D.; Parra, A.; Fàbrega, C.; Penelas-Pérez, G.; Morante, J. R.; Andreu, T. A photoelectrochemical flow cell design for the efficient CO₂ conversion to fuels. *Electrochim. Acta* **2017**, *240*, 225–230.
- (111) Irtem, E.; Andreu, T.; Parra, A.; Hernandez-Alonso, M. D.; García-Rodríguez, S.; Riesco-García, J. M.; Penelas-Pérez, G.; Morante, J. R. Low-energy formate production from CO₂ electro-reduction using electrodeposited tin on GDE. *J. Mater. Chem. A* **2016**, *4*, 13582–13588.
- (112) Arai, T.; Sato, S.; Uemura, K.; Morikawa, T.; Kajino, T.; Motohiro, T. Photoelectrochemical reduction of CO₂ in water under visible-light irradiation by a *p*-type InP photocathode modified with an electropolymerized ruthenium complex. *Chem. Commun.* **2010**, *46*, 6944–6946.
- (113) Arai, T.; Tajima, S.; Sato, S.; Uemura, K.; Morikawa, T.; Kajino, T. Selective CO₂ conversion to formate in water using a CZTS photocathode modified with a ruthenium complex polymer. *Chem. Commun.* **2011**, *47*, 12664–12666.
- (114) Zhang, M.; Cheng, J.; Xuan, X.; Zhou, J.; Cen, K. Pt/graphene aerogel deposited in Cu foam as a 3D binder-free cathode for CO₂ reduction into liquid chemicals in a TiO₂ photoanode-driven photoelectrochemical cell. *Chem. Eng. J.* **2017**, *322*, 22–32.
- (115) Ferreira de Brito, J.; Alves da Silva, A.; Cavalheiro, A. J.; Zanoni, M. V. B. Evaluation of the Parameters Affecting the Photoelectrocatalytic Reduction of CO₂ to CH₃OH at Cu/Cu₂O Electrode. *Int. J. Electrochem. Sci.* **2014**, *9*, 5961–5973.
- (116) Li, P.; Xu, J.; Jing, H.; Wu, C.; Peng, H.; Lu, J.; Yin, H. Wedged N-doped CuO with more negative conductive band and lower over potential for high efficiency photoelectric converting CO₂ to methanol. *Appl. Catal., B* **2014**, *156–157*, 134–140.
- (117) de Brito, J. F.; Araujo, A. R.; Rajeshwar, K.; Zanoni, M. V. B. Photoelectrochemical reduction of CO₂ on Cu/Cu₂O films: Product distribution and pH effects. *Chem. Eng. J.* **2015**, *264*, 302–309.
- (118) Ganesh, I. Conversion of carbon dioxide into methanol – a potential liquid fuel: Fundamental challenges and opportunities (a review). *Renewable Sustainable Energy Rev.* **2014**, *31*, 221–257.
- (119) Yuan, J.; Wang, X.; Gu, C.; Sun, J.; Ding, W.; Wei, J.; Zuo, X.; Hao, C. Photoelectrocatalytic reduction of carbon dioxide to methanol at cuprous oxide foam cathode. *RSC Adv.* **2017**, *7*, 24933–24939.
- (120) Lee, K.; Lee, S.; Cho, H.; Jeong, S.; Kim, W. D.; Lee, S.; Lee, D. C. Cu⁺-incorporated TiO₂ overlayer on Cu₂O nanowire photocathodes for enhanced photoelectrochemical conversion of CO₂ to methanol. *J. Energy Chem.* **2018**, *27*, 264–270.
- (121) Yang, Z.; Wang, H.; Song, W.; Wei, W.; Mu, Q.; Kong, B.; Li, P.; Yin, H. One dimensional SnO₂ NRs/Fe₂O₃ NTs with dual synergistic effects for photoelectrocatalytic reduction CO₂ into methanol. *J. Colloid Interface Sci.* **2017**, *486*, 232–240.
- (122) Wei, W.; Yang, Z.; Song, W.; Hu, F.; Luan, B.; Li, P.; Yin, H. Different CdSeTe structure determined photoelectrocatalytic reduction performance for carbon dioxide. *J. Colloid Interface Sci.* **2017**, *496*, 327–333.
- (123) Thompson, J. F.; Chen, B.; Kubo, M.; Londoño, N.; Minuzzo, J. Artificial photosynthesis device development for CO₂ photoelectrochemical conversion. *MRS Adv.* **2016**, *1*, 447–452.
- (124) Ampelli, C.; Passalacqua, R.; Genovese, C.; Perathoner, S.; Centi, G. A Novel Photo-electrochemical Approach for the Chemical Recycling of Carbon Dioxide to Fuels. *Chem. Eng. Trans.* **2011**, *25*, 683–688.
- (125) Yuan, J.; Xiao, B.; Hao, C. Photoelectrochemical Reduction of Carbon Dioxide to Ethanol at Cu₂O Foam Cathode. *Int. J. Electrochem. Sci.* **2017**, *12*, 8288–8294.
- (126) Qi, Y.; Xu, Q.; Wang, Y.; Yan, B.; Ren, Y.; Chen, Z. CO₂-Induced Phase Engineering: Protocol for Enhanced Photoelectrocatalytic Performance of 2D MoS₂ Nanosheets. *ACS Nano* **2016**, *10*, 2903–2909.
- (127) Kong, Q.; Kim, D.; Liu, C.; Yu, Y.; Su, Y.; Li, Y.; Yang, P. Directed Assembly of Nanoparticle Catalysts on Nanowire Photoelectrodes for Photoelectrochemical CO₂ Reduction. *Nano Lett.* **2016**, *16*, 5675–5680.
- (128) Cheng, J.; Zhang, M.; Wu, G.; Wang, X.; Zhou, J.; Cen, K. Optimizing CO₂ reduction conditions to increase carbon atom conversion using a Pt-RGO||Pt TNT photoelectrochemical cell. *Sol. Energy Mater. Sol. Cells* **2015**, *132*, 606–614.
- (129) Hasan, M. R.; Hamid, S. B. A.; Basirun, W. J.; Suhaimy, S. H. M.; Mat, A. N. C. A sol-gel derived, copper-doped, titanium dioxide-reduced graphene oxide nanocomposite electrode for the photoelectrocatalytic reduction of CO₂ to methanol and formic acid. *RSC Adv.* **2015**, *5*, 77803–77813.
- (130) Jang, Y. J.; Jeong, I.; Lee, J.; Lee, J.; Ko, M. J.; Lee, J. S. Unbiased sunlight-driven artificial photosynthesis of carbon monoxide from CO₂ using a ZnTe-based photocathode and a perovskite solar cell in tandem. *ACS Nano* **2016**, *10*, 6980–6987.
- (131) Wang, Y.; Fan, S.; AlOtaibi, B.; Wang, Y.; Li, L.; Mi, Z. A monolithically integrated gallium nitride nanowire/silicon solar cell photocathode for selective carbon dioxide reduction to methane. *Chem. - Eur. J.* **2016**, *22*, 8809–8813.
- (132) Nath, N. C. D.; Choi, S. Y.; Jeong, H. W.; Lee, J. J.; Park, H. Stand-alone photoconversion of carbon dioxide on copper oxide wire

arrays powered by tungsten trioxide/dye-sensitized solar cell dual absorbers. *Nano Energy* **2016**, *25*, 51–59.

3.2. Sergio Castro, Jonathan Albo, Ángel Irabien. 2018. Continuous conversion of CO₂ to alcohols in a TiO₂ photoanode-driven photoelectrochemical system. Journal of Chemical Technology and Biotechnology, 95, 7, 1876-1882.

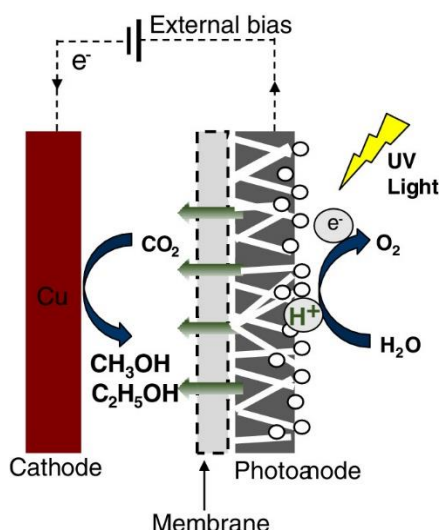


Figura 3.2. Resumen gráfico del artículo: "Continuous conversion of CO₂ to alcohols in a TiO₂ photoanode-driven photoelectrochemical system".

La reducción fotoelectroquímica de CO₂ genera un gran interés debido a los beneficios potenciales que ofrece en comparación con los enfoques electrocatalíticos y photocatalíticos. Entre los diversos materiales semiconductores disponibles, el TiO₂ es el más utilizado por su precio y disponibilidad. Además, el cobre es ampliamente reconocido como un electrocatalizador eficiente para la producción de alcoholes a partir de CO₂. Por lo tanto, el objetivo de este trabajo es acoplar un fotoánodo basado en TiO₂, iluminado con luz UV (100 mW·cm⁻²), en una celda electroquímica de tipo filtro prensa para la conversión en continuo de CO₂ a alcoholes, específicamente metanol y etanol. En este sentido, se busca reducir los requisitos de energía externa utilizando una placa de cobre como cátodo en ausencia de luz. Para lograr el objetivo general, los objetivos específicos, que se marcan en el trabajo son: (i) preparar y optimizar un fotoánodo basado en TiO₂-P25, (ii) adaptar una celda electroquímica para la conversión fotoelectroquímica de CO₂ en alcoholes y, finalmente, (iii) analizar el efecto del voltaje en el proceso en términos de velocidad de formación de productos, la eficiencia Faradaica y la eficiencia energética del proceso.

Los resultados muestran un aumento de hasta 4,3 mA·cm⁻² en la densidad de corriente al iluminar el fotoánodo y aplicar un voltaje de -2 V, medido con el electrodo de referencia de Ag/AgCl. Además, a un voltaje de -1,8 V versus Ag/AgCl, se alcanza una velocidad de producción de metanol de 9,5 µmol·m⁻²·s⁻¹, con una eficiencia Faradaica del 16,2% y una eficiencia energética del 5,2%. En el caso del etanol, se obtiene una velocidad de producción de 6,8 µmol·m⁻²·s⁻¹, con una Eficiencia Faradaica del 23,2% y una eficiencia energética del 6,8%. Estos resultados muestran los beneficios potenciales del sistema impulsado por la luz, en términos de rendimiento y eficiencia, al utilizar un fotoánodo en configuración MEA basado en TiO₂-P25 y cobre como cátodo. Además, se observa que el aumento del voltaje externo aplicado conduce a

una mayor producción de metanol, pero produce una disminución en la formación de etanol. El rendimiento del sistema supera a los sistemas anteriormente reportados en configuración fotoánodo-cátodo a oscuras para la reducción de CO₂ a alcoholes.

Continuous conversion of CO₂ to alcohols in a TiO₂ photoanode-driven photoelectrochemical system

Sergio Castro, Jonathan Albo ^{*} and Angel Irabien

Abstract

BACKGROUND: The recycling of CO₂ by photoelectrochemical reduction has attracted wide interest due to its potential benefits when compared to electro- and photo-catalytic approaches. Among the various available semiconductors, TiO₂ is the most employed material in photoelectrochemical cells. Besides, Cu is a well-known electrocatalyst for the production of alcohols from CO₂ reduction.

RESULTS: A photoelectrochemical cell consisting of a TiO₂-based membrane electrode assembly (MEA) photoanode and a Cu plate is employed to reduce CO₂ to methanol and ethanol continuously under UV illumination (100 mW cm⁻²). A maximum increment of 4.3 mA cm⁻² in current between the illuminated and dark conditions is achieved at -2 V versus Ag/AgCl. The continuous photoelectrochemical reduction process in the filter-press cell is evaluated in terms of reaction rate (*r*), as well as Faradaic efficiency (FE) and energy efficiency (EE). At -1.8 V versus Ag/AgCl, a maximum reaction rate of *r* = 9.5 μmol m⁻² s⁻¹, FE = 16.2% and EE = 5.2% for methanol and *r* = 6.8 μmol m⁻² s⁻¹, FE = 23.2% and EE = 6.8% for ethanol can be achieved.

CONCLUSIONS: The potential benefits of the photoanode-driven system, in terms of yields and efficiencies, are observed when employing a TiO₂-based MEA photoanode and Cu as dark cathode. The results demonstrate first the effect of UV illumination on current density, and then the formation of alcohols from the continuous photoreduction of CO₂. Increasing the external applied voltage leads to an enhanced production of methanol, but decreases ethanol formation. The system outperforms previous photoanode-based systems for CO₂-to-alcohols reactions.

© 2019 Society of Chemical Industry

Keywords: photoelectrocatalysis; CO₂ reduction; TiO₂; Cu; methanol; ethanol

INTRODUCTION

The concentration of CO₂ in the atmosphere has increased to worrying levels in recent years, mainly due to the burning of fossil fuels. This has accelerated research activities to obtain value-added products from residual CO₂, instead of discarding it as a residue.¹ There are various possibilities for converting CO₂ into valuable products. Among the technologies available, the electrochemical reduction of CO₂ has attracted great interest due to the potential economic and environmental benefits. This technology, apart from allowing CO₂ dissociation under ambient conditions using electricity, is also an excellent alternative for storing the intermittent energy produced from renewables in the form of chemical bonds.² Moreover, the integration of a light source in electrochemical reduction devices (a photoelectrochemical (PEC) approach) has attracted increasing interest recently because it may allow the avoidance of interconnections between devices, reducing, in principle, system capital costs and electricity losses.³ Compared to photocatalysis, the applied bias can cause band bending and help the oriented transfer of photogenerated electrons, decreasing the recombination of the photogenerated electron-hole pairs. Besides, photocatalytic materials with unfavourable band positions for CO₂ reduction and H₂O oxidation can be still used in photoelectrocatalytic systems when applying an external bias.

There are different electrode configurations for PEC systems depending on which electrode (i.e. anode, cathode or both) act as the photoelectrode.⁴ Photocathode-dark anode has been the most employed configuration.^{5–9} In this case, a *p*-type semiconductor is employed as photocathode and a metal as anode. Unfortunately, with *p*-type semiconductors, two-electron products are usually obtained and the system efficiency is low. On the other hand, CO₂ reduction in a photoanode-dark cathode PEC system is a simpler configuration and depends on the photoanode and the cathode activity independently,^{10–12} and offers the advantage of reducing the external energy requirements of the process.¹³ In this configuration, H₂O oxidation in the photoanode provides protons for CO₂ conversion in the cathode compartment. Besides, the negative potential generated in the photoanode by light supplies an additional negative potential for CO₂ reduction in the cathode.⁴ Another PEC photoelectrode configuration is a combination of a photocathode for CO₂ reduction with a photoanode

* Correspondence to: Jonathan Albo, Department of Chemical & Biomolecular Engineering, University of Cantabria, Avda Los Castros s/n, 39005 Santander, Spain. E-mail: albo@unican.es

Department of Chemical & Biomolecular Engineering, University of Cantabria, Santander, Spain

to deal with H₂O oxidation (as represented in Figure 1).^{13–15} In contrast to the previous configurations, the main advantage is that with some pairs of materials an external electrical energy supply for the redox reactions may, ideally, not be needed. However, in most cases, the voltage generated by the light source is not enough and a continuous external power supply is required.^{16,17}

The formation of alcohols from CO₂ has received increasing attention due to their proper integration in the actual fuel infrastructure, besides being considered as advantageous energy storage materials and precursors for the synthesis of other products.^{18–20} Methanol (CH₃OH) is considered an excellent energy intermediate due to its stable storage properties and high energy density. In addition to application as a fuel, CH₃OH is an intermediate to other bulk chemicals employed in everyday life products like plastics and paints.²¹ Ethanol (C₂H₅OH) is an important raw material with high heating value usually employed in disinfectants and organic materials.²² It can also replace fossil fuels in key sectors such as the transport industry.²³ Thus, both products offer an alternative to deal with climate change, reducing the dependence on fossil fuels and allowing CO₂ recycling in a neutral carbon cycle.^{18,24}

TiO₂ is the most employed semiconductor in photo-assisted processes.^{25–28} It is an *n*-type semiconductor that possesses a wide bandgap (3.0 eV) and mainly absorbs UV light.²⁹ This semiconductor has been considered a low-cost and environmentally friendly material³⁰ since the first report in 1979.²⁵ Also, Cu has been demonstrated to possess the capacity to be used to produce hydrocarbons and alcohols from CO₂.³¹ In particular, previous studies in our group employed a Cu plate for CO₂ electroreduction, with a reaction rate for CH₃OH of $r = 8.7 \mu\text{mol m}^{-2} \text{s}^{-1}$ and a Faradaic efficiency (*FE*) of 4.6% at –1.3 V versus Ag/AgCl. These values were subsequently enhanced by using Cu oxide^{31,32} and metal–organic framework-based electrodes under different experimental conditions in continuous operation mode.^{18,31–33}

Thus, the aim of the present work is the coupling of a TiO₂-based photoanode in an electrochemical filter-press cell for the continuous conversion of CO₂ to alcohols (i.e. CH₃OH and C₂H₅OH) in order to reduce the external energy requirements, and so reduce energy consumption. A Cu plate is used as dark cathode for designing a reliable photoanode–dark cathode configuration for CO₂ photoreduction. The specific objectives are as follows: (i) to prepare and optimize a TiO₂-based photoanode, (ii) to adapt an electrochemical cell for the PEC conversion of CO₂ to alcohols and finally, (iii) to analyse the effect of voltage on process performance. The results are considered a step further in the development of continuous CO₂ conversion processes using sunlight.

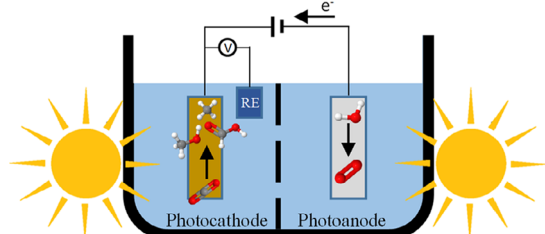


Figure 1. PEC cell in a photocathode–photoanode configuration. Reprinted with permission from.² Copyright 2018 American Chemical Society.

EXPERIMENTAL

TiO₂ photoanode preparation

A TiO₂ photoanode was fabricated by air-brushing an ink composed of a mixture of TiO₂ (Sigma Aldrich, P25), Nafion (Alfa Aesar, 5 wt%) as binder and isopropanol (99.5%, Sigma Aldrich) as vehicle, with a 70:30 wt% TiO₂/Nafion ratio in 3 wt% of solid in the final isopropanol dispersion onto a Toray carbon paper (TGP-H60). An ultrasound bath was used to homogenize the mixture. The TiO₂ loading varied from 1 to 3 mg cm^{–2}. The TiO₂ photoanode was coupled by hot-pressing with a Nafion membrane (Nafion 117), previously activated in HCl for 30 min and rinsed with deionized water before use, forming a membrane electrode assembly (MEA) able to enhance H⁺ transport, reducing mass transfer limitations.^{33,35}

Photoelectroreduction cell and experimental conditions

The continuous PEC reduction of CO₂ was carried out using a commercial filter-press cell reactor (Electrocelf, Denmark), employing a Cu plate as cathode and the prepared MEA as photoanode, which also separates the cell compartments. A 1 mol L^{–1} KOH aqueous solution was used as catholyte and anolyte and a cold UV LED light (100 mW cm^{–2}) was used to illuminate the photoactive area (10 cm²) of the TiO₂ photoanode. On the cathode side, there were two inputs: the catholyte and the CO₂ gas; and one output: the catholyte with the reaction products (liquid and gaseous). The Cu plate acted as working electrode, the TiO₂ photoelectrode as counter electrode and Ag/AgCl as reference electrode. The reduction of CO₂ was conducted under ambient conditions. Figure 2 shows a scheme of the experimental setup, while Figure 3 shows a detailed view of the cell configuration. The experimental system included four tanks for inlet and outlet electrolyte solutions, two peristaltic pumps to circulate the liquid at a flow rate of 10 mL min^{–1}, two pressure indicators and mass-flow controllers to fix the CO₂ inlet flow rate at 180 mL min^{–1}. Moreover, a potentiostat (AutoLab PGSTAT 302N) was used. The PEC behaviour of the TiO₂ photoanode was evaluated in a one-compartment glass at a scan rate of 50 mV s^{–1} after 20 cycles with and without light illumination.

Continuous experiments in the PEC cell were performed in duplicate during 50 min. Both liquid and gas samples were taken every 10 min, and a final average concentration was calculated for each test. Values that were two times lower/higher than the average value were discarded in order to calculate the reaction rate (*r*) and the *FE* with an error of less than 10%. The values were normalized to reacting CO₂ (inlet–outlet) in

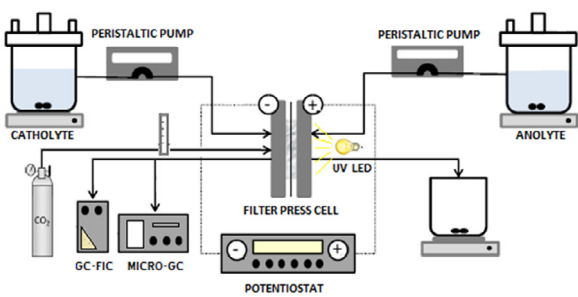


Figure 2. Experimental system for continuous PEC reduction of CO₂. Adapted with permission from.³⁶ Copyright 2017 Wiley.

the system and adjusted to $FE = 100\%$. To collect the gaseous samples, the experimental system was pressurized to 0.2 bar for subsequent analysis using an in-line gas microchromatograph (3000 Micro GC, Inficon). Liquid samples were analysed using a gas chromatograph (GCMSQP2010 Ultra, Shimadzu) equipped with a flame ionization detector. The reaction rate shows the formation rate for every product per unit of area and time ($\mu\text{mol m}^{-2} \text{s}^{-1}$) and the FE is defined as the selectivity of the reaction to form each product, calculated according to Eqn (1):

$$FE (\%) = \frac{z \cdot n \cdot F}{q} \times 100 \quad (1)$$

where z is the theoretical number of electrons exchanged to form the desired product, n is the number of moles produced, F is the Faraday constant ($96\,485 \text{ C mol}^{-1}$) and q is the total charge applied in the process. Moreover, the energy efficiency (EE), which indicates the total energy used towards the formation of the desired products, can be calculated according to Eqn (2):

$$EE (\%) = \frac{E_T}{E} \times FE \quad (2)$$

where E is the real potential applied in the system and E_T the theoretical potential needed for the formation of CH_3OH ($-0.58 \text{ V versus Ag/AgCl}$) and $\text{C}_2\text{H}_5\text{OH}$ ($-0.53 \text{ V versus Ag/AgCl}$).

RESULTS AND DISCUSSION

PEC behaviour of TiO_2 photoelectrode

Figure 4(a) shows the photocurrent response of the TiO_2 photoanode MEA during on-off illumination cycles in a one-compartment glass under UV illumination of 100 mW cm^{-2} at $-1.8 \text{ V versus Ag/AgCl}$ in the presence of CO_2 , while Figure 4(b) shows the current densities observed with and without illumination in the cell when CO_2 is continuously bubbled in a potential range between -1.2 and $-2 \text{ V versus Ag/AgCl}$ and with a TiO_2 loading of 3 mg cm^{-2} , where an optimal reduction of CO_2 to alcohols can be expected.^{34,37,38} It should be noted that the TiO_2 -based photoanode showed no changes in response (current) during on-off cycles when illuminated with visible LED light (100 mW cm^{-2}).

First, the current density of the system under UV light is larger than that in dark conditions in on-off cycles (Figure 4(a)) at $-1.8 \text{ V versus Ag/AgCl}$. Then, Figure 4(b) shows that an increase in current density under UV illumination can be observed for the whole potential range evaluated. The variation in current density

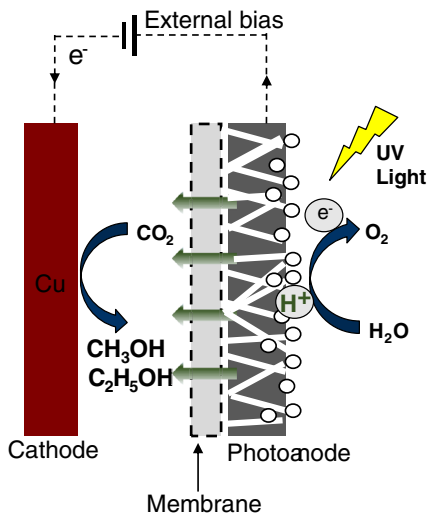


Figure 3. Detail of PEC cell configuration. Adapted with permission from.³² Copyright 2016 Elsevier.

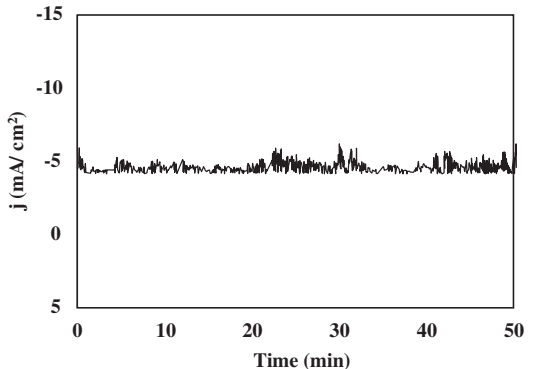


Figure 5. PEC activity, j , with time at $-1.8 \text{ V versus Ag/AgCl}$.

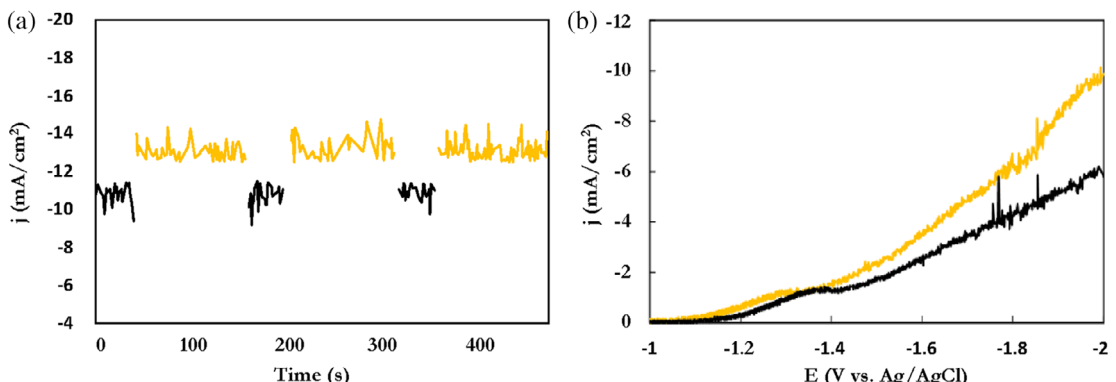


Figure 4. (a) On-off cycles for TiO_2 photoanode MEA in the dark (black) and under UV illumination (yellow) with CO_2 at $-1.8 \text{ V versus Ag/AgCl}$. (b) j - E characteristics of TiO_2 photoanode MEA in the dark (black) and under UV illumination (yellow) with CO_2 .

between illuminated and dark conditions represents the highest attainable photocurrent in the system. Of course, increases in current density are associated with higher voltage values, achieving a maximum increase of $j = 4.3 \text{ mA cm}^{-2}$ under UV illumination ($j = 9.9 \text{ mA cm}^{-2}$) with respect to the dark experiment ($j = 5.6 \text{ mA cm}^{-2}$) at -2 V versus Ag/AgCl, although this high potential could not be beneficial for alcohol production.³⁶ These results may be taken as a first indication for an enhanced PEC process performance as evaluated hereafter.

Process performance of TiO₂/Nafion/Cu plate system

The products obtained for the PEC continuous CO₂ reduction employing the TiO₂-based MEA as photoanode and Cu plate as cathode are alcohols (i.e. CH₃OH and C₂H₅OH) together with CO and C₂H₄. Their formation, and so process performance, is evaluated in terms of r and FE. Figure 5 initially shows an example of the evolution of j during the experimental time (UV illumination).

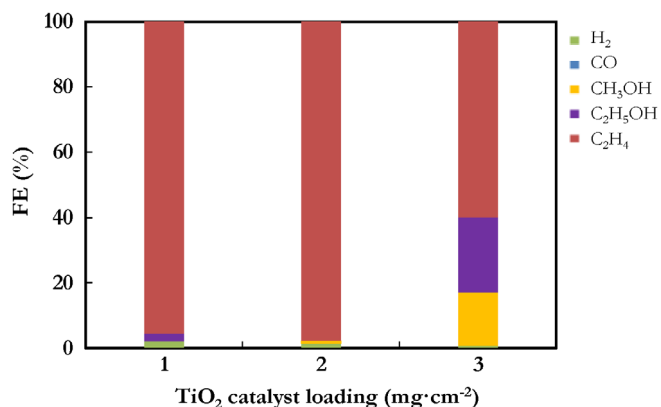


Figure 6. Effect of TiO₂ loading in the photoanode.

As can be observed, the system presents a pseudo-stable activity after 50 min of operation in continuous liquid–liquid CO₂ PEC conversion. The small fluctuations observed are commonly caused by the direct input of CO₂ gas into the cathode compartment, as well as the production of gaseous products (bubbles) on the electrode surface. The results also give an idea of the stability of the system, although, of course, longer-term tests would be needed in order to assess the feasibility of the system for real applications.

Among the key variables of the process, the TiO₂ catalyst loading can have a marked impact on process performance.³⁵ In principle, the larger the semiconductor surface, the greater the photocurrent generated as more electrons are excited in the photoanode. Therefore, Figure 6 shows the FE values at three different TiO₂ catalyst loadings in the MEA (i.e. 1, 2 and 3 mg cm⁻²). As observed, a loading of 3 mg cm⁻² seems to be the optimum

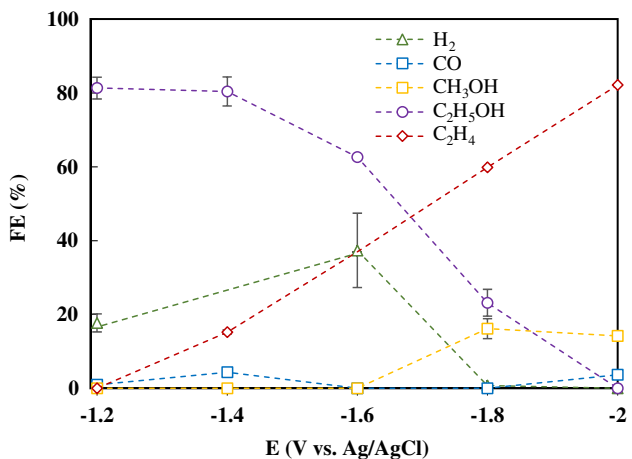


Figure 7. FE for all liquid- and gas-phase products obtained at different E .

Table 1. Production rates, r , for alcohols at different E

E (V)	j (mA cm ⁻²)	q (C)	r (μmol m ⁻² s ⁻¹)		r ($\times 10^{-8}$ μmol m ⁻² s ⁻¹ C ⁻¹)	
			CH ₃ OH	C ₂ H ₅ OH	CH ₃ OH	C ₂ H ₅ OH
-1.2	0.1	6	—	19.3	—	321.6
-1.4	1.6	21.6	—	13.9	—	64.3
-1.6	1	20.7	—	14.9	—	71.9
-1.8	5.9	102	9.5	6.8	9.3	6.6
-2	9.8	117.6	24	—	20.4	—
-1.3 ^a	10.8	584.8	8.7	—	1.5	—
-1.5 ^a	16.6	894.2	23	—	2.6	—

^a Cu plate cathode–Pt anode. Q/A = 2 mL min⁻¹ cm⁻² in an electrochemical system.³¹

Table 2. Energy efficiency (%) for alcohols

E (V versus Ag/AgCl)	-1.2	-1.4	-1.6	-1.8	-2	-1.3 ^a	-1.5 ^a
CH ₃ OH	—	—	—	5.2	4.1	2	1.4
C ₂ H ₅ OH	35.9	30.4	20.7	6.8	—	—	—

^a Cu plate cathode–Pt anode. Q/A = 2 mL min⁻¹ cm⁻² employing an electrochemical system.³¹

for both CH_3OH and $\text{C}_2\text{H}_5\text{OH}$ formation, with a *FE* value of 16.2% and 23.2%, respectively, in comparison to the value observed at 1 mg cm^{-2} , where no CH_3OH was detected and a *FE* value of 2.4% for $\text{C}_2\text{H}_5\text{OH}$ can be achieved. At catalyst loadings higher than 3 mg cm^{-2} Seger and Kamat³⁴ found that light absorption limits photocurrent generation due to particle agglomeration which hampers the access of the light to the catalytic surface. Consequently, a TiO_2 loading of 3 mg cm^{-2} is recommended to achieve the best performance in the developed TiO_2 photoanode MEA-driven system for CO_2 PEC conversion and so is applied hereafter.

The values for alcohols (i.e. CH_3OH and $\text{C}_2\text{H}_5\text{OH}$) formation in a voltage range from -1.2 to -2 V versus Ag/AgCl are presented in Table 1, while Figure 7 shows the *FE* for all liquid- and gas-phase products detected as a function of the applied voltage. The values in Table 1 are normalized by the total charge q (C) passing through the system in order to properly analyse the PEC activity. The values are also compared with our previous findings for the electrochemical conversion of CO_2 (in the dark) using a Cu plate.³¹

First, the data show that the current density values in the PEC system are significantly reduced (for a similar production of alcohols) compared to those at a Cu plate and a Pt anode in an electrochemical system (in the dark), which might initially indicate an enhancement in energy efficiency. Then, the reaction rate values, r , show similar ranges for CH_3OH for the same voltage level in electrochemical and PEC experiments. The r values per coulomb obtained in this work, however, are clearly superior in the PEC experiments ($r = 9.3 \mu\text{mol m}^{-2} \text{s}^{-1} \text{C}^{-1}$ for CH_3OH at -1.8 V versus Ag/AgCl) in comparison to those achieved in the electrochemical experiments ($r = 2.6 \mu\text{mol m}^{-2} \text{s}^{-1} \text{C}^{-1}$ for CH_3OH) showing the benefits of the PEC system. The PEC system seems also to be beneficial for the formation of $\text{C}_2\text{H}_5\text{OH}$, which requires a greater number of electrons and C–C coupling. This enhancement in CO_2 reduction to alcohols can be generally associated with two phenomena: first, the cathode potential becoming more negative (greater supply of e^-); and second, the large amount of H^+ generated from water in the photoelectrolysis, which seems to be available for CO_2 conversion to alcohols in the cathode.¹¹ The *FE* for both alcohols notably decreases at -2 V versus Ag/AgCl , which can be ascribed to an enhanced formation of C_2H_4 (Figure 7).

The highest *FE* for CH_3OH is achieved at -1.8 V versus Ag/AgCl : *FE* = 16.2%. On the other hand, the *FE* for $\text{C}_2\text{H}_5\text{OH}$ is negatively affected by increases in E , going from *FE* = 81% at -1.2 V to 23.2% at -1.8 V versus Ag/AgCl , in agreement with the values presented in Table 1. These *FE* values for $\text{C}_2\text{H}_5\text{OH}$ exceed those previously reported for other promising Cu-based systems, such as Cu-based metal–organic framework materials supported on GDEs (*FE* ~ 6% at -10 mA cm^{-2} in $[\text{Cu}_3(\mu_6-\text{C}_9\text{H}_3\text{O}_6)_2]_n$).³⁶

Besides, the formation of C_2H_4 can be expected in the potential range tested, as previously found by our group for the gas-phase CO_2 reduction at Cu-based surfaces, achieving a *FE* of 91% for C_2H_4 at -2.1 V versus Ag/AgCl ,³³ as also reported by other authors.^{39,40} Overall, an applied voltage of -1.8 V versus Ag/AgCl is preferred for the formation of both alcohols.

Furthermore, Table 2 summarizes *EE* values achieved for alcohols as a function of the applied potential. As observed, a maximum *EE* for CH_3OH can be obtained at -1.8 V versus Ag/AgCl (*EE* = 5.2%), while lowering the voltage applied seems beneficial for $\text{C}_2\text{H}_5\text{OH}$ production (*EE* = 35.9% at -1.2 V versus Ag/AgCl). These results are clearly superior to the maximum *EE* values obtained for Cu plate-based system for the electrochemical reduction of CO_2 (in the dark).

Cathode	Photoanode	Light source/intensity	E (V versus Ag/AgCl)	j (mA cm^{-2})	r ($\mu\text{mol m}^{-2} \text{s}^{-1}$)	<i>FE</i> (%)	Ref.
Cu plate	TiO_2	UV LED ($\lambda = 365 \text{ nm}$; 100 mW cm^{-2})	-1.8	5.9	$\text{CH}_3\text{OH}: 9.5; \text{C}_2\text{H}_5\text{OH}: 6.8$	$\text{CH}_3\text{OH}: 16.2; \text{C}_2\text{H}_5\text{OH}: 23.2$	This work
Cu_2O	TiO_2	AM 1.5G (100 mW cm^{-2})	-0.7	1.36	—	$\text{CH}_3\text{OH}: 1.1$	12
Pt/GA/CF	TiO_2	300 W Xe arc lamp ($320 \text{ nm} < \lambda < 410 \text{ nm}$)	-1.95	-	$\text{CH}_3\text{OH}: 0.41; \text{C}_2\text{H}_5\text{OH}: 1.25$	$\text{CH}_3\text{OH}: 5; \text{C}_2\text{H}_5\text{OH}: 29$	43
Pt	Cu-RGO-TiO ₂ /ITO	150 W Xe arc lamp ($320 \text{ nm} < \lambda < 410 \text{ nm}$)	-0.56	1.31	$\text{CH}_3\text{OH}: 52.5$	$\text{CH}_3\text{OH}: 32.5$	41
Pt-RGO	Pt-TNT ^a	300 W Xe arc lamp ($320 \text{ nm} < \lambda < 410 \text{ nm}$)	-1.95	—	$\text{CH}_3\text{OH}: 0.14$	$\text{CH}_3\text{OH}: 5$	10
Pt-RGO	Pt (5%)-TNT	300 W Xe arc lamp ($320 \text{ nm} < \lambda < 410 \text{ nm}$)	-1.95	—	$\text{CH}_3\text{OH}: 0.21; \text{C}_2\text{H}_5\text{OH}: 0.78$	—	4
Pt-RGO	Pt-TNT	300 W Xe arc lamp ($320 < \lambda < 410 \text{ nm}$)	-1.95	—	$\text{CH}_3\text{OH}: 24.3; \text{C}_2\text{H}_5\text{OH}: 3.75$	—	42

^a TNT, TiO_2 nanotubes.

Finally, the best performance results obtained at -1.8 V versus Ag/AgCl are compared (in terms of *r* and *FE*) with previous reports for alcohol production in photoanode–dark cathode PEC systems in Table 3. As observed, the values for the formation of CH₃OH and C₂H₅OH achieved using the TiO₂ photoanode MEA–Cu cathode configuration from this work are, in general, higher than those previously reported for CH₃OH production, and are only exceeded by Hasan *et al.*⁴¹ with a cathode of Pt and a photoanode of Cu-RGO-TiO₂/ITO. It should also be taken into account that other variables (reaction medium, cell configuration, experimental conditions, etc.) may affect the results. Besides, the *FE* for C₂H₅OH achieved in this work clearly surpasses that of other reports in the literature (except for the results from Hasan *et al.*⁴¹) employing the PEC configuration.

CONCLUSIONS

Coupling light to electrochemical devices for CO₂ conversion is an interesting approach for obtaining value-added products solving issues related to global warming at the same time. When the continuous PEC transformation of CO₂ is carried out in a filter-press cell employing a TiO₂ MEA photoanode, a maximum increase of 4.3 mA cm⁻² in current density is observed under UV illumination, indicating the potential benefits of the developed photoanode-driven system for an enhanced *EE*. Methanol and ethanol, as well as hydrogen, carbon monoxide and ethylene, are detected as liquid- and gas-phase products in the system employing a Cu plate as cathode. At -1.8 V versus Ag/AgCl, the maximum production of methanol is 9.5 $\mu\text{mol m}^{-2}\text{s}^{-1}$, the *FE* is 16.2% and the *EE* is 5.2%. In the case of ethanol, a reaction rate of 6.8 $\mu\text{mol m}^{-2}\text{s}^{-1}$, a *FE* of 12.1% and an *EE* of 6.8% can be achieved for a TiO₂ loading of 3 mg cm⁻² in the photoanode. In general, methanol production results are enhanced at higher voltages, while ethanol production seems to be negatively affected. All in all, the developed TiO₂ photoanode-driven system is able to enhance the production of alcohols from CO₂ under UV light, reducing the energy required in the process compared to an electrochemical system.

ACKNOWLEDGEMENTS

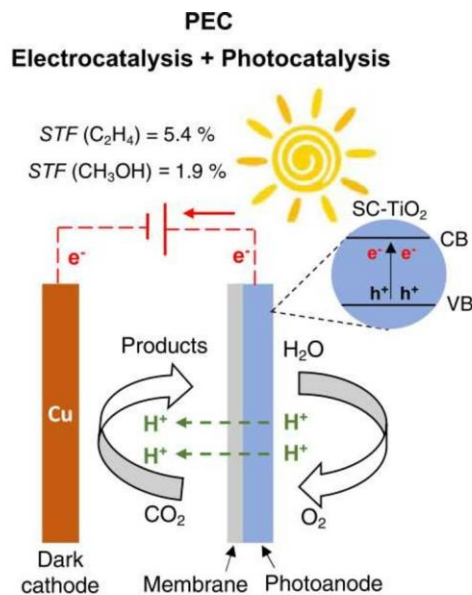
The authors gratefully acknowledge the financial support from the Spanish Ministry of Economy and Competitiveness (MINECO) through the projects CTQ2016-76231-C2-1-R and Ramón y Cajal programme (RYC-2015-17080).

REFERENCES

- Goeppert A, Czaun M, Jones JP, Prakash GKS and Olah GA, Recycling of carbon dioxide to methanol and derived products—closing the loop. *Chem Soc Rev* **43**:7995–8048 (2014).
- Castro S, Albo J and Irabien A, Photoelectrochemical reactors for CO₂ utilization. *ACS Sustainable Chem Eng* **6**:15877–15894 (2018).
- Das S and Daud WMA, Photocatalytic CO₂ transformation into fuel: a review on advances in photocatalyst and photoreactor. *Renewable Sustainable Energy Rev* **39**:765–805 (2014).
- Zhang M, Cheng J, Xuan X, Zhou J and Cen K, CO₂ synergistic reduction in a photoanode-driven photoelectrochemical cell with a Pt-modified TiO₂ nanotube photoanode and a Pt reduced graphene oxide electrocathode. *ACS Sustainable Chem Eng* **4**:6344–6354 (2016).
- Halmann M, Photoelectrochemical reduction of aqueous carbon dioxide on *p*-type gallium phosphide in liquid junction solar cells. *Nature* **275**:115–116 (1978).
- Xia S, Meng Y, Zhou X, Xue J, Pan G and Ni Z, Ti/ZnO-Fe₂O₃ composite: synthesis, characterization and application as a highly efficient photoelectrocatalyst for methanol from CO₂ reduction. *Appl Catal B* **187**:122–133 (2016).
- Wood J, Summers H, Clark A, Kaeffer N, Braeutigam M, Carbone L *et al.*, A comprehensive comparison of dye-sensitized NiO photocathodes for solar energy conversion. *Phys Chem Phys* **18**:10727–10738 (2016).
- Qin G, Zhang Y, Keb X, Tong X, Sun Z, Liang M *et al.*, Photocatalytic reduction of carbon dioxide to formic acid, formaldehyde, and methanol using dye-sensitized TiO₂ film. *Appl Catal B* **129**:599–605 (2013).
- Kaneko S, Katsumata H, Suzuki T and Ohta K, Photoelectrocatalytic reduction of CO₂ in LiOH/methanol at metal-modified p-InP electrodes. *Appl Catal B* **64**:139–145 (2006).
- Cheng J, Zhang M, Wu G, Wang X, Zhou J and Cen K, Photoelectrocatalytic reduction of CO₂ into chemicals using Pt-modified reduced graphene oxide combined with Pt-modified TiO₂ nanotubes. *Environ Sci Technol* **48**:7076–7084 (2014).
- Cheng J, Zhang M, Liu J, Zhou J and Cen K, Cu foam cathode used as Pt-RGO catalyst matrix to improve CO₂ reduction in a photoelectrocatalytic cell with TiO₂ photoanode. *J Mater Chem A* **3**:12947–12957 (2015).
- Chang X, Wang T, Zhang P, Wei Y, Zhao J and Gong J, Stable aqueous photoelectrochemical CO₂ reduction by a Cu₂O dark cathode with improved selectivity for carbonaceous products. *Angew Chem Int Ed* **55**:1–6 (2016).
- Xie S, Zhang Q, Liu G and Wang Y, Photocatalytic and photoelectrocatalytic reduction of CO₂ using heterogeneous catalysts with controlled nanostructures. *Chem Commun* **52**:35–59 (2016).
- Sato S, Arai T, Morikawa T, Uemura K, Suzuki M, Tanaka H *et al.*, Selective CO₂ conversion to formate conjugated with H₂O oxidation utilizing semiconductor/complex hybrid photocatalysts. *J Am Chem Soc* **133**:15240–15243 (2011).
- La Tempa TJ, Rani S, Bao N and Grimes CA, Generation of fuel from CO₂ saturated liquids using a p-Si nanowire//n-TiO₂ nanotube array photoelectrochemical cell. *Nanoscale* **4**:2245–2250 (2012).
- Weng B, Wei W, Wu H, Alenizi AM and Zheng G, Bifunctional CoP and CoN porous nanocatalysts derived from ZIF-67 in situ grown on nanowire photoelectrodes for efficient photoelectrochemical water splitting and CO₂ reduction. *J Mater Chem A* **4**:15353–11536 (2016).
- Sahara G, Kumagai H, Maeda K, Kaeffer N, Artero V, Higashi M *et al.*, Photoelectrochemical reduction of CO₂ coupled to water oxidation using a photocathode with a Ru(II)–Re(I) complex photocatalyst and a CoO_x/TaON photoanode. *J Am Chem Soc* **138**:14152–14158 (2016).
- Albo J, Alvarez-Guerra M, Castaño P and Irabien A, Towards the electrochemical conversion of carbon dioxide into methanol. *Green Chem* **17**:2304–2324 (2015).
- Albo J, Perfecto-Irigaray M, Beobide G and Irabien A, Cu/bi metal-organic framework-based systems for an enhanced electrochemical transformation of CO₂ to alcohols. *J CO₂ Util* **33**:157–165 (2019).
- Olah GA, Beyond oil and gas: the methanol economy. *Angew Chem Int Ed* **44**:2636–2639 (2005).
- Le M, Ren M, Zhang Z, Sprunger PT, Kurtz RL and Flake JC, Electrochemical reduction of CO₂ to CH₃OH at copper oxide surfaces. *J Electrochem Soc* **158**:E45–E49 (2011).
- Liu Y, Zhang Y, Cheng K, Quan X, Fan X, Su Y *et al.*, Selective electrochemical reduction of carbon dioxide to ethanol on a boron- and nitrogen-co-doped nanodiamond. *Angew Chem* **129**:15813–15817 (2017).
- Nitopi S, Bertheussen E, Scott SB, Liu X, Engstfeld AK, Horch S *et al.*, Progress and perspectives of electrochemical CO₂ reduction on copper in aqueous electrolyte. *Chem Rev* **119**:7610–7672 (2019).
- Yuan J, Yang MP, Zhi WY, Wang H, Wang H and Lu JX, Efficient electrochemical reduction of CO₂ to ethanol on Cu nanoparticles decorated on N-doped graphene oxide catalysts. *J CO₂ Util* **33**:452–460 (2019).
- Inoue T, Fujishima A, Konishi S and Honda K, Photoelectrocatalytic reduction of carbon dioxide in aqueous suspensions of semiconductor powders. *Nature* **277**:637–638 (1979).
- Liu L, Zhao H, Andino JM and Li Y, Photocatalytic CO₂ reduction with H₂O on TiO₂ nanocrystals: comparison of anatase, rutile, and brookite polymorphs and exploration of surface chemistry. *ACS Catal* **2**:1817–1828 (2012).
- Wang T, Meng X, Li P, Ouyang S, Chang K, Liu G *et al.*, Photoreduction of CO₂ over the well-crystallized ordered mesoporous TiO₂ with the confined space effect. *Nano Energy* **9**:50–60 (2014).
- Zhao H, Pan F and Li Y, A review on the effects of TiO₂ surface point defects on CO₂ photoreduction with H₂O. *J Materiomics* **3**:17–32 (2017).

- 29 Ibrahim N, Kamarudin SK and Minggu LJ, Biofuel from biomass via photo-electrochemical reactions: an overview. *J Power Sources* **259**: 33–42 (2014).
- 30 Haberreutinger SN, Schmidt-Mende L and Stolarsky JK, Photocatalytic reduction of CO₂ on TiO₂ and other semiconductors. *Angew Chem Int Ed* **52**: 7372–7408 (2013).
- 31 Albo J, Sáez A, Solla-Gullón J, Montiel V and Irabien A, Production of methanol from CO₂ electroreduction at Cu₂O and Cu₂O/ZnO-based electrodes in aqueous solution. *Appl Catal Environ* **176–177**: 709–717 (2015).
- 32 Albo J and Irabien A, Cu₂O-loaded gas diffusion electrodes for the continuous electrochemical reduction of CO₂ to methanol. *J Catal* **343**: 232–239 (2016).
- 33 Merino-García I, Albo J and Irabien A, Tailoring gas-phase CO₂ electro-reduction selectivity to hydrocarbons at Cu nanoparticles. *Nanotechnology* **29**: 014001 (2018).
- 34 Seger B and Kamat PV, Fuel cell geared in reverse: photocatalytic hydrogen production using a TiO₂/Nafion/Pt membrane assembly with no applied bias. *J Phys Chem C* **113**: 18946–18952 (2009).
- 35 Merino-García I, Albo J and Irabien A, Productivity and selectivity of gas-phase CO₂ electroreduction to methane at copper nanoparticle-based electrodes. *Energy Technol* **5**: 922–928 (2017).
- 36 Albo J, Vallejo D, Beobide G, Castillo O, Castaño P and Irabien A, Copper-based metal–organic porous materials for CO₂ electrocatalytic reduction to alcohols. *ChemSusChem* **10**: 1100–1109 (2017).
- 37 Qiao J, Liu Y, Hong F and Zhang J, A review of catalysts for the electro-reduction of carbon dioxide to produce low-carbon fuels. *Chem Soc Rev* **43**: 631–675 (2014).
- 38 Irabien A, Alvarez-Guerra M, Albo J and Dominguez-Ramos A, Electrochemical conversion of CO₂ to value-added products, in *Electrochemical Water and Wastewater Treatment*, ed. by Martínez-Huitl CA, Rodrigo MA and Scialdone O. Elsevier, Oxford, pp. 29–59 (2018).
- 39 Komatsu S, Tanaka M, Okumura A and Kungi A, Preparation of Cu-solid polymer electrolyte composite electrodes and application to gas-phase electrochemical reduction of CO₂. *Electrochim Acta* **40**: 745–753 (1995).
- 40 Cook RL, Macduff RC and Sammells AF, High rate gas phase CO₂ reduction to ethylene and methane using gas diffusion electrodes. *J Electrochem Soc* **137**: 607–608 (1990).
- 41 Hasan MR, Hamid SBA, Basirun WJ, Suhamy SHM and Mat ANC, A sol-gel derived, copper-doped, titanium dioxide-reduced graphene oxide nanocomposite electrode for the photoelectrocatalytic reduction of CO₂ to methanol and formic acid. *RSC Adv* **5**: 77803–77813 (2015).
- 42 Cheng J, Zhang M, Wu G, Wang X, Zhou J and Cen K, Optimizing CO₂ reduction conditions to increase carbon atom conversion using a Pt-RGO||Pt TNT photoelectrochemical cell. *Sol Energy Mater Sol Cells* **132**: 606–614 (2015).
- 43 Zhang M, Cheng J, Xuan X, Zhou J and Cen K, Pt/graphene aerogel deposited in Cu foam as a 3D binder-free cathode for CO₂ reduction into liquid chemicals in a TiO₂ photoanode-driven photoelectrochemical cell. *Chem Eng J* **322**: 22–32 (2017).

3.3. Iván Merino García, Sergio Castro, Ángel Irabien, Ignacio Hernández, Verónica Rodríguez, Rafael Camarillo, Jesusa Rincón, Jonathan Albo. 2022. Efficient photoelectrochemical conversion of CO₂ to ethylene and methanol using a Cu cathode and TiO₂ nanoparticles synthesized in supercritical medium as photoanode. Journal of Environmental Chemical Engineering, 10, 3, 107441.



Continuous PEC CO₂ reduction in a photoanode/dark cathode configuration

Figura 3.3. Resumen gráfico del artículo: "Efficient photoelectrochemical conversion of CO₂ to ethylene and methanol using a Cu cathode and TiO₂ nanoparticles synthesized in supercritical medium as photoanode".

La conversión fotoelectroquímica de CO₂ en productos de alto valor añadido es una alternativa atractiva para reducir la necesidad de voltaje externo y, por tanto, del consumo de energía de los procesos de conversión electroquímica. En este trabajo se sintetizan nanopartículas de TiO₂ en medio supercrítico (TiO₂-SC) con mayor cristalinidad en forma de anatasa, lo que resulta en propiedades ópticas mejoradas, una mayor área superficial y, una adecuada morfología para la separación de cargas. Estas características permiten la producción de fotoánodos eficientes, que se incorporan en un reactor fotoelectroquímico tipo filtro prensa para lograr una conversión más eficiente de CO₂ de manera continua. Se analiza el rendimiento del sistema en términos de la velocidad de formación de productos, la eficiencia Faradaica, la eficiencia energética y la eficiencia de la conversión de energía solar a combustibles. Los resultados se comparan con el comportamiento de los fotoánodos de TiO₂-P25 en la misma configuración de reactor y condiciones de operación. La novedad de este trabajo radica en: i) el suministro de CO₂ como gas en el cátodo junto con un catolito líquido, lo que permite mejorar la producción de etileno; ii) la síntesis de nanopartículas de TiO₂-SC para mejorar las propiedades del TiO₂-P25,

incluyendo el área superficial BET, la absorción de luz, el *bandgap* o la cristalinidad; y iii) el uso de una configuración de ensamblaje membrana-electrodo (MEA) en el fotoánodo, lo que actúa como separador de los compartimentos de la celda fotoelectroquímica y mejora el transporte de materia y cargas en el sistema fotoelectroquímico, disminuyendo así la resistencia interna de la celda.

La caracterización fotoelectroquímica de los fotoánodos muestra que la densidad de corriente alcanzada es mayor a la reportada en sistemas fotoelectrocatalíticos similares, alcanzando el valor significativamente alto de $12,31 \text{ mA}\cdot\text{cm}^{-2}$ en comparación con el sistema a oscuras que alcanza un valor de $7,18 \text{ mA}\cdot\text{cm}^{-2}$. Este nivel de corriente también supera el obtenido con los fotoánodos preparados con TiO₂-P25 ($5,9 \text{ mA}\cdot\text{cm}^{-2}$) en las mismas condiciones. La disminución del *bandgap* para el TiO₂-SC, observada en los análisis de absorción diferencial, permite la excitación de electrones a energías mucho más bajas, lo que podría ser responsable de mejorar el rendimiento del proceso impulsado por la luz.

Se realizaron pruebas de reducción fotoelectroquímica de CO₂ en continuo utilizando un reactor de tipo filtro-prensa impulsado por un fotoánodo iluminado con luces LED UV ($100 \text{ mW}\cdot\text{cm}^{-2}$). El reactor está compuesto por las nanopartículas de TiO₂-SC ($3 \text{ mg}\cdot\text{cm}^{-2}$) soportadas en papel de carbono poroso como fotoánodo, una placa de cobre como cátodo y una disolución acuosa de 1 M KOH como medio de reacción. Los resultados obtenidos muestran que los principales productos obtenidos a partir del CO₂ son etileno, en fase gaseosa, y metanol, en fase líquida. Además, se demuestra que la reacción es más eficiente bajo irradiación, logrando una velocidad de producción de etileno de $147,4 \text{ }\mu\text{mol}\cdot\text{m}^{-2}\cdot\text{s}^{-1}$ y una eficiencia Faradaica del 46,6%. En relación al metanol, se obtiene una velocidad de producción de $4,72 \text{ }\mu\text{mol}\cdot\text{m}^{-2}\cdot\text{s}^{-1}$ y una eficiencia Faradaica del 15,3%. En comparación, el rendimiento del sistema a oscuras es considerablemente inferior, obteniéndose una velocidad de producción de etileno de $24,2 \text{ }\mu\text{mol}\cdot\text{m}^{-2}\cdot\text{s}^{-1}$ y una eficiencia Faradaica del 38,2%, mientras que no se detecta metanol. Este aumento en la eficiencia se puede atribuir, principalmente, a las mayores densidades de photocorriente que se alcanzan bajo irradiación UV, lo que afecta significativamente a la selectividad de la reacción. Además, los valores máximos de conversión de luz solar a combustibles obtenidos para etileno (5,4%) y metanol (1,9%) son considerablemente superiores a los observados con fotoánodos basados en TiO₂-P25 bajo la misma configuración de reactor y condiciones experimentales (3,7% y 1%, respectivamente). Los resultados demuestran, por tanto, los beneficios de utilizar fotoánodos basados en TiO₂-SC para una reducción fotoelectroquímica de CO₂ en continuo más eficiente.



Efficient photoelectrochemical conversion of CO₂ to ethylene and methanol using a Cu cathode and TiO₂ nanoparticles synthesized in supercritical medium as photoanode

Ivan Merino-Garcia ^{a,*}, Sergio Castro ^{a,1}, Angel Irabien ^a, Ignacio Hernández ^b, Verónica Rodríguez ^c, Rafael Camarillo ^c, Jesusa Rincón ^c, Jonathan Albo ^{a,*}

^a Departamento de Ingenierías Química y Biomolecular, Universidad de Cantabria, Avda. Los Castros, s/n, 39005 Santander, Spain

^b Departamento CITIMAC, Universidad de Cantabria, Avda. Los Castros, s/n, 39005 Santander, Spain

^c Department of Chemical Engineering, Faculty of Environmental Sciences and Biochemistry, Universidad de Castilla-La Mancha, Avda. Carlos III, s/n, 45071 Toledo, Spain

ARTICLE INFO

Editor: Vítor J.P. Vilar

Keywords:

Photoelectrocatalysis
Continuous CO₂ conversion
Photoanode-driven system
TiO₂ in supercritical medium
Ethylene
Methanol

ABSTRACT

The photoelectrochemical conversion of CO₂ into valuable products represents an attractive method to decrease the external electrical bias required in electrochemical approaches. In this work, TiO₂ nanoparticles with enhanced optical properties, large surface area, appropriate morphology, and superior crystallinity are synthesized in supercritical medium to manufacture light-responsive photoanodes. The photoelectrochemical CO₂ reduction tests are carried out in continuous mode using a photoanode-driven filter-press cell illuminated with UV LED lights (100 mW cm⁻²), consisting on TiO₂ nanoparticles synthesized in supercritical medium (3 mg cm⁻²) supported onto porous carbon paper as the photoanode, a Cu plate cathode, and 1 M KOH aqueous solution as the reaction medium. The main products obtained from CO₂ are ethylene in the gas phase, together with methanol in the liquid phase. The results show that reaction performance is improved under UV irradiation towards ethylene ($r = 147.4 \mu\text{mol m}^{-2} \text{s}^{-1}$; FE = 46.6%) and methanol ($r = 4.72 \mu\text{mol m}^{-2} \text{s}^{-1}$; FE = 15.3%) in comparison with the system performance in the dark (ethylene: $r = 24.2 \mu\text{mol m}^{-2} \text{s}^{-1}$ and FE = 38.2%; methanol not detected), which can be mainly ascribed to the superior photocurrent densities reached that affect the selectivity of the reaction. Besides, the maximum solar-to-fuels values achieved for ethylene (5.4%) and methanol (1.9%) are markedly superior to those observed with illuminated TiO₂-P25 photoanodes under the same reactor configuration and experimental conditions (3.7% and 1%, respectively). Therefore, these results demonstrate the benefits of using TiO₂-based materials synthesized in supercritical medium for a more efficient continuous photoelectroreduction of CO₂ to value-added products.

1. Introduction

The intensification of human industrial activities is causing an unbalanced CO₂ produced and consumed on Earth [1,2]. Among the available sustainable possibilities to accelerate an energy transition away from fossil fuels, the chemical conversion of CO₂ and water into valuable products represents a promising direction to equilibrate the system and close the carbon cycle [3–5]. Several approaches can be considered to meet the target, namely mineralization [6], enzymatic [7], thermochemical [8], electrochemical [9,10], photoelectrochemical

(PEC) [11–13], and photochemical processes [14,15]. In particular, the transformation of CO₂ via PEC provides greener CO₂ utilization routes towards the generation of fuels and chemicals under light irradiation, integrating the benefits of both electrocatalytic and photocatalytic conversion approaches, and promoting the separation efficiency of photogenerated electron-hole pairs [12,16–19]. Besides, the production of ethylene (C₂H₄) from CO₂ utilization is interesting, since this hydrocarbon represents an energy-dense chemical feedstock used in several applications as energy vector and chemical building blocks [20, 21]. The production of alcohols such as methanol (CH₃OH) is also of

* Corresponding authors.

E-mail addresses: merino@unican.es (I. Merino-Garcia), alboj@unican.es (J. Albo).

¹ I. Merino-Garcia and S. Castro contributed equally to this work as first authors.

utmost importance, owing to its key role in several applications, namely as a chemical storage carrier for hydrogen or as a platform product in gasoline and biodiesel [22–24].

Depending on the nature of the (photo)electrodes used in two-compartment PEC cells, four different photoreactor configurations can be applied: i) photoanode/dark cathode [25–27], ii) dark anode/photocathode [28], iii) photoanode/photocathode [29,30], and iv) hybrid PEC-solar cell tandem [31]. The first PEC configuration is simpler and usually preferred to improve the energy efficiency of the process since the photoanode provides extra photogenerated electrons from water oxidation to the cathode compartment for CO₂ reduction, decreasing the requirements of external electrical energy [31]. Thus, photoanode-driven PEC processes can lead to decreased cell bias, which makes this strategy the most suitable option from energy efficiency and practical application viewpoints [32–34].

Although a wide variety of photoactive materials can be seen in PEC systems as photoanodes, such as WO₃, BiVO₄, Fe₂O₃, or ZnO [31,35–40], among others, TiO₂-P25 has been the most investigated light-responsive material in photoanode-driven PEC systems, owing to its low cost, non-toxic characteristics, photo-stability, wide bandgap (> 3.0 eV), chemical inertness, large resistance to photo-corrosion, and UV light absorption properties [36,41,42]. Nevertheless, TiO₂-P25 presents several limitations [31,43], mainly: i) fast recombination of electron-hole pairs and ii) low purity and crystallinity. In this respect, different morphologies (e.g., nanotubes, nanospheres) of TiO₂ have been recently investigated to improve electron mobility, chemical stability, and surface area, among others [18,44]. Moreover, the modification of these structures (i.e., titania nanotubes) with noble metal particles such as Au and Ag has also been proposed to decrease the photogenerated carrier recombination efficiency of TiO₂ [18,45], which should allow for achieving a higher photoelectrochemical conversion performance. On the other hand, alternative synthesis methods have been proposed to overcome the main shortcomings of benchmark TiO₂ [46,47]. Among them, the preparation of TiO₂ in supercritical medium led to improved photocatalytic properties compared to those prepared under conventional procedures [47–50]. Specifically, several properties such as surface area, light absorption, optical bandgap energy, presence of surface hydroxyl groups, and appropriate morphology (for enhanced charge separation) are improved in comparison with commercial TiO₂-P25 [43].

Previous studies in our group reported the preparation, characterization, and use of commercial TiO₂-P25 nanoparticulated electrodes as light-responsive photoanodes in a continuous photoanode-driven PEC process illuminated with UV LED lights. A Cu plate was utilized as a dark cathode to reduce CO₂ in a filter-press PEC cell divided by a Nafion® 117 membrane [25]. The energy requirements to carry out the CO₂ conversion process decreased compared to an electrochemical system (energy efficiency of 5.2% and 1.4% for PEC and electrochemical system, respectively). However, further efforts are still required to improve the overall process performance. This work, therefore, focuses on the preparation, characterization, and evaluation of TiO₂ nanoparticles synthesized in supercritical medium (SC-TiO₂) for the continuous photoelectrochemical conversion of CO₂ in an illuminated photoanode-driven filter-press reactor. The performance of the novel light-responsive materials is analyzed in terms of production rate (*r*), Faradaic efficiency (FE), energy efficiency (EE), and solar-to-fuel (STF) efficiency. The results are compared with the behavior of TiO₂-P25 surfaces in the same reactor configuration to demonstrate the potential applicability of supercritical fluid-based methods for the synthesis of photoactive materials with improved properties. The novelty of the present work lays on: i) CO₂ supplied as gas in the cathode (together with a liquid catholyte), measuring gas-phase chemicals (e.g., C₂H₄) and thus closing all products produced; ii) TiO₂ nanoparticles are synthesized in supercritical medium to improve the properties of benchmark TiO₂-P25, namely BET surface area, light absorption, optical bandgap, or crystallinity; and iii) the use of a membrane electrode assembly

(MEA) configuration by coupling the membrane to the photoanode surface, acting as a separator of the PEC cell compartments, for an improved mass/ion/electron transport in the PEC system, thus decreasing the internal cell resistance.

All in all, this work represents a step forward in the development of photoanode-driven PEC systems for a more efficient transformation of CO₂ in continuous mode.

2. Materials and methods

2.1. Synthesis and characterization of SC-TiO₂ nanoparticles

The synthesis of TiO₂ nanoparticles in supercritical CO₂ was performed in an ad hoc designed experimental set-up, which has been described in detail elsewhere [43]. In brief, a thermostatic bath, a high-pressure pump, and a high-pressure synthesis reactor represent the main core of the setup. The powder was obtained by thermal hydrolysis of titanium isopropoxide (TTIP; precursor) with ethanol using supercritical CO₂ as the reaction medium. The synthesis conditions were 20 MPa pressure, 300 °C temperature, 28 mmol precursor/mmol alcohol molar ratio, and reaction time of 2 h. After the synthesis procedure, solids obtained were removed from the reactor and dried at 105 °C for 12 h. The solids were then calcined at 400 °C for 6 h to remove C pollution and to increase TiO₂ crystallinity. The prepared photoactive materials were comprehensively characterized by several techniques in a previous work [43], namely scanning electron microscopy (SEM), X-ray diffraction (XRD), BET analyses, and Fourier transform infrared (FTIR) spectroscopy. A Cary 6000i Spectrometer equipped with an integrating sphere for powder samples was used for diffuse reflectance spectroscopy (DRS) measurements in the UV-Vis-NIR range, and an Edinburgh Instruments FLSP 920 double grating fluorometer equipped with a Xe lamp and Hamamatsu R928 photomultiplier tube, allowed complementing the characterization with photoluminescence (PL) analyses (emission and excitation) to study the optical properties of both SC-TiO₂ and TiO₂-P25 (dry powder).

2.2. Photoanode preparation and characterization

The light-responsive SC-TiO₂ photoanodes are manufactured by an air-brushing method [21,25]. In brief, SC-TiO₂-based catalytic inks are homogeneously deposited over the surface of porous Toray carbon paper (TGP-H-60). The catalytic ink is composed of a mixture of the synthesized SC-TiO₂ photocatalyst, a Nafion® solution (Alfa Aesar, 5 wt%, copolymer polytetrafluoroethylene) as a binder, and isopropanol (Sigma Aldrich, 99.5%) as a vehicle, with a 70:30 SC-TiO₂/Nafion mass ratio and a 3 wt% of total solids (photocatalyst + Nafion) in the isopropanol dispersion. The obtained dispersion is sonicated for at least 30 min to obtain a homogeneous slurry that is subsequently airbrushed on the surface of the carbon paper support. The airbrushing process is carried out at 100 °C to ensure the complete evaporation of the solvent. The photoactive surfaces are prepared by simple accumulation of layers, reaching a final photocatalytic loading of 3 mg cm⁻² (experimentally determined by continuous weighing), which is selected based on previous findings [25]. A Nafion® 117 membrane, previously activated in HCl solution for 30 min and rinsed with deionized water, is finally coupled with the prepared photoanode to obtain a photoactive MEA.

The PEC properties of the photoanodes are firstly characterized by linear sweep voltammetry (LSV) with and without LED light illumination when CO₂ is continuously fed into the reactor. Moreover, the prepared light-responsive surfaces are characterized by XRD (Phillips X'Pert MDP X-ray powder diffractometer) before and after 150 min of continuous operation under light irradiation in the photoanode-driven PEC reactor to determine the composition and crystallinity of the photocatalysts.

2.3. PEC cell description and experimental conditions

The light-responsive photoanodes (10 cm^2) are tested at ambient conditions in a commercial filter-press cell reactor (Electrocell A/S), that is adapted to be illuminated with cold UV LED lights (365 nm; 100 mW cm^{-2}) in the anodic compartment, as displayed in Fig. 1. The light intensity is measured by a radiometer (Photoradiometer Delta OMH) and controlled by adjusting the LED intensity and the distance between the microreactor and the LED. The photoanode/dark cathode configuration consists of an illuminated SC-TiO₂/carbon paper as the photoanode, a Cu plate as the dark cathode, and a thin leak-free Ag/AgCl (1 mm) as the reference electrode. The Cu plate is cleaned before each experiment with a HCl solution (37%) to ensure a Cu(0)-based surface [51].

The cell compartments are separated by the MEA (SC-TiO₂ photoanode + Nafion® 117 membrane). Both catholyte and anolyte aqueous solutions (1 M KOH) are continuously fed to the reactor through two independent peristaltic pumps at flow rates of 10 mL min^{-1} , whereas a constant gas CO₂ feed (180 mL min^{-1}) is introduced into the cathodic compartment of the PEC cell. Finally, a potentiostat (AutoLabPGSTAT 302N) is used to control the applied potential (E) and measure the generated current density (j). A detailed description of both the experimental setup and the PEC cell configuration can be seen in Fig. 2.

The photoelectrochemical CO₂ reduction tests are carried out by duplicate in continuous mode for 50 min, when a pseudo-stable performance is reached. Besides, the behavior of the photoanodes is investigated during three consecutive runs of 50 min under on/off UV irradiation.

Gas and liquid samples are measured at the reactor outlet (cathode side) every 10 min to calculate the concentration of products obtained in each experiment. A gas chromatograph (GCMSQP2010 Ultra, Shimadzu) equipped with a flame ionization detector (GC-FID) is used to measure the formation of liquid products (i.e., alcohols). The production of formate in the liquid phase is also analyzed with ion chromatography (IC, Dionex ICS 1100). Moreover, gaseous samples are taken and measured using an online gas microchromatograph (3000 Micro GC, Inficon). The concentration results that are two times lower/higher than the average value are discarded (experimental error of $< 16.1\%$) to calculate the following figures of merit:

i) the formation rate for each product per unit of area and time, r ($\mu\text{mol m}^{-2}\text{ s}^{-1}$);

ii) the Faradaic efficiency (FE), which indicates the selectivity of the reaction towards each product, calculated according to Eq. (1):

$$FE(\%) = \frac{z n F}{q} \times 100, \quad (1)$$

where z is the theoretical number of electrons exchanged to form the target product, n is the number of moles produced, F represents the Faraday constant (96485 C mol^{-1}), and q is the total charge (C) applied in the process. The concentration of products is normalized to the reacting CO₂ (inlet-outlet) in the system and adjusted to close the balance of products in the photoelectrochemical system;

iii) the energy efficiency (EE), defined as the total energy used towards the formation of the desired product, calculated according to Eq. (2):

$$EE(\%) = \frac{E_T}{E} \times FE, \quad (2)$$

where E is the external (experimentally) applied potential and E_T represents the theoretical voltage needed for the formation of each product. The theoretical potentials for C₂H₄ and CH₃OH (V vs. Ag/AgCl at pH 7) are -0.539 V and -0.589 V , respectively [52];

iv) the solar-to-fuel (STF) parameter, which represents the efficiency of the process to produce valuable products with light. In PEC approaches, STF takes into account not only the input power from light irradiation but also the input electrical power (applied voltage – external bias). STF can be calculated as follows:

$$STF = \frac{P_{f,o} + P_{e,o}}{P_s + P_{e,i}} = \frac{A \cdot J_{op} \cdot E_{f,o} \cdot FE}{P_s + P_{e,i}}, \quad (3)$$

where $P_{f,o}$ is the output power contained in the chemical fuel (W), $P_{e,o}$ the output power in the form of electricity (W), P_s the input power from solar irradiation (W), and $P_{e,i}$ the external input electrical power (W).

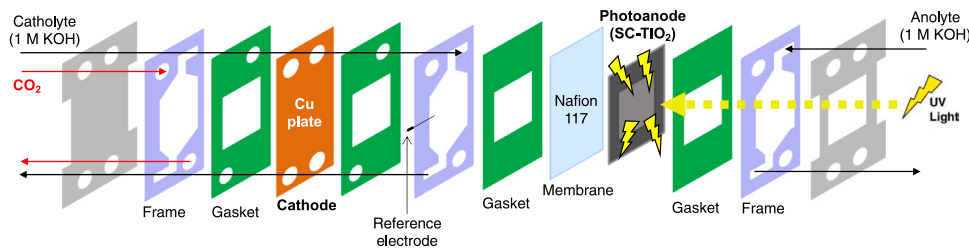
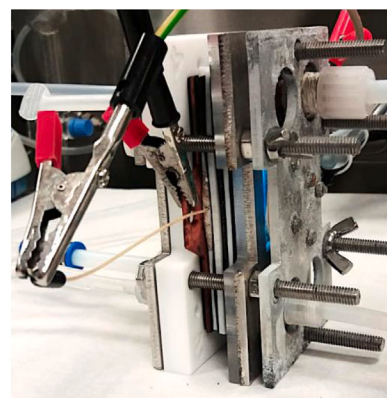


Fig. 1. Illuminated filter-press PEC reactor (above) and graphical illustration of the internal cell components (below).

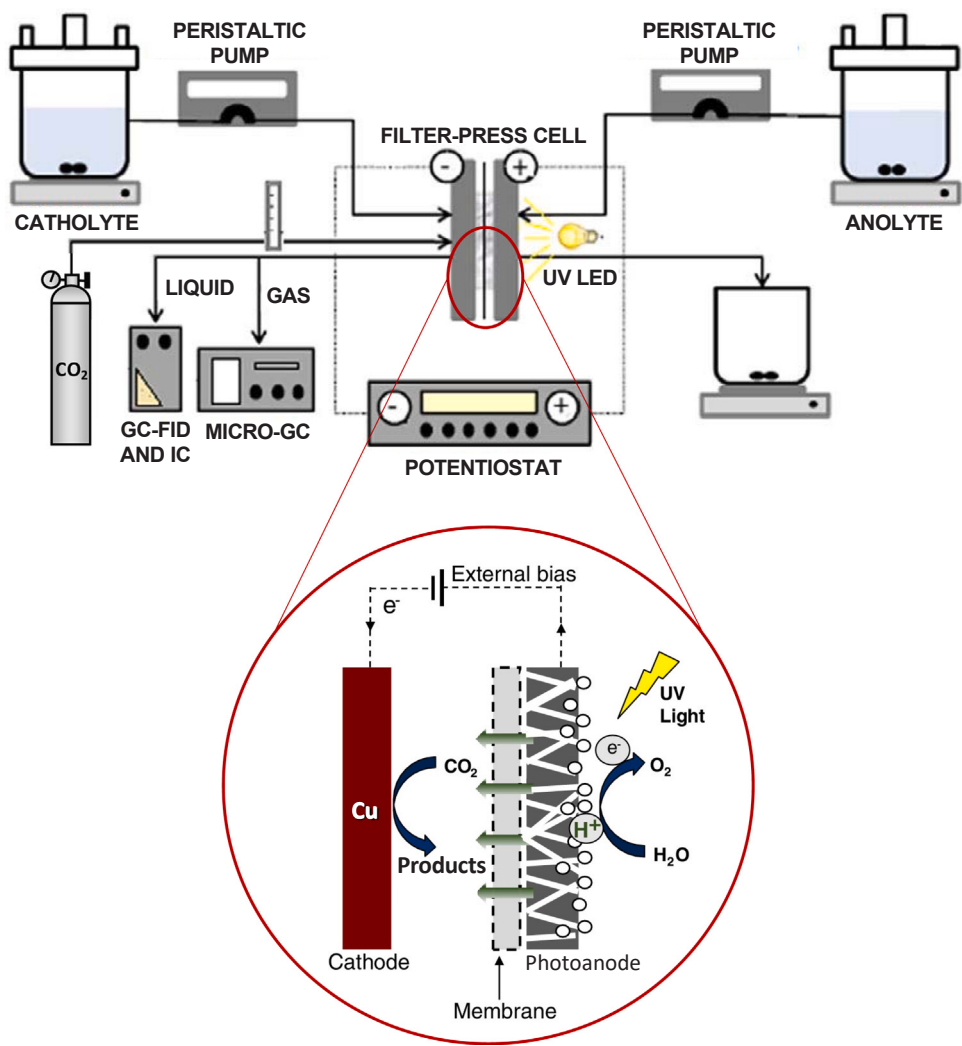


Fig. 2. Experimental system for the continuous PEC conversion of CO₂ including a schematic representation of the photoanode (MEA)/dark cathode configuration. Adapted from [25].

Besides, A represents the geometric area (cm²), J_{op} the operating current density (A cm⁻²), $E_{f,o}$ the potential difference (V) between the two half-reactions (i.e., CO₂ reduction product and O₂ from water oxidation) and FE is the Faradaic efficiency.

3. Results and discussion

3.1. Optical properties

The optical properties of the nanoparticles are investigated through DRS and PL analyses, as displayed in Fig. 3. The results show significant differences in reflectance between SC-TiO₂ and commercial TiO₂-P25, as given in the differential spectrum. In particular, the main differences occur under 400 nm, where TiO₂-P25 starts its absorption front (please see DRS of TiO₂-P25 powder as a reference). Both samples show analogous PL spectra at energies below the gap (luminescence maximum: 460 nm), with comparable photoluminescence lifetime for such a blue emission. Nevertheless, their excitation spectroscopy at $\lambda_{\text{max}} = 460$ nm is dissimilar. Interestingly, SC-TiO₂ emits for excitation below the P25 gap, peaking at an excitation wavelength around 400 nm (Fig. 3, inset). This implies the existence of low energy states at these energies and a large effective redshift of the gap, of nearly 0.5 eV, in agreement with the absorption spectrum. The comparable luminescence suggests that the emitting traps are similar in nature, and can also be populated upon

UV excitation. At 365 nm, SC-TiO₂ shows a factor 1.5 higher extinction. In short, the larger decreased gap energy and optical lower-lying states for SC-TiO₂ allow the creation of excitations at much lower energies. This may contribute to reduce the external bias of the process (and thus the overall energy efficiency) in the presence of light, in contrast with the behavior of commercial TiO₂-P25 photocatalysts.

3.2. PEC characterization

The current densities reached in the filter-press PEC cell as a function of the applied potential (from -1.2 to -2 V vs. Ag/AgCl) and UV light illumination when CO₂ is continuously bubbled into the reactor are displayed in Fig. 4a. As expected, the differences in current density between dark and illuminated conditions become more relevant as the applied voltage increases, owing to a stronger band bending effect that leads to a more efficient charge separation upon light absorption [53, 54]. The current density gap observed represents the highest attainable photocurrent in the PEC system, with a maximum gap of 8.5 mA cm⁻² at -2 V vs Ag/AgCl ($j_{UV} = 21.6$ mA cm⁻²; $j_{dark} = 13.1$ mA cm⁻²). This result represents a two-fold improvement in comparison with commercial TiO₂-P25 photoanodes (current increase: 4.3 mA cm⁻² [25]) at the same potential level. The current density achieved is comparable (and usually higher) with those results reported so far in TiO₂-based photoanode-driven PEC systems for CO₂ conversion. For example,

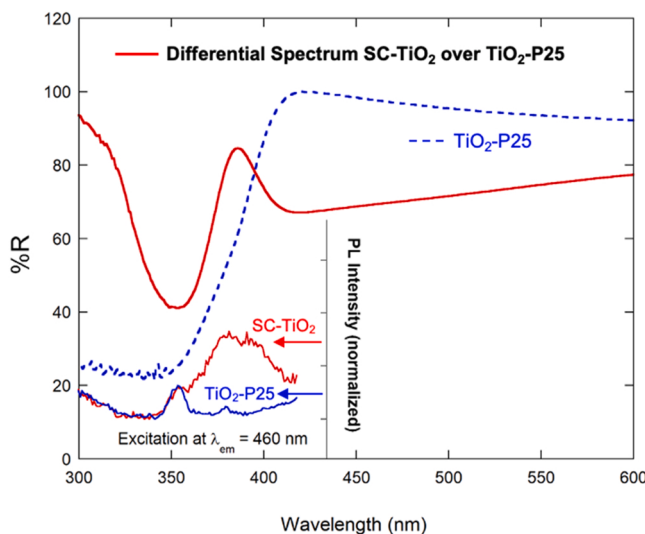


Fig. 3. Differential reflectance spectrum taken for SC-TiO₂ with TiO₂-P25 as the reference signal (DRS for TiO₂-P25 as a blue dotted line). Inset: PL excitation spectra for SC-TiO₂ (red) and TiO₂-P25 (blue) dry powder. The photoexcitation spectra are taken at 460 nm emission. (For interpretation of the references to colour in this figure legend, the reader is referred to the web version of this article).

Yamamoto et al. reported a current density of 2.4 mA cm⁻² using TiO₂ nanotube photoanodes (6 cm²) and a metal dark cathode (Pb or Ag) in a divided H-type PEC cell with a methanol-based electrolyte [55]. Similarly, Cheng et al. reported an increased current density (14 mA cm⁻²) using the same PEC reactor setup with a TiO₂ nanotube photoanode and a Cu foam combined with Pt-modified graphene oxide (Pt-RGO) cathode, with a photoanode/cathode area ratio of 6/1 [38]. More recently, a TiO₂ photoanode and a gas diffusion electrode (GDE) cathode configuration led to a photocurrent density of 1.27 mA cm⁻² with a low cell voltage bias of 0.8 V [32], whereas higher current densities (9 mA cm⁻²) have been reported using TiO₂ nanotube arrays (7 cm²) in a photoanode-driven PEC cell [56]. The values from this work (21.6 mA cm⁻² with a photocurrent gap of 8.5 mA cm⁻² at -2 V, and 12.31 mA cm⁻² with a gap of 4.81 mA cm⁻² at -1.8 V) may thus demonstrate the potential of the SC-TiO₂ photoanodes developed.

Besides, the current density evolution over SC-TiO₂ and TiO₂-P25 photoanodes at constant voltage (-1.8 V vs. Ag/AgCl) is shown in Fig. 4b. It should be noted that a potential of -2 V vs. Ag/AgCl (or more negative) is not considered since it may be undesirable for the production of hydrocarbons [57] and alcohols [58] from CO₂ conversion (due mainly to enhanced H₂ generation), but it might also lead to increased energy consumption, which negatively affects the overall efficiency of the PEC process.

As expected, the illumination of the SC-TiO₂ light-responsive surfaces involves a higher current density ($j \sim 12\text{--}13$ mA cm⁻²) compared to the same system under dark conditions ($j \sim 7.5$ mA cm⁻²). Besides, the

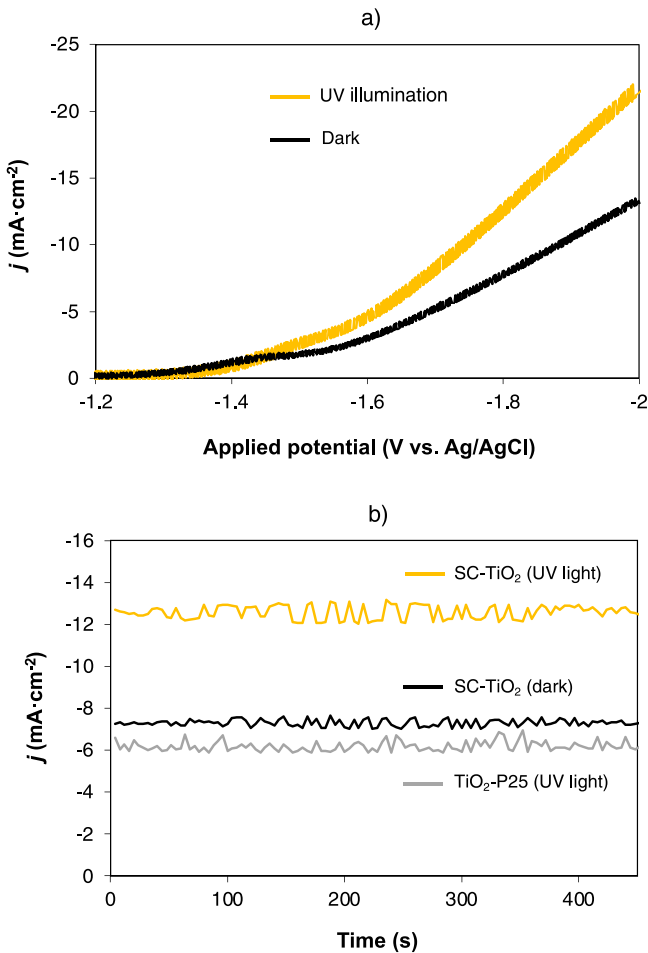


Fig. 4. PEC characterization: a) current-voltage responses of SC-TiO₂ photoanodes with (yellow) and without (black) UV illumination; b) current density evolution at -1.8 V vs. Ag/AgCl for SC-TiO₂ photoanodes with (yellow) and without (black) LED illumination, compared with TiO₂-P25 photoanodes under illumination (grey). (For interpretation of the references to colour in this figure legend, the reader is referred to the web version of this article).

use of TiO₂-P25 photoanodes leads to significantly decreased current densities in the presence of light ($j \sim 6 \text{ mA cm}^{-2}$), which proves the enhanced properties of TiO₂ synthesized in supercritical CO₂, such as specific morphology and crystallinity, surface area, light absorption, and optical bandgap energy [43,47]. In particular, the prepared photoactive materials exhibited large surface area than commercial TiO₂-P25 (152 vs. 50 m² g⁻¹), as well as a narrow bandgap energy (0.3 eV lower for SC-TiO₂), higher purity (predominant anatase phase), and specific morphology (mixture of particle shapes) [43]. Higher photocatalytic activities are therefore expected for SC-TiO₂ nanoparticles, with easier access of reactant molecules to photoactive sites and a better charge separation and transport.

Then, the stability of the prepared SC-TiO₂ photoanodes is tested under UV light for three consecutive on-off runs of 50 min (Fig. 5). The experiment starts with the UV light on, while the LED lights are turned off at the end of each run ($t = 50, 100, 150 \text{ min}$). The analysis shows how the production of CH₃OH, as an example, decays progressively after three consecutive runs. Despite this fact, the increase in CH₃OH yield at the beginning of each run may indicate that the activity loss, partially associated with the blocking of photoactive sites in the photoanode during water oxidation [59], can be mitigated from one on-off cycle to another upon light irradiation. Altogether, pseudo-stable values can be reached at the end of each cycle (4.72, 4.73, and 4.6 μmol m⁻² s⁻¹, respectively), thus showing a stable PEC conversion of CO₂ under UV light illumination.

To evaluate the composition and crystallinity of the prepared photoactive surfaces, Fig. 6 shows the XRD diffractograms of SC-TiO₂ photoanodes before and after use, including the response of P25-TiO₂ surfaces for comparison. As expected, the XRD response of TiO₂-P25 shows not only peaks related to anatase, but also peaks that can be ascribed to the presence of rutile, since both anatase and rutile are the two main physico-chemically distinct polymorphs in P25 (Sigma-Aldrich, P25). However, the homemade synthesized TiO₂ nanoparticles (SC-TiO₂) exhibit a nearly pure anatase composition, in accordance with previous studies [43,49,60,61]. It should be noted that anatase represents a more photoactive phase than rutile due to surface properties (better response to adsorbates in electron transfer reactions) and solid-state features (improved light absorption and charge transfer) [62], which might lead to an enhanced PEC performance.

Moreover, the diffractograms also reveal that SC-TiO₂ displays higher crystallinity than P25-TiO₂ if we compare the peak height (especially at 25–26°) and resolution of both diffractograms. The results, therefore, show that the calcination process (after synthesis of SC-TiO₂) has been successfully carried out, which should involve more favorable conditions for charge separation [43]. It can be finally noticed that the responses of fresh and used surfaces are very similar, which can be linked to the stability of the system for continuous light-driven PEC

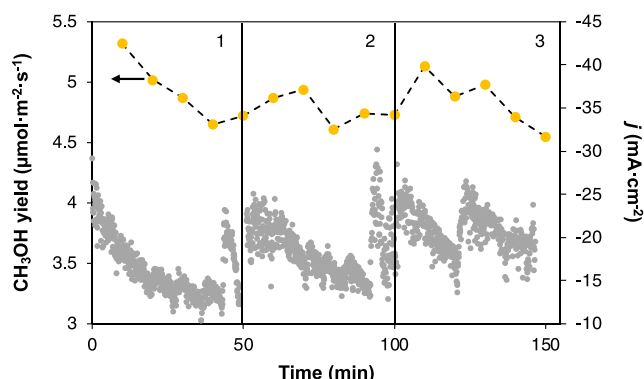


Fig. 5. Time course for the light-driven PEC production of CH₃OH (yellow) and current density (grey) using SC-TiO₂ photoanodes in three consecutive runs (−1.8 V vs. Ag/AgCl).

operation.

3.3. Product distribution and process efficiency in PEC cell

The effect of UV light irradiation on the continuous performance of the PEC cell including the SC-TiO₂ photoanodes is studied at constant voltage (−1.8 V vs. Ag/AgCl). The products obtained from CO₂ conversion in the outlet stream are C₂H₄ in the gas phase (with traces of CO) and CH₃OH (with small quantities of C₂H₅OH) in the liquid phase.

The formation rates (r) obtained as a function of light conditions (UV illumination or dark mode) are presented in Table 1. As can be seen, the performance of the UV illuminated PEC system is not only improved in terms of current density (current gap: 5.1 mA cm⁻²) but also reaction selectivity. Specifically, the increase in current under UV light allows a six-fold enhanced production of C₂H₄ (147.4 vs. 24.2 μmol m⁻² s⁻¹) and allows the formation of CH₃OH (4.72 μmol m⁻² s⁻¹), which might be explained by the specific optical properties of SC-TiO₂ photocatalysts (light absorption) and their specific morphology and crystallinity for an enhanced charge separation and transfer in the presence of light [43]. As a result, a high number of electrons (migrating from the photoanode towards the cathode) might be available to proceed with the continuous PEC conversion of CO₂. The production of H₂ also becomes more relevant at higher current densities.

The production rates presented in Table 1 are also normalized by the total charge, q (C), to properly evaluate the activity and selectivity of the process. Interestingly, the production of C₂H₄ is significantly enhanced in the presence of light regardless of the total charge passed through the system during 50 min of continuous PEC operation (0.4 μmol m⁻² s⁻¹ C⁻¹ vs. 0.11 μmol m⁻² s⁻¹ C⁻¹), which denotes that the selectivity of the reaction is altered at higher current densities (UV illumination).

Similar trends can be seen for FE (Fig. 7). The formation of C₂H₄ is improved and the generation of alcohols (i.e., CH₃OH) can be seen. The change in reaction selectivity towards C₂H₄ (FE C₂H₄ from 38.2% to 46.6%) and CH₃OH (FE CH₃OH = 15.3%) under light irradiation highlights again the improved CO₂ conversion in the cathode at higher current densities, due to the superior photoactivity of SC-TiO₂ photoanodes under the light (improved charge separation and transfer). This leads to an improved PEC process performance with decreased external bias, which is essential from a practical application viewpoint. Besides, the HER is clearly suppressed under UV light irradiation (FE H₂ = 38%) since most of the charge passed seems to be used for the selective formation of C₂H₄ and CH₃OH. In the dark, however, H₂ represents the main product at the reactor outlet (FE H₂ = 61.5%).

Finally, Table 2 shows STF and EE, which are crucial figures of merit to evaluate the overall efficiency of the PEC system. The results obtained in the present study are compared to those achieved using illuminated TiO₂-P25 surfaces in our previous work [25].

The use of illuminated SC-TiO₂ surfaces, in comparison with TiO₂-P25 photoanodes, seems to be beneficial for enhanced charge separation and transfer from the photoanode that leads to an improved generation of C₂H₄ from CO₂ conversion at the cathode. The improved characteristics of the synthesized nanoparticles in supercritical CO₂ (i.e., enhanced morphology and high crystallinity) might lead to more efficient separation of electron-hole pairs (suppressing recombination) [43] as well as an increased current density that leads to a more selective formation of C₂H₄ and CH₃OH from CO₂ at the surface of the Cu plate. The STF results for C₂H₄ and CH₃OH are enhanced in comparison with the behavior of illuminated TiO₂-P25 photoactive surfaces (5.4% vs. 3.7% for C₂H₄ and 1.9% vs. 1% for CH₃OH) under the same conditions, which once again denotes the enhanced properties of the SC-TiO₂ photoanodes and the effect of the current density on reaction selectivity (especially at high current levels). This result agrees with the decreased gap observed for SC-TiO₂ by differential reflectance analysis (Fig. 3), which allows the creation of excitations at much lower energies. Besides, as expected, the EE results under UV irradiation are improved with respect to the behavior of this material in the dark, due to the increased

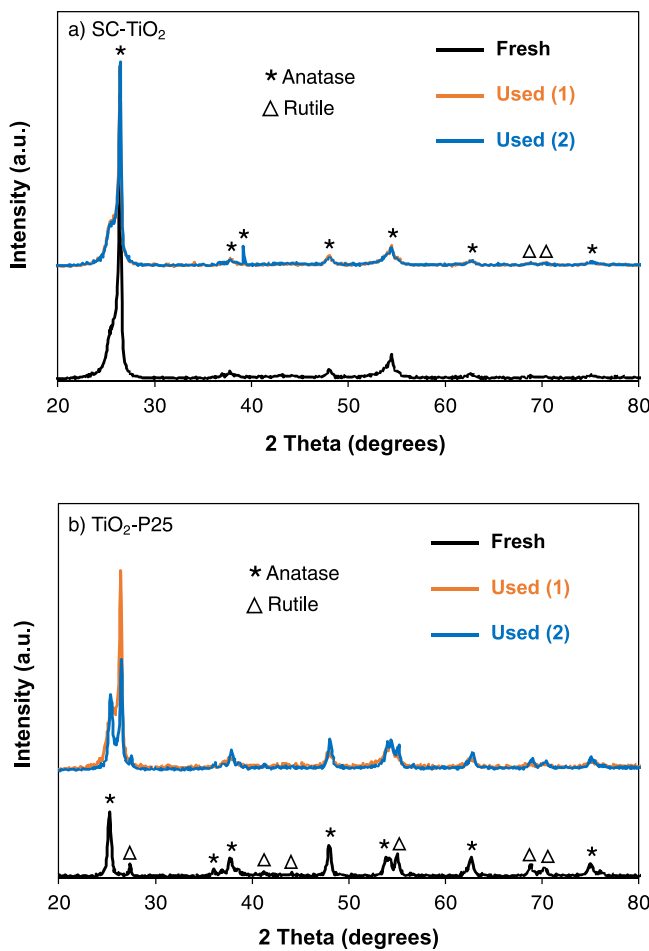


Fig. 6. XRD diffractograms of fresh and used photoactive surfaces: a) SC-TiO₂; b) TiO₂-P25.

Table 1

Production rates (*r*) for CO₂ reduction products and H₂ with and without illumination (−1.8 V vs. Ag/AgCl).

Photoanode	<i>j</i> (mA cm ^{−2})	<i>q</i> (C)	<i>r</i> (μmol m ^{−2} s ^{−1})				<i>r/q</i> (μmol m ^{−2} s ^{−1} C ^{−1})
			C ₂ H ₄	C ₂ H ₅ OH	CH ₃ OH	H ₂	
SC-TiO ₂ (UV illumination)	12.31	369.3	147.4	0.32	4.72	721.5	0.4
SC-TiO ₂ (dark)	7.18	215.4	24.2	—	—	233.1	0.11

photocurrent density generated at −1.8 V vs. Ag/AgCl (Fig. 4a and 4b). The lower *EE* under illumination for C₂H₄ at SC-TiO₂ surfaces (14%) in comparison with the performance of TiO₂-P25 (17.8%) and the invariable *EE* for CH₃OH (5% vs. 5.2%, respectively) can be linked to an increased production of H₂ in the system with SC-TiO₂ photoanodes, due to the higher current density achieved at the cathode.

Fig. 8 shows a schematic representation of the proposed reaction pathways for the generation of C₂H₄ and CH₃OH at the surface of the Cu cathode [63–68].

If we compare the *FEs* obtained for C₂H₄ (as main product) in this work (*FE* C₂H₄ = 46.6%) with other photoanode-driven PEC systems (Table 3), the results outperform the data reported in 1996 when employing a TiO₂ photoanode combined with a Cu-based cathode, where a *FE* C₂H₄ = 24% was obtained, although CH₄ was the main product [69]. Other studies also reported the generation of C₂H₄, as a minor product, in several PEC systems combining different photoanodes and Cu cathodes. For instance, Magesh et al. showed in 2014 a maximum *FE* C₂H₄ = 4.5% for C₂H₄ at WO₃ photoanodes with a Cu cathode [70], whereas this product was not detected when substituting the Cu cathode with Sn/SnO_x electrodes, which indicates the key role of

Cu. One year later, the use of a BiVO₄/WO₃ photoanode with a Cu cathode led to a *FE* C₂H₄ = 17.7% [71]. Besides, C₂H₄ was a minor product (*FE* C₂H₄ = 2.5%) from CO₂ reduction at a Cu cathode combined with photoanodes based on AlGaN/GaN heterostructures [72].

Thus, the maximum *FE* for C₂H₄ reached in this work is markedly superior to those values reported so far in different photoanode-driven PEC systems, which highlights the relevance of the present study. It should also be mentioned that although a lower *FE* for C₂H₄ was achieved in this work in comparison with our previous study at TiO₂-P25 photoanodes (*FE* C₂H₄ = 59.3%), the *STF* is nevertheless clearly superior due to an increased current density (two-fold improved) at the same potential level, thus demonstrating a more efficient PEC CO₂-to-C₂H₄ process.

Overall, this work represents a step forward into developing more effective PEC systems for CO₂ conversion in continuous mode, which may be helpful to get closer to real applications.

4. Conclusions

In this work, TiO₂ nanoparticles synthesized in supercritical medium

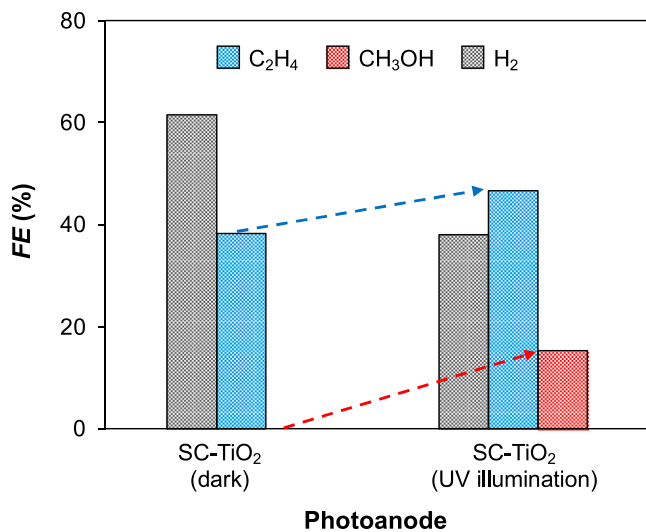


Fig. 7. FE results with SC-TiO₂ photoanodes with/without UV illumination (−1.8 V vs. Ag/AgCl).

Table 2

STF and EE for CO₂ reduction in the PEC system (−1.8 V vs. Ag/AgCl).

Photoanode	j (mA cm ^{−2})	STF (%)		EE (%)		Ref.
		C ₂ H ₄	CH ₃ OH	C ₂ H ₄	CH ₃ OH	
SC-TiO ₂ (UV illumination)	12.31	5.4	1.9	14	5	This work
SC-TiO ₂ (dark)	7.18	—	—	11.5	—	This work
TiO ₂ -P25 (UV illumination)	5.9	3.7	1	17.8	5.2	[25]

(SC-TiO₂), with a nearly pure anatase composition and improved crystallinity, are investigated in a photoanode-driven photoelectrochemical filter-press reactor for a more efficient transformation of CO₂ into value-added products (i.e., ethylene and methanol) in continuous mode.

The characterization of the photoanodes shows that photocurrent

density is higher than most of the values reported in similar photoelectrocatalytic systems and significantly superior (12.31 mA cm^{−2}) than the system in the dark (7.18 mA cm^{−2}). This current level is also higher than that reached with commercial TiO₂-P25 electrodes (5.9 mA cm^{−2}) under the same conditions. The greater decreased gap for SC-TiO₂ observed in differential absorption analyses allows the creation of excitations at much lower energies, which might be responsible for enhancing light-driven process performance.

As a result, the production of ethylene from CO₂ is six-fold improved (147.4 μmol m^{−2} s^{−1}) when using SC-TiO₂ surfaces as photoanodes in comparison with the process performance in the dark. The formation of

Table 3

PEC systems reported for CO₂ conversion to C₂H₄ at Cu-based cathodes in photoanode/dark cathode configurations.

Photoanode	Cathode	Potential and light source	Reaction medium	FE (%)	STF (%)	Ref.
SC-TiO ₂	Cu	−1.8 V vs. Ag/AgCl* UV LED (365 nm)	1 M KOH	46.6	5.4	This work
TiO ₂	Cu	−1.8 V vs. Ag/AgCl* UV LED (365 nm)	1 M KOH	59.3	3.7	[25]
TiO ₂	Cu/ZnO	Pulsed bias** Sunlight	0.1 M KHCO ₃	24	—	[69]
WO ₃	Cu	0.65 V vs. RHE*** Hg lamp (> 420 nm)	0.5 M KHCO ₃	4.5	—	[70]
BiVO ₄ /WO ₃	Cu	0.4 V vs. RHE*** Hg lamp (> 420 nm)	0.5 M KHCO ₃	17.7	—	[71]
AlGaN/GaN	Cu	−1.47 V vs. Ag/AgCl* Xe lamp (365 nm)	3 M KCl	2.5	—	[72]

Notation: * Cathode potential, ** Potential not available, *** Photoanode potential.

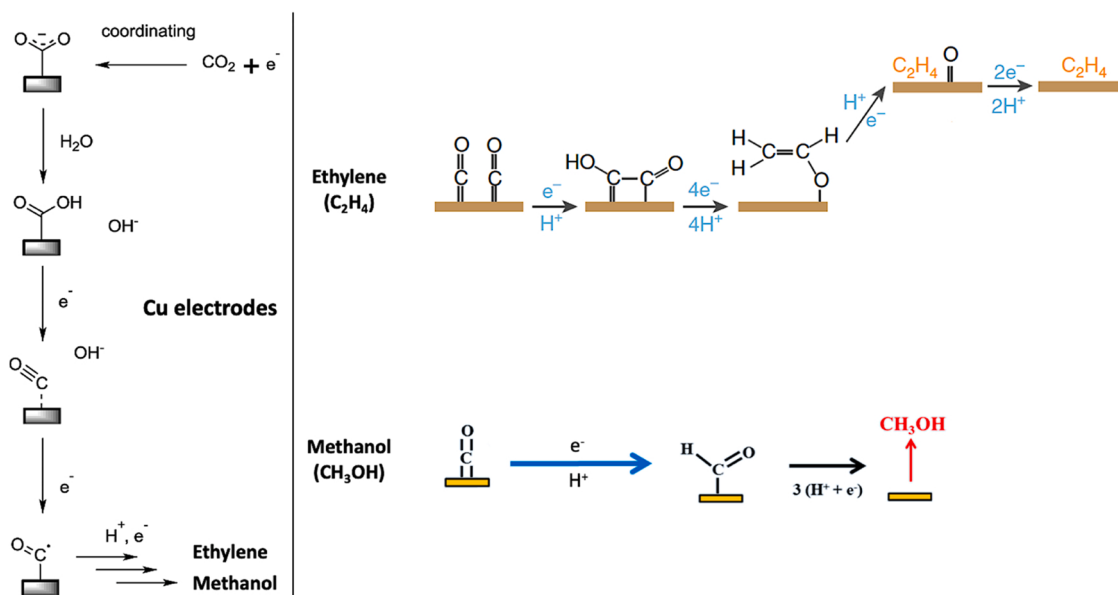


Fig. 8. Reaction mechanisms for the formation of C₂H₄ and CH₃OH from CO₂ at Cu cathodes.
Adapted from [63,66,68].

methanol is also favored under illumination ($4.72 \mu\text{mol m}^{-2} \text{s}^{-1}$). Furthermore, the Faradaic efficiencies for both ethylene and methanol (46.6% and 15.3%, respectively) are enhanced under light irradiation, outperforming previous photoanode-driven photoelectrochemical systems reported in the literature. Accordingly, the solar-to-fuel results are improved in the system with illuminated SC-TiO₂ photoactive surfaces (5.4% for ethylene and 1.9% for methanol), in comparison with the behavior of TiO₂-P25 photoanodes (3.7% for ethylene and 1% for methanol).

To sum up, this work reports the continuous light-driven photoelectrochemical conversion of CO₂ using SC-TiO₂photoanodes, promoting a more efficient photoelectrochemical transformation of CO₂ to valuable products.

CRediT authorship contribution statement

Jonathan Albo, Angel Irabien, Rafael Camarillo, Jesusa Rincón, Methodology, Resources, Validation, Supervision, Funding acquisition; **Jonathan Albo, Rafael Camarillo,** Conceptualization; **Ivan Merino-Garcia, Sergio Castro, Jonathan Albo, Ignacio Hernández, Verónica Rodríguez, Rafael Camarillo,** Formal analysis; **Ivan Merino-Garcia, Sergio Castro, Jonathan Albo, Rafael Camarillo, Ignacio Hernández:** Investigation, Roles/Writing – original draft; **Jonathan Albo, Angel Irabien:** Project administration; **Ivan Merino-Garcia, Jonathan Albo, Angel Irabien, Ignacio Hernández, Rafael Camarillo:** Visualization, Writing – review & editing.

Declaration of Competing Interest

The authors declare that they have no known competing financial interests or personal relationships that could have appeared to influence the work reported in this paper.

Acknowledgements

The authors gratefully acknowledge the financial support from Ministerio de Ciencia e Innovación (MCIN), under Ramón y Cajal programme (RYC-2015-17080), and Spanish Ministry of Economy and Competitiveness (MINECO), projects PID2019-104050RA-I00 funded by MCIN/AEI/10.13039/501100011033 and CTQ2016-76231-C2-1-R (MINECO). V.R., R.C., and J.R. wish to thank the Regional Government of Castilla-La Mancha (Project SBPLY/19/180501/000318 and Grants for the training of research personal in public research centers and companies [2016/9989]), as well as the project PID2019-111416RB-I00 funded by MCIN/AEI/10.13039/501100011033. I.H. also acknowledges the funding by the Spanish Ministry of Science, Grant No. MAT2016-80438-P.

References

- [1] J. Qiao, Y. Liu, F. Hong, J. Zhang, A review of catalysts for the electroreduction of carbon dioxide to produce low-carbon fuels, *Chem. Soc. Rev.* 43 (2014) 631–675, <https://doi.org/10.1039/c3cs60323g>.
- [2] W. Zhang, Y. Hu, L. Ma, G. Zhu, Y. Wang, X. Xue, R. Chen, S. Yang, Z. Jin, Progress and perspective of electrocatalytic CO₂ reduction for renewable carbonaceous fuels and chemicals, *Adv. Sci. Sci.* 5 (2018), 1700275, <https://doi.org/10.1002/advs.201700275>.
- [3] E.V. Kondratenko, G. Mul, J. Baltrusaitis, G.O. Larrazábal, J. Pérez-Ramírez, Status and perspectives of CO₂ conversion into fuels and chemicals by catalytic, photocatalytic and electrocatalytic processes, *Energy Environ. Sci.* 6 (2013) 3112–3135, <https://doi.org/10.1039/c3ee41272e>.
- [4] T. Burdyny, W.A. Smith, CO₂ reduction on gas-diffusion electrodes and why catalytic performance must be assessed at commercially-relevant conditions, *Energy Environ. Sci.* 12 (2019) 1442–1453, <https://doi.org/10.1039/c8ee03134g>.
- [5] I. Merino-Garcia, L. Tinat, J. Albo, M. Alvarez-Guerra, A. Irabien, O. Durupthy, V. Vivier, C.M. Sánchez-Sánchez, Continuous electroconversion of CO₂ into formate using 2 nm tin oxide nanoparticles, *Appl. Catal. B Environ.* 297 (2021), 120447, <https://doi.org/10.1016/j.apcatb.2021.120447>.
- [6] A. Sanna, M.R. Hall, M. Maroto-Valer, Post-processing pathways in carbon capture and storage by mineral carbonation (CCSM) towards the introduction of carbon neutral materials, *Energy Environ. Sci.* 5 (2012) 7781–7796, <https://doi.org/10.1039/c2ee03455g>.
- [7] Y. Zheng, W. Zhang, Y. Li, J. Chen, B. Yu, J. Wang, L. Zhang, J. Zhang, Energy related CO₂ conversion and utilization: advanced materials/nanomaterials, reaction mechanisms and technologies, *Nano Energy* 40 (2017) 512–539, <https://doi.org/10.1016/j.nanoen.2017.08.049>.
- [8] G.D. Takalkar, R.R. Bhosale, Application of cobalt incorporated Iron oxide catalytic nanoparticles for thermochemical conversion of CO₂, *Appl. Surf. Sci.* 495 (2019), 143508, <https://doi.org/10.1016/j.apsusc.2019.07.250>.
- [9] I. Merino-Garcia, J. Albo, A. Irabien, Tailoring gas-phase CO₂ electroreduction selectivity to hydrocarbons at Cu nanoparticles, *Nanotechnology* 29 (2018), 014001, <https://doi.org/10.1088/1361-6528/aa994e>.
- [10] A.A. Al-Omari, Z.H. Yamani, H.L. Nguyen, Electrocatalytic CO₂ reduction: from homogeneous catalysts to heterogeneous-based reticular chemistry, *Molecules* 23 (2018) 1–12, <https://doi.org/10.3390/molecules23112835>.
- [11] A.U. Pawar, C.W. Kim, M.T. Nguyen-Le, Y.S. Kang, General review on the components and parameters of photoelectrochemical system for CO₂ reduction with in situ analysis, *ACS Sustain. Chem. Eng.* 7 (2019) 7431–7455, <https://doi.org/10.1021/acssuschemeng.8b06303>.
- [12] P. Chen, Y. Zhang, Y. Zhou, F. Dong, Photoelectrocatalytic carbon dioxide reduction: fundamental, advances and challenges, *Nano Mater. Sci.* (2021), <https://doi.org/10.1016/j.nanoms.2021.05.003>.
- [13] N. Nandal, S.L. Jain, A review on progress and perspective of molecular catalysis in photoelectrochemical reduction of CO₂, *Coord. Chem. Rev.* 451 (2022), 214271, <https://doi.org/10.1016/j.ccr.2021.214271>.
- [14] J. Albo, M. Alvarez-Guerra, A. Irabien, Electro-, photo- and-photoelectro-chemical reduction of CO₂, in: *Heterogeneous Catalysts: Advanced Design, Characterization and Applications*, Wiley-VCH GmbH, 2021, <https://doi.org/10.1002/9783527813599.ch36>.
- [15] K. Li, X. An, K.H. Park, M. Khrasheh, J. Tang, A critical review of CO₂ photoconversion: catalysts and reactors, *Catal. Today* 224 (2014) 3–12, <https://doi.org/10.1016/j.cattod.2013.12.006>.
- [16] D. Pan, X. Ye, Y. Cao, S. Zhu, X. Chen, M. Chen, D. Zhang, G. Li, Photoanode driven photoelectrocatalytic system for CO₂ reduction to formic acid by using CoOx cathode, *Appl. Surf. Sci.* 511 (2020), 145497, <https://doi.org/10.1016/j.apsusc.2020.145497>.
- [17] J. Wang, J. Ma, Q. Zhang, Y. Chen, L. Hong, B. Wang, J. Chen, H. Jing, New heterojunctions of CN/TiO₂ with different band structure as highly efficient catalysts for artificial photosynthesis, *Appl. Catal. B Environ.* 285 (2021), 119781, <https://doi.org/10.1016/j.apcatb.2020.119781>.
- [18] A.G. Karthick Raj, C. Murugan, A. Pandikumar, Efficient photoelectrochemical reduction of carbon dioxide into alcohol assisted by photoanode driven water oxidation with gold nanoparticles decorated titania nanotubes, *J. CO₂ Util.* 52 (2021), 101684, <https://doi.org/10.1016/j.jcou.2021.101684>.
- [19] E. Kalamaras, M.M. Maroto-Valer, M. Shao, J. Xuan, H. Wang, Solar carbon fuel via photoelectrochemistry, *Catal. Today* 317 (2018) 56–75, <https://doi.org/10.1016/j.cattod.2018.02.045>.
- [20] H.J. Yang, H. Yang, Y.H. Hong, P.Y. Zhang, T. Wang, L.N. Chen, F.Y. Zhang, Q. H. Wu, N. Tian, Z.Y. Zhou, S.G. Sun, Promoting ethylene selectivity from CO₂ electroreduction on CuO supported onto CO₂ capture materials, *ChemSusChem* 11 (2018) 881–887, <https://doi.org/10.1002/cssc.201702338>.
- [21] I. Merino-Garcia, J. Albo, J. Solla-Gullón, V. Montiel, A. Irabien, Cu oxide/ZnO-based surfaces for a selective ethylene production from gas-phase CO₂ electroconversion, *J. CO₂ Util.* 31 (2019) 135–142, <https://doi.org/10.1016/j.jcou.2019.03.002>.
- [22] J. Albo, A. Irabien, CuO-loaded gas diffusion electrodes for the continuous electrochemical reduction of CO₂ to methanol, *J. Catal.* 343 (2016) 232–239, <https://doi.org/10.1016/j.jcat.2015.11.014>.
- [23] J. Albo, M. Alvarez-Guerra, P. Castaño, A. Irabien, Towards the electrochemical conversion of carbon dioxide into methanol, *Green Chem.* 17 (2015) 2304–2324, <https://doi.org/10.1039/c4gc02453b>.
- [24] W. Zhang, Q. Qin, L. Dai, R. Qin, X. Zhao, X. Chen, D. Ou, J. Chen, T.T. Chuong, B. Wu, N. Zheng, Electrochemical reduction of carbon dioxide to methanol on hierarchical Pd/SnO₂ nanosheets with abundant Pd–O–Sn interfaces, *Angew. Chem. Int. Ed.* 57 (2018) 9475–9479, <https://doi.org/10.1002/anie.201804142>.
- [25] S. Castro, J. Albo, A. Irabien, Continuous conversion of CO₂ to alcohols in a TiO₂ photoanode-driven photoelectrochemical system, *J. Chem. Technol. Biotechnol.* 95 (2020) 1876–1882, <https://doi.org/10.1002/jctb.6315>.
- [26] M. Zhang, J. Cheng, X. Xuan, J. Zhou, K. Cen, CO₂ synergistic reduction in a photoanode-driven photoelectrochemical cell with Pt-modified TiO₂ nanoparticle photoanode and a Pt reduced graphene oxide electrocathode, *ACS Sustain. Chem. Eng.* 4 (2016) 6344–6354, <https://doi.org/10.1021/acssuschemeng.6b00909>.
- [27] M.R. Singh, E.L. Clark, A.T. Bell, Effects of electrolyte, catalyst, and membrane composition and operating conditions on the performance of solar-driven electrochemical reduction of carbon dioxide, *Phys. Chem. Chem. Phys.* 17 (2015) 18924–18936, <https://doi.org/10.1039/c5cp03283k>.
- [28] J.F. de Brito, A.A. da Silva, A.J. Cavalheiro, M.V.B. Zanoni, Evaluation of the parameters affecting the photoelectrocatalytic reduction of CO₂ to CH₃OH at Cu/Cu₂O electrode, *Int. J. Electrochim. Sci.* 9 (2014) 5961–5973.
- [29] S. Castro, J. Albo, A. Irabien, Photoelectrochemical reactors for CO₂ utilization, *ACS Sustain. Chem. Eng.* 6 (2018) 15877–15894, <https://doi.org/10.1021/acssuschemeng.8b03706>.
- [30] S. Xie, Q. Zhang, G. Liu, Y. Wang, Photocatalytic and photoelectrocatalytic reduction of CO₂ using heterogeneous catalysts with controlled nanostructures, *Chem. Commun.* 52 (2016) 35–59, <https://doi.org/10.1039/c5cc07613g>.

- [31] P. Wang, S. Wang, H. Wang, Z. Wu, L. Wang, Recent progress on photoelectrocatalytic reduction of carbon dioxide, Part. Part. Syst. Charact. 35 (2018), 1700371, <https://doi.org/10.1002/ppsc.201700371>.
- [32] K. Kobayashi, S.N. Lou, Y. Takatsuji, T. Haruyama, Y. Shimizu, T. Ohno, Photoelectrochemical reduction of CO₂ using a TiO₂ photoanode and a gas diffusion electrode modified with a metal phthalocyanine catalyst, *Electrochim. Acta* 338 (2020), 135805, <https://doi.org/10.1016/j.electacta.2020.135805>.
- [33] H. Li, Y. Shi, H. Shang, W. Wang, J. Lu, A.A. Zakharov, L. Hultman, R.I.G. Uhrberg, M. Syväjärvi, R. Yakimova, L. Zhang, J. Sun, Atomic-scale tuning of graphene/cubic SiC Schottky junction for stable low-bias photoelectrochemical solar-to-fuel conversion, *ACS Nano* 14 (2020) 4905–4915, <https://doi.org/10.1021/acsnano.0c00986>.
- [34] J.F. de Brito, C. Genovese, F. Tavella, C. Ampelli, M.V. Boldrin Zanoni, G. Centi, S. Perathoner, CO₂ reduction of hybrid Cu₂O–Cu/gas diffusion layer electrodes and their integration in a Cu-based photoelectrocatalytic cell, *ChemSusChem* 12 (2019) 4274–4284, <https://doi.org/10.1002/cssc.201901352>.
- [35] M. Marszewski, S. Cao, J. Yu, M. Jaroniec, Semiconductor-based photocatalytic CO₂ conversion, *Mater. Horiz.* 2 (2015) 261–278, <https://doi.org/10.1039/c4mh00176a>.
- [36] S.N. Haberreutinger, L. Schmidt-Mende, J.K. Stolarczyk, Photocatalytic reduction of CO₂ on TiO₂ and other semiconductors, *Angew. Chem. Int. Ed.* 52 (2013) 7372–7408, <https://doi.org/10.1002/anie.201207199>.
- [37] J. Cheng, M. Zhang, G. Wu, X. Wang, J. Zhou, K. Cen, Photoelectrocatalytic reduction of CO₂ into chemicals using Pt-modified reduced graphene oxide combined with Pt-modified TiO₂ nanotubes, *Environ. Sci. Technol.* 48 (2014) 7076–7084, <https://doi.org/10.1021/es500364g>.
- [38] J. Cheng, M. Zhang, J. Liu, J. Zhou, K. Cen, A. Cu, foam cathode used as a Pt-RGO catalyst matrix to improve CO₂ reduction in a photoelectrocatalytic cell with a TiO₂ photoanode, *J. Mater. Chem. A* 3 (2015) 12947–12957, <https://doi.org/10.1039/c5ta03026a>.
- [39] P. Ding, T. Jiang, N. Han, Y. Li, Photocathode engineering for efficient photoelectrochemical CO₂ reduction, *Mater. Today Nano* 10 (2020), 100077, <https://doi.org/10.1016/j.mtnano.2020.100077>.
- [40] V. Kumaravel, J. Bartlett, S.C. Pillai, Photoelectrochemical conversion of carbon dioxide (CO₂) into fuels and value-added products, *ACS Energy Lett.* 5 (2020) 486–519, <https://doi.org/10.1021/acsenergylett.9b02585>.
- [41] T.P. Nguyen, D.L.T. Nguyen, V.H. Nguyen, T.H. Le, D.V.N. Vo, Q.T. Trinh, S.R. Bae, S.Y. Chae, S.Y. Kim, Q. Van Le, Recent advances in TiO₂-based photocatalysts for reduction of CO₂ to fuels, *Nanomaterials* 10 (2020) 337, <https://doi.org/10.3390/nano10020337>.
- [42] R. Camarillo, J. Rincón, Photocatalytic discoloration of dyes: relation between effect of operating parameters and dye structure, *Chem. Eng. Technol.* 34 (2011) 1675–1684, <https://doi.org/10.1002/ceat.201100063>.
- [43] R. Camarillo, S. Tostón, F. Martínez, C. Jiménez, J. Rincón, Preparation of TiO₂-based catalysts with supercritical fluid technology: characterization and photocatalytic activity in CO₂ reduction, *J. Chem. Technol. Biotechnol.* 92 (2017) 1710–1720, <https://doi.org/10.1002/jctb.5169>.
- [44] J.F. de Brito, J.A.L. Perini, S. Perathoner, M.V.B. Zanoni, Turning carbon dioxide into fuel concomitantly to the photoanode-driven process of organic pollutant degradation by photoelectrocatalysis, *Electrochim. Acta* 306 (2019) 277–284, <https://doi.org/10.1016/j.electacta.2019.03.134>.
- [45] A.G.K. Raj, C. Murugan, P. Rameshkumar, A. Pandikumar, Growth of silver nanodendrites on titania nanotubes array for photoanode driven photoelectrocatalytic reduction of carbon dioxide, *Appl. Surf. Sci. Adv.* 2 (2020), 100035, <https://doi.org/10.1016/j.apsadv.2020.100035>.
- [46] E. Alonso, I. Montequi, M.J. Cocero, Effect of synthesis conditions on photocatalytic activity of TiO₂ powders synthesized in supercritical CO₂, *J. Supercrit. Fluids* 49 (2009) 233–238, <https://doi.org/10.1016/j.supflu.2009.01.005>.
- [47] J. Jung, M. Perrut, Particle design using supercritical fluids: literature and patent survey, *J. Supercrit. Fluids* 20 (2001) 179–219. (<http://linkinghub.elsevier.com/retrieve/pii/S089684460100064X>).
- [48] R. Camarillo, S. Tostón, F. Martínez, C. Jiménez, J. Rincón, Enhancing the photocatalytic reduction of CO₂ through engineering of catalysts with high pressure technology: Pd/TiO₂ photocatalysts, *J. Supercrit. Fluids* 123 (2017) 18–27, <https://doi.org/10.1016/j.supflu.2016.12.010>.
- [49] E. Alonso, I. Montequi, S. Lucas, M.J. Cocero, Synthesis of titanium oxide particles in supercritical CO₂: effect of operational variables in the characteristics of the final product, *J. Supercrit. Fluids* 39 (2007) 453–461, <https://doi.org/10.1016/j.supflu.2006.03.006>.
- [50] B.L. Cushing, V.L. Kolesnichenko, C.J. O'Connor, Recent advances in the liquid-phase syntheses of inorganic nanoparticles, *Chem. Rev.* 104 (2004) 3893–3946, <https://doi.org/10.1021/cr030027b>.
- [51] J.J. Kim, D.P. Summers, K.W. Frese, Reduction of CO₂ and CO to methane on Cu foil electrodes, *J. Electroanal. Chem. Interfacial Electrochem.* 245 (1988) 223–244, [https://doi.org/10.1016/0022-0728\(88\)80071-8](https://doi.org/10.1016/0022-0728(88)80071-8).
- [52] A. Irabien, M. Alvarez-Guerra, J. Albo, A. Dominguez-Ramos, *Electrochemical conversion of CO₂ to value-added products*, in: *Electrochem. Water Wastewater Treat.*, Elsevier, Amsterdam, 2018, pp. 29–59.
- [53] Z. Zhang, J.T. Yates, Band bending in semiconductors: chemical and physical consequences at surfaces and interfaces, *Chem. Rev.* 112 (2012) 5520–5551, <https://doi.org/10.1021/cr3000626>.
- [54] Y. Hermans, S. Murcia-López, A. Klein, R. Van De Krol, T. Andreu, J.R. Morante, T. Toupanie, W. Jaegermann, Analysis of the interfacial characteristics of BiVO₄/metal oxide heterostructures and its implication on their junction properties, *Phys. Chem. Chem. Phys.* 21 (2019) 5086–5096, <https://doi.org/10.1039/c8cp07483f>.
- [55] T. Yamamoto, H. Katsumata, T. Suzuki, S. Kaneko, Photoelectrochemical reduction of CO₂ in methanol with TiO₂ photoanode and metal cathode, *ECS Trans.* 75 (2017) 31–37, <https://doi.org/10.1149/07550.0031ecst>.
- [56] M. Zhang, J. Cheng, X. Xuan, J. Zhou, K. Cen, Pt/graphene aerogel deposited in Cu foam as a 3D binder-free cathode for CO₂ reduction into liquid chemicals in a TiO₂ photoanode-driven photoelectrochemical cell, *Chem. Eng. J.* 322 (2017) 22–32, <https://doi.org/10.1016/j.cej.2017.03.126>.
- [57] I. Merino-Garcia, J. Albo, A. Irabien, Productivity and selectivity of gas-phase CO₂ electroreduction to methane at copper nanoparticle-based electrodes, *Energy Technol.* 5 (2017) 922–928, <https://doi.org/10.1002/ente.201600616>.
- [58] J. Albo, D. Vallejo, G. Beobide, O. Castillo, P. Castaño, A. Irabien, Copper-based metal–organic porous materials for CO₂ electrocatalytic reduction to alcohols, *ChemSusChem* 10 (2017) 1100–1109, <https://doi.org/10.1002/cssc.201600693>.
- [59] J. Albo, M.I. Qadir, M. Samperi, J.A. Fernandes, I. de Pedro, J. Dupont, Use of an optofluidic microreactor and Cu nanoparticles synthesized in ionic liquid and embedded in TiO₂ for an efficient photoreduction of CO₂ to methanol, *Chem. Eng. J.* 404 (2021), 126643, <https://doi.org/10.1016/j.cej.2020.126643>.
- [60] Q. Wang, D. Yang, D. Chen, Y. Wang, Z. Jiang, Synthesis of anatase titania-carbon nanotubes nanocomposites with enhanced photocatalytic activity through a nano-coating-hydrothermal process, *J. Nanopart. Res.* 9 (2007) 1087–1096, <https://doi.org/10.1007/s11051-006-9199-x>.
- [61] Y.C. Wu, Y.C. Tai, Effects of alcohol solvents on anatase TiO₂ nanocrystals prepared by microwave-assisted solvothermal method, *J. Nanopart. Res.* 15 (2013) 1686, <https://doi.org/10.1007/s11051-013-1686-2>.
- [62] M.A. Henderson, A surface science perspective on TiO₂ photocatalysis, *Surf. Sci. Rep.* 66 (2011) 185–297, <https://doi.org/10.1016/j.surrep.2011.01.001>.
- [63] R. Kortlever, J. Shen, K.J.P. Schouten, F. Calle-Vallejo, M.T.M. Koper, Catalysts and reaction pathways for the electrochemical reduction of carbon dioxide, *J. Phys. Chem. Lett.* 6 (2015) 4073–4082, <https://doi.org/10.1021/acs.jpclett.5b01559>.
- [64] K.P. Kuhl, E.R. Cave, D.N. Abram, T.F. Jaramillo, New insights into the electrochemical reduction of carbon dioxide on metallic copper surfaces, *Energy Environ. Sci.* 5 (2012) 7050–7059, <https://doi.org/10.1039/c2ee21234j>.
- [65] A.A. Peterson, F. Abild-Pedersen, F. Studt, J. Rossmeisl, J.K. Nørskov, How copper catalyzes the electroreduction of carbon dioxide into hydrocarbon fuels, *Energy Environ. Sci.* 3 (2010) 1311–1315, <https://doi.org/10.1039/c0ee00071j>.
- [66] J.P. Jones, G.K.S. Prakash, G.A. Olah, Electrochemical CO₂ reduction: recent advances and current trends, *Isr. J. Chem.* 54 (2014) 1451–1466, <https://doi.org/10.1002/ijch.201400081>.
- [67] A.J. Garza, A.T. Bell, M. Head-Gordon, Mechanism of CO₂ reduction at copper surfaces: pathways to C₂ products, *ACS Catal.* 8 (2018) 1490–1499, <https://doi.org/10.1021/acscatal.7b03477>.
- [68] D. Ren, J. Fong, B.S. Yeo, The effects of currents and potentials on the selectivities of copper toward carbon dioxide electroreduction, *Nat. Commun.* 9 (2018) 925, <https://doi.org/10.1038/s41467-018-03286-w>.
- [69] S. Ichikawa, R. Doi, Hydrogen production from water and conversion of carbon dioxide to useful chemicals by room temperature photoelectrocatalysis, *Catal. Today* 27 (1996) 271–277, [https://doi.org/10.1016/0920-5861\(95\)00198-0](https://doi.org/10.1016/0920-5861(95)00198-0).
- [70] G. Magesh, E.S. Kim, H.J. Kang, M. Banu, J.Y. Kim, J.H. Kim, J.S. Lee, A versatile photoanode-driven photoelectrochemical system for conversion of CO₂ to fuels with high faradaic efficiencies at low bias potentials, *J. Mater. Chem. A* 2 (2014) 2044–2049, <https://doi.org/10.1039/c3ta14408a>.
- [71] J.H. Kim, G. Magesh, H.J. Kang, M. Banu, J.H. Kim, J. Lee, J.S. Lee, Carbonate-coordinated cobalt co-catalyzed BiVO₄/WO₃ composite photoanode tailored for CO₂ reduction to fuels, *Nano Energy* 15 (2015) 153–163, <https://doi.org/10.1016/j.nanoen.2015.04.022>.
- [72] M. Deguchi, S. Yotsuhashi, H. Hashiba, Y. Yamada, K. Ohkawa, Enhanced capability of photoelectrochemical CO₂ conversion system using an AlGaN/GaN photoelectrode, *Jpn. J. Appl. Phys.* 52 (2013) 08JF07, <https://doi.org/10.7567/JJAP.52.08JF07>.

Resumen de resultados y conclusiones

CAPÍTULO 4. RESUMEN DE RESULTADOS Y CONCLUSIONES

4.1 Resumen de los principales resultados

La presente Tesis Doctoral presenta un proceso de conversión fotoelectroquímica de CO₂ en continuo utilizando fotoánodos basados en TiO₂ comercial (TiO₂-P25) y TiO₂ con propiedades mejoradas (TiO₂-SC), junto con cátodos basados en Cu, para la producción de alcoholes e hidrocarburos.

Para lograrlo, se ha realizado inicialmente una exhaustiva revisión del estado del arte, donde la fotoelectrocatalisis destaca como una alternativa prometedora que combina las ventajas de la electrocatalisis y la fotocatalisis, reduciendo el voltaje requerido en la conversión electroquímica de CO₂ en productos químicos útiles mediante el aprovechamiento de la luz. Como se ha discutido a lo largo de este documento, el diseño de un reactor PEC debe realizarse en base a una cuidadosa evaluación de diversos factores, como son la fuente de luz, la configuración geométrica, el material de construcción, así como características de mezcla y flujo, e intercambio de calor, entre otros. Dos de los parámetros clave del proceso son las fases involucradas y el modo de operación (es decir, discontinuo, semicontinuo o continuo). Además, el ánodo y el cátodo en la celda PEC deben estar preferiblemente en forma de películas delgadas separadas por una membrana conductora de protones y depositadas sobre sustratos porosos. Esto favorece el transporte de electrones, así como la difusión de protones a través de la membrana. El proceso requiere además que se dé eficientemente la reacción de evolución de oxígeno en el lado del ánodo y una difusión eficiente de CO₂ en el lado del cátodo.

La literatura muestra que se ha empleado con mayor frecuencia la configuración de fotoánodo-cátodo a oscuras, aprovechando los beneficios de usar semiconductores tipo *n* (en lugar de semiconductores tipo *p*), más abundantes, económicos y estables para la oxidación de H₂O. En una configuración fotocátodo-ánodo a oscuras, el fotocátodo está compuesto por un semiconductor tipo *p* debido a su alta energía de banda de conducción, que es adecuada para la reducción de CO₂, pero su eficiencia es limitada. Otra opción para la disposición de los fotoelectrodos es la combinación de un fotocátodo con un semiconductor tipo *p* para la reducción de CO₂ con un fotoánodo de semiconductor tipo *n* para la oxidación de H₂O. A diferencia de las otras dos configuraciones, esta permite, idealmente, realizar la reducción de CO₂ sin necesidad de aplicar corriente eléctrica externa. Por último, la configuración de reactor PEC tandem (o híbrida) combina la reducción de CO₂ con la generación de energía fotovoltaica en el mismo dispositivo, mediante: (i) la utilización de elementos fotovoltaicos exteriores al reactor, capaces de suministrar un flujo extra de electrones para la reducción de CO₂ y (ii) la integración de materiales fotovoltaicos en la estructura de los fotoelectrodos del sistema, maximizando el aprovechamiento de la luz y la separación de cargas.

Tras la revisión del estado del arte, se ha diseñado y construido un sistema experimental para llevar a cabo la fotoelectroreducción de CO₂ a metanol y etanol en continuo. Se utiliza una celda PEC compuesta inicialmente por un fotoánodo basado TiO₂-P25 en configuración MEA que se ilumina con luz LED UV (100 mW·cm⁻²), junto con una placa de Cu a oscuras. Con esta configuración, se ha logrado un incremento de hasta 4,3 mA·cm⁻² (2 V vs. Ag/AgCl) al iluminar la superficie del fotoánodo. El funcionamiento del sistema se ve favorecido al aplicar -1,8 V vs. Ag/AgCl con una carga catalítica de TiO₂-P25 de 3 mg·cm⁻², donde se alcanza una velocidad de producción de 9,5 µmol·m⁻²·s⁻¹, una eficiencia Faradaica del 16,2% y una eficiencia energética del 5,2% para metanol, y una velocidad de producción de 6,8 µmol·m⁻²·s⁻¹, eficiencia Faradaica del 23,2% y eficiencia energética del 6,8% para etanol. La producción de metanol se ve favorecida con el incremento de voltaje, mientras que la producción de etanol se ve afectada negativamente. Se concluye que es posible mejorar la producción de alcoholes a partir de CO₂ con luz UV, reduciendo la energía requerida en un sistema electroquímico (a oscuras).

Posteriormente se investiga el empleo de nanopartículas de TiO₂-SC para la preparación de fotoánodos con el objetivo de mejorar la eficiencia del proceso. La caracterización fotoelectroquímica de los fotoánodos revela que la densidad de corriente alcanzada es significativamente más elevada (12,31 mA·cm⁻²) que la alcanzada en el sistema en ausencia de luz (7,18 mA·cm⁻²). Esta corriente también supera la obtenida anteriormente con los fotoánodos fabricados con nanopartículas comerciales de TiO₂-P25 (5,9 mA·cm⁻²) en las mismas condiciones. Esta mejora se atribuye a las propiedades mejoradas del TiO₂-SC, como es la morfología, la cristalinidad y el área superficial, con influencia en la absorción de luz y *bandgap*, que se traduce en un mejor acceso de reactivos a los sitios fotoactivos y una mejor separación de cargas, lo que permite mejorar la eficiencia del proceso. Como resultado, la producción de etileno, producto de gran interés comercial, se mejora hasta en seis veces (147,4 µmol·m⁻²·s⁻¹) cuando se utilizan superficies de TiO₂-SC como fotoánodos en comparación con el rendimiento del proceso a oscuras. La formación de metanol también se ve favorecida bajo la luz (4,72 µmol·m⁻²·s⁻¹). Además, las eficiencias Faradaicas tanto para el etileno como para el metanol (46,6% y 15,3%, respectivamente), aumentan con la irradiación de luz, superando los resultados reportados en la literatura para sistemas fotoelectroquímicos en configuración fotoánodo-cátodo. En consecuencia, la eficiencia en la conversión de energía solar en productos mejora en el sistema basado en TiO₂-SC (5,4% para etileno y 1,9% para metanol), en comparación con el comportamiento de los fotoánodos de TiO₂-P25 (3,7% para etileno y 1 % de metanol).

4.2 Conclusiones

Las conclusiones obtenidas a lo largo de la presente Tesis Doctoral han sido difundidas a través 3 artículos en revistas científicas incluidas en el InCites™ Journal of Citation Reports-Science Edition (JCR), en posiciones del primer decil (D1), primer cuartil (Q1) o segundo cuartil (Q2) y 5 comunicaciones presentadas en congresos internacionales y nacionales (2 de las mismas recogidas en libros o proceedings con ISBN). El listado completo de contribuciones a congresos se detalla en el anexo, especificando, en cada caso, el tipo de comunicación realizada, oral o póster.

A continuación, se enumeran las 3 publicaciones en revistas científicas, indicando lista de autores por orden de firma, título del artículo, nombre de la revista, número de la revista, año de publicación, índice de impacto disponible correspondiente al año de publicación, denominación del área temática de la revista, cuartil en el área temática y posición relativa en el área temática:

1. Sergio Castro, Jonathan Albo, Ángel Irabien, **2018**. Photoelectrochemical reactors for CO₂ utilization. ACS Sustainable Chemistry & Engineering, 6, 15877-15894. Índice de impacto: 6,970. Q1 y D1; Chemical Engineering 9/138.
2. Sergio Castro, Jonathan Albo, Ángel Irabien, **2020**. Continuous conversion of CO₂ to alcohols in a TiO₂ photoanode-driven photoelectrochemical system. Journal of Chemical Technology & Biotechnology, 95, 1876-1882. Índice de impacto: 3,174. Q2; Chemical Engineering 63/143.
3. Iván Merino-García¹, Sergio Castro¹, Ángel Irabien, Ignacio Hernández, Verónica Rodríguez, Rafael Camarillo, Jesusa Rincón, Jonathan Albo, **2022**. Efficient photoelectrochemical conversion of CO₂ to ethylene and methanol using a Cu cathode and TiO₂ nanoparticles synthesized in supercritical medium as photoanode. Journal of Environmental Chemical Engineering, 10, 107441. Índice de impacto: 7,7. Q1; Chemical Engineering 16/140. ¹Iván Merino-García y Sergio Castro han contribuido igualmente a este trabajo como primeros autores.

Se presentan a continuación las principales conclusiones recogidas en los citados artículos:

- 1) Se ha demostrado las posibilidades técnicas de llevar a cabo el proceso de fotoelectroreducción de CO₂ en modo continuo a productos de alto valor añadido utilizando materiales semiconductores de TiO₂-P25 y TiO₂-SC. Este enfoque permite reducir significativamente la energía requerida en un sistema electroquímico convencional. Los resultados muestran el potencial de la fotoelectrocatalisis para la conversión eficiente de CO₂, lo que contribuye al mismo tiempo a mitigar el cambio climático.

2) Tras una revisión exhaustiva del estado del arte en el campo de la fotoelectroreducción de CO₂ a productos de alto valor añadido, se ha observado que la configuración más reportada en la actualidad es aquella que utiliza un fotoánodo junto con un cátodo a oscuras. Esto se debe a los beneficios asociados al uso de semiconductores tipo *n*, en lugar de los semiconductores tipo *p*, que son abundantes, económicos y estables para la oxidación de H₂O. Además, otra opción prometedora para la disposición de los fotoelectrodos es la combinación de un photocátodo de semiconductor tipo *p* para la reducción de CO₂ con un fotoánodo de semiconductor tipo *n* para la oxidación de H₂O. Esta configuración, permite llevar a cabo la reducción de CO₂ junto con la oxidación de H₂O sin necesidad de un aporte eléctrico externo, idealmente, lo cual simplifica el sistema y reduce los consumos del proceso electroquímico. Los sistemas PEC tandem, que incorporan elementos fotovoltaicos, permiten un mejor aprovechamiento de la luz y mejoran la separación de cargas.

3) Posteriormente, se diseña y construye un sistema experimental para la fotoelectroreducción en continuo de CO₂ a productos de alto valor añadido. Para ello, se emplea un reactor PEC equipado con un fotoánodo de TiO₂-P25 en una configuración MEA. Durante las pruebas bajo iluminación de luz UV, se observa un incremento notable en la densidad de corriente (4,3 mA·cm⁻²). Este resultado muestra los potenciales beneficios del fotoánodo desarrollado.

Además, se observa como al utilizar una carga de TiO₂-P25 de 3 mg·cm⁻² en el fotoánodo y aplicar un potencial de -1,8 V frente a Ag/AgCl, se alcanza una velocidad de producción de metanol de 9,5 µmol·m⁻²·s⁻¹, con una eficiencia Faradaica del 16,2% y una eficiencia energética del 5,2%. En el caso del etanol, se obtiene una velocidad de producción de 6,8 µmol·m⁻²·s⁻¹, una eficiencia Faradaica del 12,1% y una eficiencia energética del 6,8% en las mismas condiciones. La selectividad de la reacción puede ser modulada con el voltaje aplicado, resultando favorecida la producción de metanol con voltajes más elevados.

4) Se emplean por último nanopartículas de TiO₂ sintetizadas en medio supercrítico (TiO₂-SC), donde la producción de etileno experimenta un incremento de hasta seis veces (147,4 µmol·m⁻²·s⁻¹) en comparación con el sistema a oscuras. Asimismo, la formación de metanol también se ve favorecida bajo iluminación, alcanzando una velocidad de formación de 4,72 µmol·m⁻²·s⁻¹. Además, las eficiencias Faradaicas tanto para el etileno como para el metanol (46,6% y 15,3%, respectivamente) aumentan con la irradiación de luz, superando los resultados reportados en la literatura para sistemas fotoelectroquímicos en configuración fotoánodo-cátodo. En consecuencia, la eficiencia en la conversión de energía solar en productos mejora en el sistema basado en TiO₂-SC (5,4% para etileno y 1,9% para metanol), en comparación con el comportamiento de los fotoánodos de TiO₂-P25 (3,7% para etileno y 1 % de metanol).

4.3 Trabajo futuro

Tras analizar los principales resultados obtenidos en esta Tesis Doctoral, se identifican las siguientes líneas de investigación como relevantes para el futuro avance científico y técnico del proceso, de tal forma que sea posible acercar la fotoelectrocatalisis a su implementación a escala industrial:

- 1) Continuar con el desarrollo y empleo de nuevos materiales fotoactivos para la fabricación de fotoánodos, incluyendo materiales basados en óxidos de Cu, Bi, Fe o W, entre otros. Se destaca la prometedora utilización de materiales basados en perovskitas, lo cual puede ser abordado a través de colaboraciones con grupos de investigación nacionales e internacionales especializados en la síntesis de estos compuestos. Además, se debe hacer especial énfasis en el diseño y optimización de nuevas configuraciones de fotoelectroreactores, que incluyan configuraciones de photocátodos-ánodo, photocátodo-fotoánodo y fotoelectrolizadores tandem, con el objetivo principal de lograr la producción de hidrocarburos con alto valor añadido, como el etileno, operando en fase gaseosa en el compartimento catódico del reactor PEC y sin aporte externo de energía. Esta estrategia permite aumentar tanto el rendimiento como la concentración de los productos objetivo, minimizando al mismo tiempo la necesidad de etapas adicionales de separación.
- 2) Avanzar en las técnicas de fabricación de los electrodos, ya que este aspecto supone un paso crucial hacia la futura implementación industrial de la reducción fotoelectroquímica de CO₂. En los últimos años han surgido nuevas técnicas de deposición de catalizadores para la fabricación de electrodos como, por ejemplo, la deposición de vapor químico, la pirólisis por pulverización, la galvanoplastia y los métodos de impresión, que están captando un gran interés. Además, es importante considerar posibles tratamientos de modificación de la estructura y superficies de los fotoelectrodos, como la deposición capa por capa y el tratamiento de la superficie con plasma, ya que pueden mejorar el rendimiento y la estabilidad del electrodo.
- 3) Explorar reacciones de mayor interés que puedan llevarse a cabo en el compartimento anódico del reactor PEC con el objetivo de aumentar su viabilidad económica. Cabe destacar, por ejemplo, la reacción de oxidación del glicerol, debido a que es un subproducto importante en la producción de biodiesel, o la electrooxidación del metano a hidrocarburos líquidos debido al alto consumo energético del proceso industrial de conversión de metano. Esto supondría un gran progreso en el proceso ya que permitiría obtener productos de interés tanto en el compartimento catódico como anódico del reactor fotoelectroquímico, buscando, al mismo tiempo, reducir el consumo energético del proceso global.
- 4) Optimización del sistema experimental y de las variables para acercar la fotoelectroreducción a la aplicación real. Entre estas variables, es importante considerar la fuente de luz (luz visible o solar), su intensidad, el potencial de polarización, la densidad de corriente, el caudal de CO₂ y el

contenido de agua en la corriente cuando se opera en fase gaseosa. Además, para superar las limitaciones inherentes de los electrodos, se debe evaluar la relación de área geométrica entre el cátodo y el ánodo, y la viabilidad de utilizar elementos fotovoltaicos ensamblados tanto fuera como dentro del reactor.

Ante lo expuesto, queda patente que, aunque a lo largo de esta Tesis Doctoral se han alcanzado avances significativos en el proceso de fotoelectroreducción de CO₂ en modo continuo, aún existen desafíos por abordar para lograr la implementación industrial de este proceso. Por lo tanto, es crucial seguir dedicando esfuerzos a la investigación en este campo.

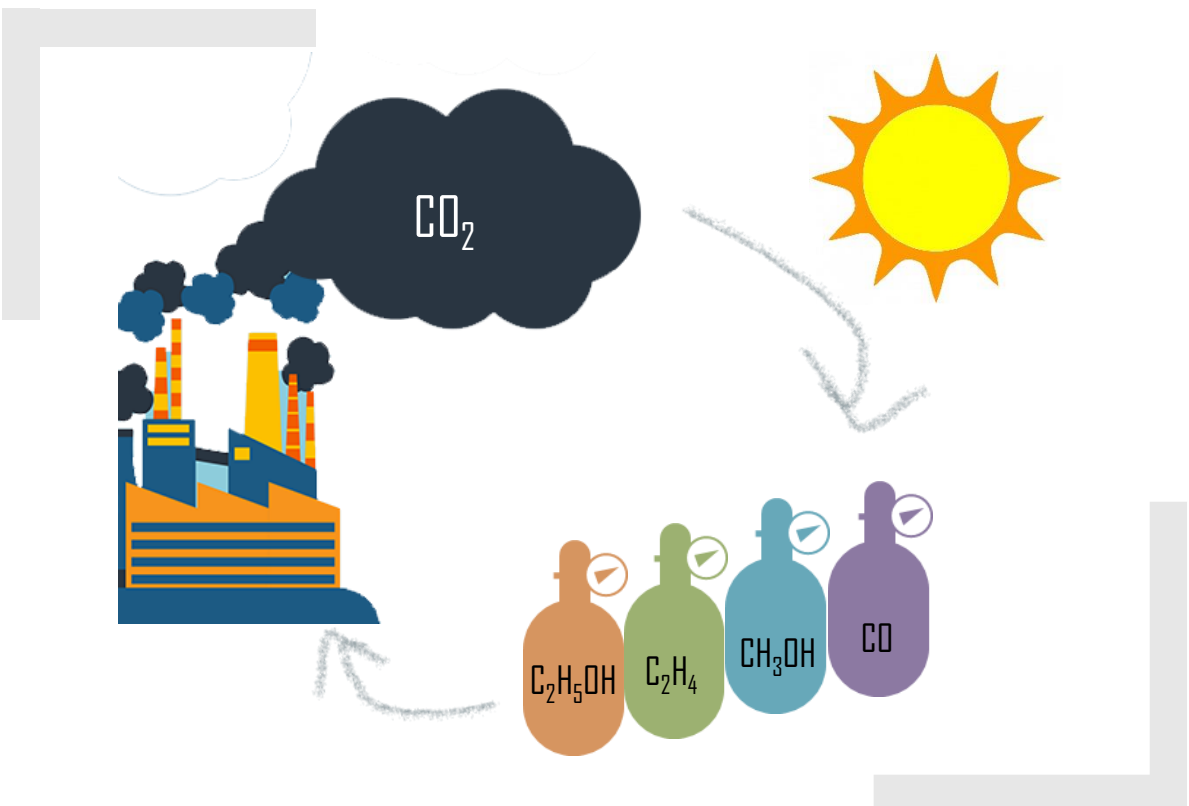
Anexo

ANEXO**DIFUSIÓN DE RESULTADOS EN CONGRESOS NACIONALES E INTERNACIONALES**

A continuación, se enumeran las contribuciones a congresos nacionales e internacionales en el ámbito de la Ingeniería Química a través de los cuales se ha difundido los resultados de la presente Tesis Doctoral:

1. Sergio Castro, Jonathan Albo, Ángel Irabien, Photoelectrochemical reactors for CO₂ utilization, 4th International Symposium on the Catalysis for Clean Energy and Sustainable Chemistry (CCESC). 9 - 11 julio **2018**, Bilbao (España). Comunicación oral.
2. Sergio Castro, Jonathan Albo, Ángel Irabien, TiO₂ photoanode-driven electrochemical system for CO₂ transformation, XXXVII Reunión Bienal de la Real Sociedad Española de Química. 26 - 30 mayo **2019**, San Sebastián (España). Comunicación oral.
3. Sergio Castro, Jonathan Albo, Ángel Irabien, Continuous photo-electrochemical reduction of CO₂ in a TiO₂ photoanode-driven system, 3rd ANQUE-ICCE International Congress of Chemical Engineering. 19 - 21 junio **2019**, Santander (España). ISBN: 978-84-09-12430-5. Comunicación oral.
4. Sergio Castro, Jonathan Albo, Verónica Rodríguez, Rafael Camarillo, Jesusa Rincón, Ángel Irabien, Reducción en continuo de CO₂ utilizando nanopartículas de TiO₂ en una celda fotoelectroquímica, V Workshop de la Red E3TECH / I Workshop Iberoamericano a Distancia E3TECH "Aplicaciones Medioambientales y Energéticas de la Tecnología Electroquímica". 28 – 31 octubre **2020**, Online. ISBN: 978-84-09-24561-1. Comunicación póster.
5. Sergio Castro, Jonathan Albo, Verónica Rodríguez, Rafael Camarillo, Jesusa Rincón, Ángel Irabien, TiO₂ synthesized in supercritical medium for continuous CO₂ photoelectrocatalytic conversion, 24th International Congress of Chemical and Process Engineering (CHISA 2021). 15 - 18 marzo **2021**, Online. Comunicación póster.





La captura, almacenamiento y utilización de CO₂ (CAUC) se considera una de las opciones más prometedoras para mitigar el cambio climático. En particular, la reducción electroquímica del CO₂, que tiene el propósito de transformar esta molécula en productos de alto valor añadido, está atrayendo una atención cada vez mayor. En este sentido, la fotoelectrocatalísia, el acoplamiento de luz en sistemas electroquímicos, emerge como una potencial alternativa que combina los beneficios de la electrocatalísia y la fotocatalísia. La presente Tesis Doctoral, desarrollada en el grupo de investigación DePRO del Departamento de Ingenierías Químicas y Biomolecular de la Universidad de Cantabria, tiene como objetivo establecer un proceso continuo de conversión de CO₂ por vía photoelectroquímica, con el propósito de reducir los sobrepotenciales necesarios para la conversión electroquímica de CO₂ al hacer uso de la luz. Esta investigación representa una nueva línea de estudio dentro del grupo.

The capture, storage, and utilization of CO₂ (CCUS) is considered one of the most promising strategies for mitigating climate change. In particular, the electrochemical reduction of CO₂, which has the goal of converting this molecule into high-value-added products, is attracting increasing interest. In this context, photoelectrocatalysis, which couples light to electrochemical systems, emerges as a promising solution, combining the advantages of electrocatalysis and photocatalysis. The focus of this doctoral thesis, conducted in DePRO research group within the Department of Chemical and Biomolecular Engineering of the University of Cantabria, aims to establish a continuous CO₂ photoelectrochemical conversion process. The objective is to reduce the overpotentials required for CO₂ electrochemical conversion by harnessing the power of light. This represents the start of a new research line within the scope of the research group.